Manitoba
Energy and Mines
Geological Services

ERRATA: Economic Geology Report ER87-1

Page 33: Figure 24 caption. Last line should read: bro; • 'Knotted gabbro'; and, – related(?) rocks.

Page 35: Figure 25 caption. Last part should read: Symbology as in Figure 24.

Economic Geology Report ER87-1

Geological Setting of the Tartan Lake Gold Deposit

By G.H. Gale and K.J. Ferreira

Winnipeg, 1988

Energy and Mines

Hon. Harold J. Neufeld
Minister

Charles S. Kang
Deputy Minister

Minerals Division

Sobharam Singh
Assistant Deputy Minister

Geological Services
W.D. McRitchie
Director

TABLE OF CONTENTS

Page

ABSTRACT vi
INTRODUCTION 1
Location and Access 1
Acknowledgments 1
GENERAL GEOLOGY 2
Regional geology 2
Geology of the Tartan Lake area 2
PETROGRAPHY 6
Volcanic and Sedimentary rocks 6
Basaltic Andesite Rocks 6
Volcaniclastic and Sedimentary rocks 6
Mafic volcaniclastic and sedimentary rocks 6
Mafic volcanic-derived wacke 6
Mafic siltstone 7
Felsic to intermediate volcaniclastic rocks 7
Felsic tuffaceous rocks 7
Intermediate tuffaceous rocks 8
Intermediate volcaniclastic siltstone 8
Chloritized mafic rocks 8
Intrusive Rocks 9
'Knotted' gabbro 9
Poikiloblastic 'knotted' gabbro 9
Microphyric gabbro 9
Gabbroic complex 9
Medium grained gabbro 9
Fine grained gabbro 10
Igneous breccia 10
Altered gabbro 10
Ruby Lake gabbro 12
Porphyritic Felsic Dykes 12
Mine Pensinsula 13
South Block 14
Ruby Lake 14
Felsic intrusive vs. extrusive rocks 14
STRUCTURE 15
Mine Peninsula 15
Planar fabrics 15
Folds 15
First phase (F_1) 15
Second phase (F_2) 16
Third phase 19
Post F_2 (?) cleavage 19
Faults 19
South Block 19
General Statement 19
Type I Alteration Zones 19
Type II Alteration Zones 23
Type III Alteration Zones 27
Deformational Events 27
Structural History of the South Block (Gabbro), Summary 28

Page

ROCK GEOCHEMISTRY 31
Volcanic rocks 31
Basalt 31
Basaltic andesite 31
Felsic volcanic rocks 31
Intrusive rocks 32
Medium- to coarse-grained gabbro 32
Fine grained gabbro 33
'Knotted' gabbro 34
Ruby Lake gabbro 35
Feldspar-porphyritic felsic intrusions 36
Chloritic Rocks 36
Trace Element Geochemistry 36
MINERALIZATION 47
Summary of Exploration History 47
Zones of Mineralization 47
Main Zone 47
South Zone, 5 East Zone, Baseline Zone 47
Other zones 47
Exploration Potential 48
REFERENCES 50
APPENDIX 1: Major element analyses 51
APPENDIX 2: ICP analyses 52
APPENDIX 3: Au and Ag analyses, grab samples 55
APPENDIX 4: Sample locations 57
APPENDIX 5: Selected petrographic descriptions 61

FIGURES

Figure 1: Regional geology of the Tartan Lake area. 3
Figure 2: General geology of the Tartan Lake area. 4
Figure 3: Geological map of the Tartan Lake Mine area (1:1200 scale). . . . . in pocket
Figure 4: Geographic subareas within the Tartan Lake area. 5
Figure 5: Igneous breccia. 10
Figure 6: Pillow lavas, Mine Peninsula. 11
Figure 7: Altered gabbro, South Zone. 11
Figure 8: Crenulated chlorite schist, South Zone. 13
Figure 9: Compositional layering developed in mafic volcanic rocks. 15
Figure 10: F_1 minor folds. 16
Figure 11: F_2 minor folds. 17
Figure 12: Sketches of F_1 and F_2 minor structures. 18
Figure 13: Major F_2 structure reconstructed from minor F_2 fold observations. 20
Figure 14: Crenulation fold in sheared and altered gabbro. 21
Figure 15: Rhyolitic tuff with well developed cleavage or mylonite fabric. 21
Figure 16: Minor structures in the Tartan Lake area. 22
Figure 17: Major faults identified in the Tartan Lake area. 23
Figure 18: Zones of alteration identified in gabbroic rocks in the South Block. 24
Figure 19: Detailed geology of a part of the South Zone. 25

Page

Figure 20: Detailed geology of a part of the 5 East Zone. 26
Figure 21: Quartz vein mobilizate in altered and schistose rocks of the South Zone and 5 East Zone. 27
Figure 22: Structural features in alteration zones. 28
Figure 23: Schematic structural history of the mineralized zones in the South Block gabbro. 30
Figure 24: Silicate whole rock oxide plots for analyses of various rock types. 33
Figure 25: TiO_2 vs. Mn and TiO_2 vs. P_2O_5 variation diagrams. 35
Figure 26: Cross section of the Tartan Lake Main Zone. 48
Figure A: Sample locations for the Mine Peninsula area. 57
Figure B: Sample locations for the South Block. 58
Figure C: Sample locations for the Ruby Lake grid. 59
Figure D: Sample locations for the Tartan Lake (1:5000) grid. 60

TABLES

Table 1: Silicate whole rock analyses of basaltic andesite rocks. 31
Table 2: Silicate whole rock analyses of felsic rocks. 32
Table 3: Silicate whole rock analyses of medium- to coarse-grained gabbroic rocks. 34
Table 4: Silicate whole rock analyses of fine grained gabbroic rocks. 34
Table 5: Silicate whole rock analyses of 'knotted' gabbro and related(?) fine- to medium-grained gabbroic rocks. 35
Table 6: Silicate whole rock analyses of chloritized mafic rocks. 36
Table 7: Silicate whole rock analyses of mafic volcaniclastic and sedimentary rocks. 37
Table 8: Partial chemical analyses of basaltic andesite volcanic rocks. 38
Table 9: Silicate whole rock analyses of schistose gabbroic rocks. 38
Table 10: Partial chemical analyses of altered and schistose gabbroic rocks. 39
Table 11: Partial chemical analyses of chloritic and schistose gabbroic rocks. 40
Table 12: Partial chemical anlayses of intermediate tuffaceous and sedimentary rocks. 41
Table 13: Partial chemical analyses of feldspar and feldspar-quartz porphyry 42
Table 14: Gold and silver analyses for grab samples of vein quartz and some quartz-rich rocks. 44
Table 15: Gold and silver analyses for grab samples of schistose rocks. 45
Table 16: Gold and silver analyses for grab samples of sulphide- and graphite-rich rocks. 45
Table 17: Gold and silver analyses for grab samples of various rock types. 46
Table 18: Exploration history of the Tartan Lake deposit. 47

ABSTRACT

The Main Zone of the Tartan Lake gold deposit occurs in a volcanic and volcaniclastic supracrustal sequence at the margin of a gabbroic complex. Geological mapping at scales of 1:5000 and 1:1200 typified the lithologies in a 4 km^2 area surrounding the mine, and provided an initial investigation of the gabbroic complex and its association with numerous gold occurrences.

The dominant lithologies in the supracrustal sequence include basalt and pyroxene-phyric basaltic andesite flows and pyroclastic rocks, volcaniclastic sedimentary mafic and felsic tuffs, intermediate and mafic wacke and siltstone, and chloritized mafic rocks. The gabbro complex is a multiple intrusion characterized by textural and compositional variability. Medium- to coarse-grained leucogabbro is the most prevalent phase. Fine grained gabbro, 'knotted' gabbro with poikiloblastic hornblende, and a distinctive igneous breccia can be differentiated in the field and on the basis of limited whole rock and trace element geochemical analyses. Feldspar ± quartz porphyry dykes intrude the volcanic and sedimentary rocks and, to a lesser extent, the northwestern portion of the gabbroic complex.

Complex structural deformation has affected volcanic and sedimentary rocks near the Main Zone and includes: 1) development of a regional schistosity (S_1) mostly parallel to compositional layering; 2) a postulated major early folding event (F_1); 3) a prominent second folding event (F_2); and 4) development of box-type folds and a late post-F_2(?) cleavage. Numerous faults range from 225° to 245° in strike. The gabbroic complex has undergone early fracturing and/or faulting and subsequent alteration including chloritization, carbonatization, tourmalinization and gold-bearing pyritization. A superimposed schistosity is defined by chlorite. Subsequent deformation produced crenulation folds. Late faults, along the pre-existing alteration zones, produced local shearing and strain-slip cleavages.

Gold is identified in three geological settings in the Tartan Lake area: 1) in late auriferous quartz veins and lenses of gold- and pyrite-bearing disrupted schistose feldspar porphyry and chlorite schist (typified by the Main Zone), 2) in carbonatized, pyritized and tourmalinized zones of chlorite schist (e.g., South Zone, Baseline Zone, 5 East Zone), and 3) narrow fracture-filling quartz veins with abundant visible gold.

INTRODUCTION

Gold mineralization has been known in the Tartan Lake area since 1931 (Bateman, 1945). Considerable surface work was done in 1932 and 1933 and diamond drilling undertaken in 1945-46. Although a number of intersections with more than 0.5 oz/ton Au were encountered, no further major work was reported until 1984 when Granges Exploration Ltd. began a diamond drill investigation of a V.L.F. anomaly that led to the definition of the Main Zone and the South Zone. This mineralization was developed as the Tartan Lake Mine, which began production in 1987.

The Main Zone occurs in volcanic rocks at the margin of a gabbroic complex. A number of other gold occurrences in the area are either spatially associated with or occur at the margin of gabbroic rocks (Fig. 1). A detailed metallogenetic examination of the Tartan Lake deposit was initiated to provide a basis for further studies of other known occurrences in the area.

This project was designed to provide a synthesis of the geology of the area immediately surrounding the Tartan Lake gold deposit to be utilized as a geological framework within which detailed mineral deposit studies could be undertaken. The initial six week field program provided a 1:5000 geological base (Peloquin and Gale, 1985) and revealed that portions of the area were too complex to be represented at that scale of mapping. Consequently, part of the area was remapped at a scale of 1:1200 using cut grid lines for reference and carrying out extensive outcrop stripping during a five week field program in 1986 (Peloquin et al., 1986).

This report deals mainly with petrographic descriptions of the main rock types. Structural, geochemical and mineralization descriptions are brief since those aspects of the study were not emphasized during the initial mapping due to time limitations. Detailed structural, geochemical and mineralogical studies of the mineralized zones, that had been postponed pending underground development of the Tartan Lake Mine, were initiated in 1987 as an M.Sc. thesis study by John Fedorowich at the University of Saskatchewan.

LOCATION AND ACCESS

The Tartan Lake Mine is located 10 km northeast of Flin Flon. It is accessible by bush aircraft from Channing or via an 18 km private road that starts several kilometres west of the town of Creighton, Saskatchewan.

ACKNOWLEDGEMENTS

The authors gratefully acknowledge S. Peloquin and B. Tannahill for their field mapping work on this project. P. Deveaux, M. Kreczmer, W. Hansen and other staff of Granges Exploration Ltd. provded valuable information and discussions. M. Fedikow, P. Gilbert and B. Bannatyne critically reviewed the manuscript. Computer manipulation of geochemical data was done by G. Conley. S. Weselak and D. Kircz typed the manuscript.

GENERAL GEOLOGY

REGIONAL GEOLOGY

The area around Tartan Lake was mapped by Bateman and Harrison (1945) and Tanton (1938) at a scale of one inch to one mile (1:63 360). An area of approximately one square mile was mapped at 1:5000 scale by Peloquin and Gale (1985). Gilbert (1986) conducted a reconnaissance of parts of the Tartan Lake area during a 1:15 000 scale regional mapping project. Examination of the one inch to one mile maps suggests that this area is underlain by rocks that are contiguous with those of the Flin Flon-White Lake area mapped by Balles and Syme (1987; cf. Fig. 1).

The Tartan Lake area is situated in the western part of the Flin Flon greenstone belt near its northern margin with the Kisseynew gneisses. Both intrusive and extrusive rocks of this greenstone belt yield Proterozoic radiometric dates of 1737 to 1930 Ma (Mukherjee et al., 1971; Stauffer et al., 1975; Josse, 1974) and indicate a probable Aphebian age for the volcanism. The volcanic and volcano-sedimentary rocks of the belt belong to the Amisk Group that is unconformably overlain by sedimentary and subaerial volcanic rocks of the Missi Group (Bruce, 1918).

Mafic flows and derived volcanogenic sedimentary rocks and volcaniclastic rocks constitute approximately 90% of the Amisk group. Abundant pillow lava, hyaloclastite and volcanogenic sedimentary rocks indicate a dominantly subaqueous environment of deposition for most of the Amisk Group. The mafic flows range in composition from basalt to andesite; however, most have basalt to basaltic andesite compositions (i.e., less than 55% SiO_2) and have tholeiitic to calc-alkaline affinities in the vicinity of Flin Flon (Stauffer et al., 1975). Felsic flow rocks include both dacite and rhyolite. The volcanic rocks have been compared with Cenozoic and younger island arc complexes by Balles (1971) and Stauffer et al. (1975).

The Missi Group in the Flin Flon area was deposited with angular unconformity upon a regolith developed on the Amisk volcanic rocks. The Missi Group at Flin Flon consists of conglomerate, subarkose and feldspathic greywacke (Mukherjee et al., 1971). In the Snow Lake area, the Missi Group has been reported to contain subaerial mafic to felsic volcanic rocks (Shanks and Balles, 1977).

Mafic and felsic subvolcanic and plutonic rocks intrude the Amisk volcanic rocks in the Flin Flon area. A number of different types of intrusive rocks occur as cobbles in the Missi conglomerates at Flin Flon.

GEOLOGY OF THE TARTAN LAKE AREA

For the purposes of this report the Tartan Lake area is an approximately 4 km^2 area bisected by the south arm of Tartan Lake (Fig. 2, 3). It is underlain predominantly by mafic volcanic rocks and the northwestern tip of a large gabbroic complex (Fig. 1). The map area is divided into three geographic subareas for descriptive purposes, namely: 1) the Mine Peninsula; 2) the Ruby Lake area; and 3) the South Block (Fig. 4).

The Mine Peninsula is underlain predominantly by mafic and felsic tuffaceous rocks, pyroxene-phyric basaltic andesite flows, gabbroic and dacitic dykes and clastic sedimentary rocks. These rocks appear to be the continuation along strike of rocks in the Ruby Lake area to the west.

The Ruby Lake subarea is underlain mainly by flow and volcaniclastic rocks. From south to north these rocks consist of basaltic flows, pyroxene-phyric basaltic andesite flows and pyroclastic rocks, mafic and felsic tuffaceous rocks, and minor epiclastic rocks. Gabbroic and feldspar-porphyritic dacitic dykes occur throughout the area.

The South Block is underlain predominantly by various gabbroic intrusive rocks that have been referred to collectively as the "Gabbroic complex" (Peloquin and Gale, 1985). This "Gabbroic complex" is a multiple intrusion of fine- to coarse-grained gabbroic rock that consists mainly of medium- to coarse-grained leucogabbro, which varies in composition to a coarse grained melanocratic gabbro. Subangular pods or blocks of pyroxenite tens of centimetres across occur locally. Aphanitic intermediate dykes, fine grained gabbro and feldspar-porphyritic felsic dykes are present locally. A distinctive igneous breccia, consisting of angular medium- to coarse-grained gabbroic to pyroxenitic clasts in a matrix of fine grained gabbro (Fig. 5), was delineated towards the central part of the area (Peloquin and Gale, 1985). Gilbert (1987) reports evidence for a synvolcanic (Amisk) age for several gabbroic intrusions in the area.

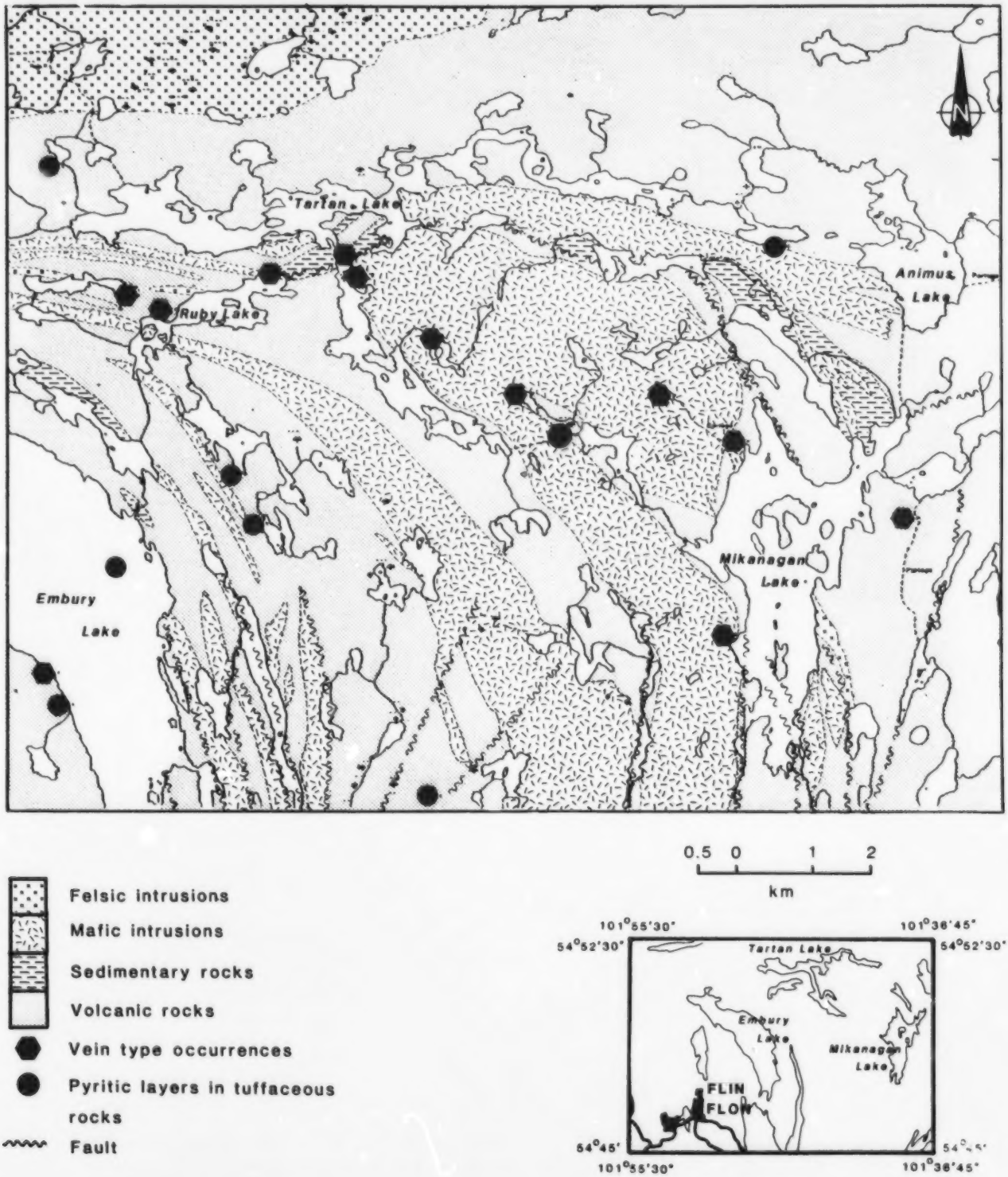

Figure 1: Regional geology of the Tartan Lake area with location of known mineral occurrences.

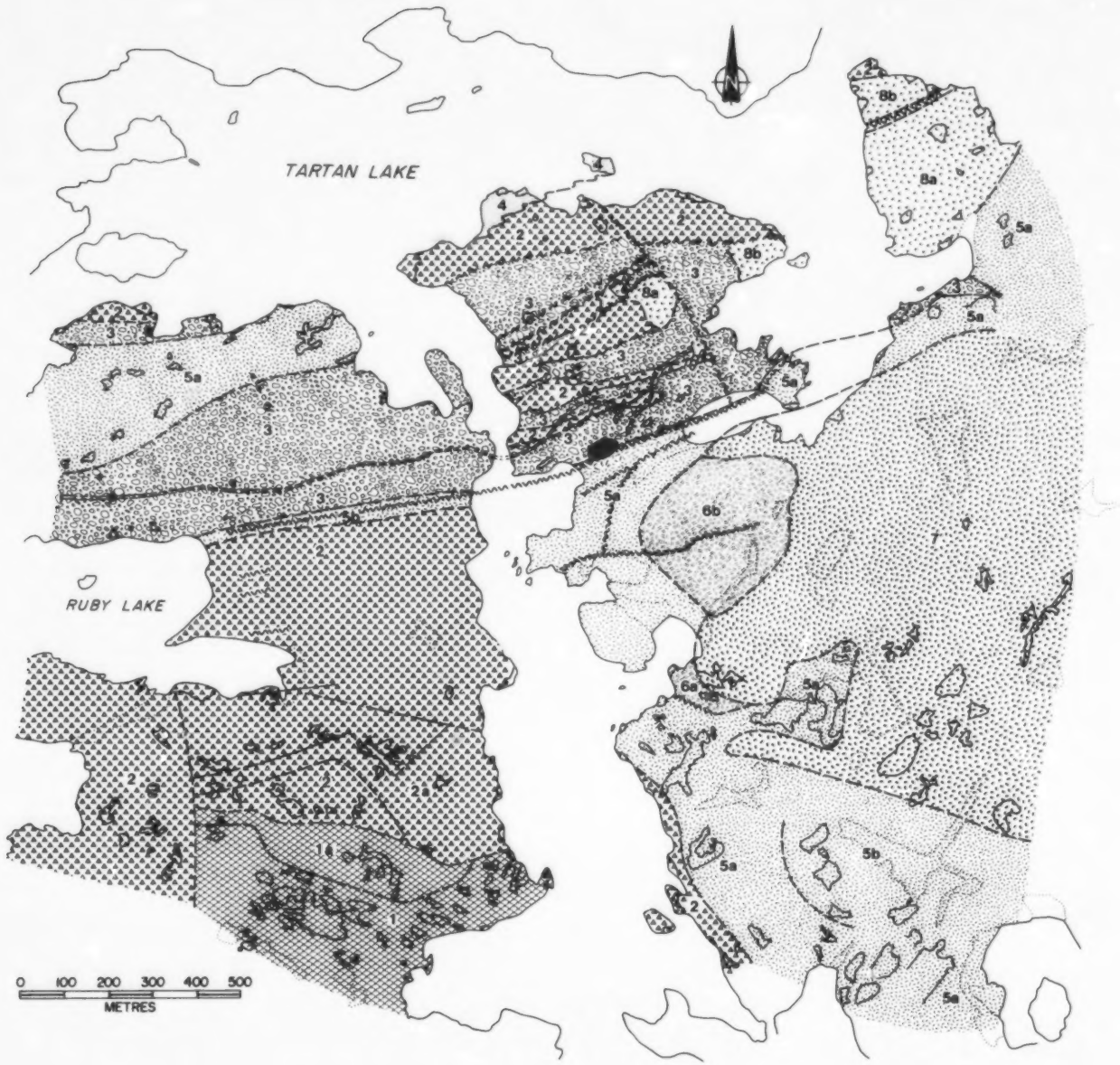

Figure 2: *General geology of the Tartan Lake area (after Peloquin et al., 1986). Area outlined was mapped at a scale of 1:1200. The location of the Main Zone of the Tartan Lake Mine is indicated by the black dot. Legend. 1) Basaltic flows, 1a) Basaltic breccia; 2) Basaltic andesite flows and fragmental rocks, 2a) Pyroxene-phyric pyroclastic rocks; 3) Volcanogenic sedimentary rocks; 4) Dacitic(?) flows; 5a) Leucogabbro, 5b) Melanogabbro; 6a) Fine grained gabbro, 6b) Fine grained gabbro intruded into leucogabbro; 7) Igneous breccia; 8a) Fine grained gabbro, 8b) 'Knotted' gabbro.*

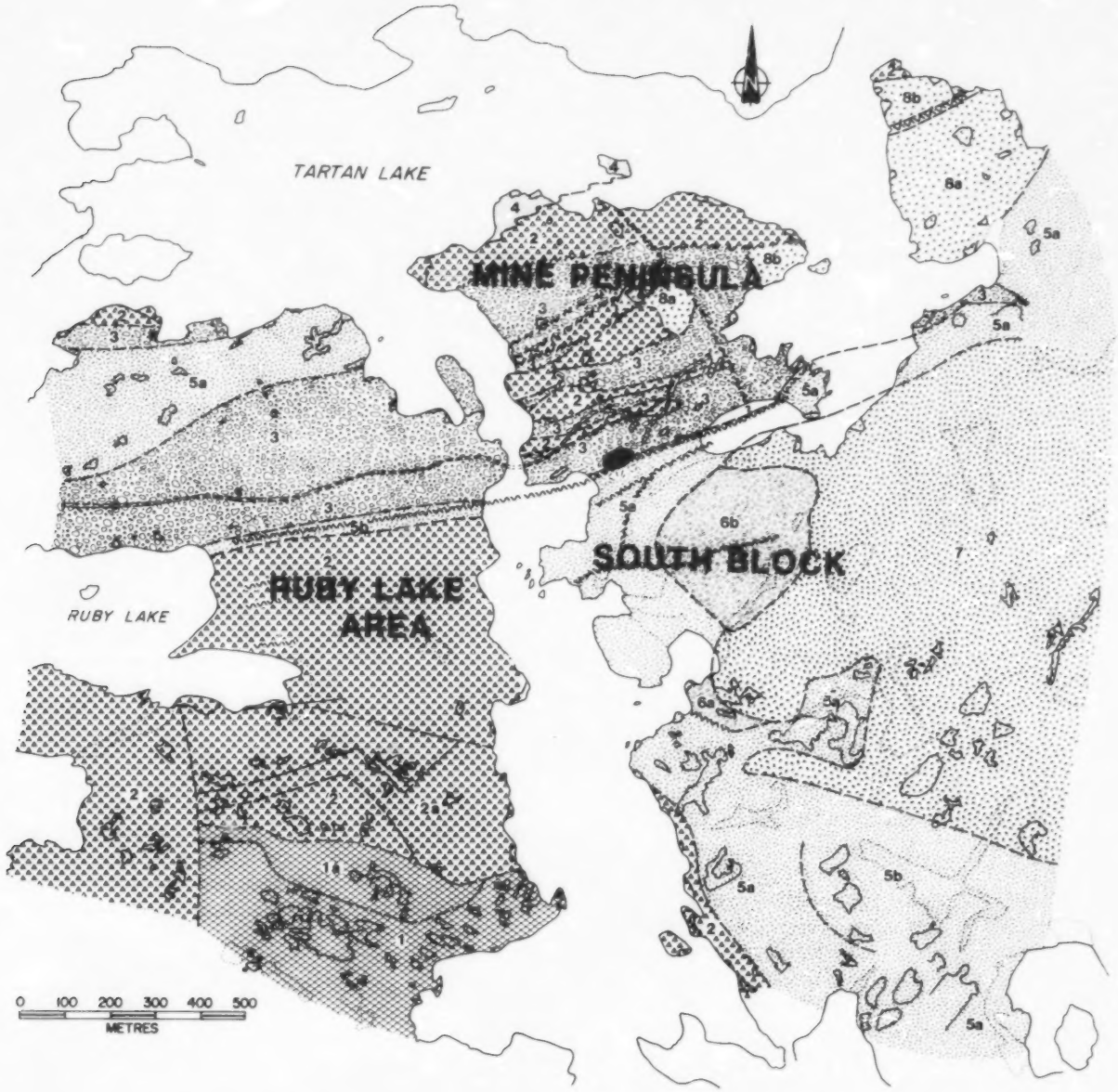

Figure 4: *Geographic subareas for the Tartan Lake area. The boundary between the Mine Peninsula and South Block is a natural bog-filled depression at the approximate location of the Main Zone (see Fig. 2 for symbology).*

PETROGRAPHY

VOLCANIC AND SEDIMENTARY ROCKS

Basaltic Rocks

The rocks mapped as basalt in the southwestern extremity of the map area (unit 1, Fig. 2) form a sequence of fine grained pillowed flows, breccia and tuff that are darker coloured than the basaltic andesite flow rocks (unit 2), rarely contain pyroxene phenocrysts and are commonly vesicular. Individual flow units are generally several tens of metres thick and commonly consist of a pillowed (1-1.5 m average diameter) central zone and marginal zones of flow breccia and tuff. In several places cherty tuffaceous layers occur at the top of the north-facing flow units.

A thick unit of basaltic breccia (Unit 1a, Fig. 2) overlying pillowed flows consists of variably textured basaltic fragments in a basaltic matrix that is commonly vesicular. This map unit appears to have been the result of a different effusive event from the pillowed rocks to the south and represents several individual flow units separated by clastic layers.

A thin section from a pyroxene-phyric flow in unit 1 contained several per cent augite phenocrysts that range in size from 0.17 to 1.5 mm (average 0.6 mm) in diameter. The phenocrysts are equant to elongate, subhedral to anhedral, commonly twinned and partly uralitized. The very fine grained anhedral groundmass consists of epidote (60%), tremolite-actinolite (30%), carbonate (10%), quartz (10%) and trace leucoxene and hematite. Amygdules, which constitute less than 5% of the rock, are 1-3 mm in diameter and filled with epidote, quartz, plagioclase, carbonate and trace chalcopyrite.

The aphyric basaltic rocks consist of very fine grained (0.25 mm) tremolite-actinolite (55%), epidote and carbonate after plagioclase (35%), lath-shaped remnant plagioclase (5%) and amygdules (5%).

Basaltic Andesite Rocks

Basaltic andesite flows and pyroclastic rocks are exposed in a 400 m wide zone in the Ruby Lake area and in several narrow bands in the Mine Peninsula area (Fig. 2 and 3). These flows are commonly pillowed and pyroxene-phyric. Tuffaceous rocks and breccia are minor components throughout the basaltic andesite rocks (unit 2). A unit of pyroxene-phyric pyroclastic rocks (unit 2a) is exposed over an extensive area north of the basaltic rocks in the southwestern part of the map area (Fig. 2); stratigraphic thickness is not known.

Flow contacts in the Ruby Lake area appear to be irregular but are rarely exposed. Pillows have an overall east-west elongation with average lengths of 1.5 m and thicknesses of 0.5 m. On the Mine Peninsula the pillows are intensely deformed (see Fig. 6 and Peloquin et al., 1986, Fig. GS-11-8, p. 64) and original sizes are difficult to estimate. Top determinations from pillows in basaltic andesite flows in the Ruby Lake area are inconclusive but locally indicate a north-facing sequence. Gilbert (1987) indicates the sequence of basaltic andesite flows form the north limb of a southeasterly-trending syncline.

The basaltic andesite flows are dark green to beige (C.I. = 60-80) on weathered surfaces. Pyroxene phenocrysts and amphibole pseudomorphs after pyroxene are up to 3 mm in diameter and constitute 3-15% of the rock. The phenocrysts have subhedral to euhedral shapes and locally are glomerophyric. Amygdules are generally rounded, up to 5 mm in diameter, and constitute less than 1% to more than 30% of the rock. The amygdules are filled with either quartz, carbonate, quartz + carbonate ± plagioclase or quartz rimmed by epidote. The very fine grained groundmass, commonly less than 0.01 mm, consists of epidote, biotite, plagioclase, pyroxene, chlorite and quartz.

Carbonate crystals and crystal aggregates are present locally. Anhedral to euhedral pyrite, up to 3%, is commonly associated with chlorite. Trace amounts of tourmaline may be present together with pyrite in the sheared flow rocks.

A distinctive basaltic andesite tuff and breccia sequence (unit 2a, Fig. 2) has been delineated in the southwestern part of the map area. Exposures of this unit along the shoreline of Tartan Lake consist mainly of subangular fragments, 15-30 cm, of amygdaloidal basaltic andesite in a tuffaceous matrix. South and southeast of Ruby Lake this unit contains a number of layers of crystal tuff with 30-60% pyroxene crystals, up to 1 cm in diameter, interlayered with pyroxene-bearing breccias.

Volcaniclastic and Sedimentary Rocks

Mafic to felsic volcaniclastic and sedimentary rocks are present north of the basaltic andesite flows in the Ruby Lake area and north of the mine road on the Mine Peninsula. These rocks have been separated into three separate units in Figure 3: namely, 1) mafic volcaniclastic rocks and sedimentary rocks, 2) felsic to intermediate volcaniclastic rocks, and 3) chloritized mafic rocks. These rocks are diffusely to well layered and generally fine grained. Pillowed andesitic flows occur within these rocks, but the contacts are either not exposed or are faulted. Mafic and felsic dykes intrude these rocks locally.

MAFIC VOLCANICLASTIC AND SEDIMENTARY ROCKS

Mafic volcaniclastic and sedimentary rocks occur in the northern part of the Ruby Lake area in association with felsic to intermediate volcaniclastic rocks. A thickness of at least 90 m of mafic volcaniclastic rocks occurs

north of the gabbroic sill that separates volcaniclastic rocks from the basaltic andesite flows to the south (Fig. 3). These rocks include volcanic-derived wacke and siltstone, and very fine to fine siltstone. Gabbro sills, possibly related to the "Tartan Lake gabbro sill", disrupt the mafic volcaniclastic rocks (cf. Ruby Lake grid, approximately 5+50N/0+00BL to 5+50N/5+00W, and 6+00N/19+00W). These units have limited exposure due to their relatively small stratigraphic thickness and paucity of outcrop; the petrographic and geochemical data are based on only three samples.

Mafic volcanic-derived wacke (unit 2a, Fig. 3). The 4.5 m thick mafic volcanic-derived wacke weathers medium green (C.I. = 55-60), is very fine grained with a moderate foliation and locally contains distinctive layers differentiated by grain size. Plagioclase, the primary mineral, occurs with variable grain sizes in an apparent bimodal distribution. It has an average groundmass size of 0.2 mm and crystals with an average size of 1.5 mm. These large crystals of plagioclase, which constitute 3% of the rock, contain minute biotite and epidote inclusions, and in places are broken *in situ* with the intervening space infilled with quartz ± carbonate ± biotite ± epidote ± tourmaline. More commonly the crystals were broken prior to deposition or during deformation since broken fragments have been displaced and cannot be rematched. A very fine grained mafic matrix composed of biotite, epidote and hornblende is interstitial to the plagioclase. Local, lithic clasts are defined by variably shaped, very fine grained, granular aggregates of plagioclase or epidote (± carbonate). The abundance of mafic material, the lack of rounding, and poor sorting attest to minimal reworking. This mafic volcanic-derived wacke has a slightly coarser grain size and a greater abundance of visible plagioclase in hand specimen than mafic siltstone; originally, from field examinations, this rock was considered to be a crystal tuff.

Mafic siltstone (unit 2b, Fig. 3). Mafic tuff-derived siltstone is medium green-grey on weathered surfaces (C.I. = 50) with well developed foliation defined by the orientation of biotite. Subhedral to euhedral plagioclase (10-15%) with an average size of 0.2 mm occurs as broken crystals and rounded grains. The matrix has a grain size of 0.015-0.2 mm and is composed of plagioclase, biotite, epidote and quartz. Carbonate minerals (3%) have an average size of 0.3 mm and occur in elongate crystals and polycrystalline patches parallel to biotite foliation; locally, the carbonate is concentrated in layers.

Very fine grained mafic siltstone weathers dark greenish grey and has an average grain size of 0.02 mm. This siltstone is thinly laminated and the laminae are attenuated and discontinuous; locally the laminae are readily discernible, whereas in other places the rock appears massive. The rock is composed of biotite, epidote, plagioclase, quartz, and minor sulphide minerals. Grain shapes, probably anhedral, are difficult to discern. Elongate lensoidal areas constitute 3-5% of the rock, are up to 0.75 mm in diameter and consist of 0.1 mm undulatory quartz, interstitial biotite, anhedral epidote, and anhedral sulphide minerals. Tourmaline, less than 1%, occurs in prismatic crystals up to 0.5 mm long.

FELSIC TO INTERMEDIATE VOLCANICLASTIC ROCKS (unit 3, Fig. 3)

Felsic to intermediate volcaniclastic rocks are interlayered with mafic volcanic rocks immediately north of the basaltic andesite rocks in the Ruby Lake area and on the Mine Peninsula (Fig. 3). Similar rocks occur immediately north of the Tartan Lake road in the Ruby Lake area (Fig. 2). These rocks are subdivided into three types: a) felsic tuffaceous rocks; b) intermediate tuffaceous rocks; and c) intermediate volcaniclastic rocks, in part greywacke. These rock types (especially 3a) may form continuous layers but commonly have lensoidal and discontinuous outcrop patterns.

Felsic tuffaceous rocks (unit 3a, Fig. 3). Thin layers of white to buff weathering, tuffaceous rhyolite occur throughout the dominantly intermediate tuffaceous rock unit. The thickest layer, observed at 13+00N/0+25E, exceeds 10 m in thickness. Locally the felsic rocks contain quartz crystals that are irregularly scattered throughout an aphanitic matrix and are considered to be rhyolitic tuffs. In other places these white weathering felsic rocks have higher contents (greater than 20%) of feldspar crystals and it is not clear from field examinations, because of a lack of outcropping contact relationships, whether they represent felsic crystal tuff or thin feldspar-phyric felsic dykes .

An exposure immediately north of the basaltic andesite flows in the Ruby Lake area (4+00N/8+50W; Fig. 3) consists of a number of 10-50 cm thick layers of felsic tuff interlayered with intermediate tuffaceous rocks. The felsic layers vary from aphyric and schistose to quartz-, quartz and feldspar-, and feldspar-bearing varieties. The feldspar- and quartz-bearing layers are often interbedded with finer grained, thinly layered felsic tuffaceous rocks with only a few crystals. The finer grained layers have bimodal grain sizes of 0.1 and 0.5 mm. Compositional and grain size layering are discernible within some of these thinly layered felsic tuffaceus rocks.

In thin section the crystal-bearing felsic tuffaceous rocks consist of 2-8 mm plagioclase crystals and/or 1-3 mm quartz grains in a granular matrix of 0.5 mm plagioclase and quartz, epidote, biotite, muscovite, carbonate and opaque oxide minerals. Trace pyrite may be concentrated in some carbonate-rich areas. Commonly the feldspar crystals are euhedral and appear to overgrow the schistosity. In the Mine Peninsula area the white weathering felsic tuffaceous rocks are generally aphyric

and constitute less than 5% of the exposed rocks.

Bedding and internal organization of beds in the felsic tuffs are commonly obscured by structural deformation. Discontinuous attenuated layering is present but its relationship to bedding was not determined. Contacts with adjacent intermediate tuffs are generally sharp and probably of structural origin (e.g. transposition along shear planes or faults; see also Fig. 15).

Intermediate tuffaceous rocks (unit 3b, Fig. 3). Intermediate tuffaceous rock weathers reddish brown to buff. It is thinly layered with variable composition; locally, grain size differences may be distinguished among layers. The reddish brown weathering tuffaceous rock, more common than the buff weathering tuffaceous rock, is commonly interbedded with siliceous tuff at and north of base line 14 + 25N on the Mine Peninsula. It may contain up to 10% plagioclase crystals that are less than 1 mm. The lighter coloured tuffaceous rock is interbedded with intermediate volcaniclastic rocks in outcrops along the mine road, and may contain 15-20% plagioclase crystals that are 1-2 mm in diameter. The rock is locally grey east of the Crusher Fault and north of base line 14 + 25N.

Millimetre-thick layers are compositionally differentiated; felsic layers are more abundant than mafic layers by a ratio of about 4:1. Felsic layers consist of quartz and plagioclase with about 15% biotite and lesser carbonate, epidote and opaque oxide minerals. Mafic layers are composed of biotite and epidote with 20-30% plagioclase, quartz, carbonate, chlorite and opaque oxide minerals; biotite and epidote crystals have a subparallel arrangement. The average grain size is less than or equal to 0.05 mm; however, in mafic layers the biotite may be up to 0.1 mm long. Grain size differences are commonly distinguishable among layers.

Plagioclase and quartz crystals as well as polycrystalline mosaics of plagioclase and/or quartz are up to 0.4 mm long. Polycrystalline aggregates, up to 3%, are porphyroblastic and nucleate from an anhedral to subhedral feldspar crystal whose grain size is larger than that of the matrix. Plagioclase porphyroblasts are complexly twinned and contain inclusion trails composed of epidote or sericite. Undulatory extinction in quartz is a ubiquitous strain feature. Mosaics of quartz ± feldspar are generally rounded to augen-shaped; however, where elongated, they parallel layering/foliation.

In thin section lithic clasts are lensoidal aggregates, up to 1 mm, that contain variable percentages of very fine grained carbonate, quartz, plagioclase, biotite and muscovite. Epidosite pods, 0.35-2 cm in diameter, consist mainly of very fine grained epidote. Minor plagioclase, quartz, and biotite occur as discrete crystals, crystalline patches, and infill multidirectional microfractures within the pods. Very fine grained opaque minerals are disseminated throughout the pods. The foliation in the rock commonly bends around the margins of the pods.

Minor intermediate lapilli-tuff is locally associated with the intermediate tuff. It has a reddish brown weathering matrix, lacks notable feldspar crystals, and contains 1-2 cm, nongraded pods of epidosite.

Intermediate volcaniclastic siltstone (unit 3c, Fig. 3). Intermediate volcaniclastic siltstone is a fine grained grey to buff weathering rock. The grey weathering variety with indistinct to weakly defined layering occurs also within the chloritic rocks (unit 4) south of the mine portal. The buff weathering rock with moderately to well defined layering is located between aphyric and pyroxene-phyric mafic flow units and occurs also directly south of the decline. The two rock types appear to be petrographically similar on the basis of a very limited number of thin section descriptions.

The intermediate volcaniclastic siltstone has a mostly uniform grain size of 0.025 mm and is generally better sorted than the felsic and intermediate tuffaceous rocks. The mineral grains have angular to subangular shapes, and layering is defined by a subparallel concentration and alignment of mafic minerals. Quartz and plagioclase are the major minerals present; however, epidote and biotite constitute up to 30% of the rock. Carbonate, 1-3%, occurs as 0.10-0.15 mm crystals that form irregular aggregates up to 1 mm that are elongated parallel to layering. Up to 1% anhedral tourmaline (var. schorl) and anhedral to cubic pyrite, less than 1%, are also present. Epidote and/or quartz ± carbonate ± opaque minerals form 0.1-10 mm pods and lenses elongated parallel to layering and probably represent lithic clasts.

This rock is distinguished from the intermediate tuff in hand specimen by slightly finer grain size, a browner tone, and thinner layers. Polycrystalline feldspar (± quartz) porphyroblasts that appear as small white specks in the intermediate tuffaceous rock are not common in the intermediate volcaniclastic siltstone.

Chloritized Mafic Rocks (unit 4, Fig. 3)

Chloritized mafic rocks were mapped south of the mine road on the Mine Peninsula and in a narrow band north of base line 14 + 25 (Fig. 3); the latter is a gabbroic dyke. Two units of chloritic rocks south of the mine road are separated by thin units of felsic to intermediate volcaniclastic rocks. These rocks are generally very fine grained, but crystals and crystal aggregates may exhibit considerable variability from average grain sizes of 0.02 mm up to 3 mm in diameter. The composition ranges from primarily chlorite with only small amounts of very fine grained epidotized plagioclase, carbonate, quartz and sericite, to a mafic schist that is composed mostly of tremolite-actinolite pseudomorphing pyroxene, epidotized plagioclase, epidote and carbonate. Trace amounts of pyrite are common in anhedral to euhedral crystals up to 0.5 mm. Opaque oxide minerals rim pyrite

in places or form very fine grained streaks and anhedral crystals.

Relict textures in rocks of unit 4 north of base line 14 + 25N and some rocks in the lens of unit 4 south of the mine road indicate that they may have been derived in part from gabbroic rocks. Reworked tuffaceous material appears to have been the original rock in other sections. Other portions of this unit appear to have been derived from volcaniclastic rocks.

Foliation is well developed and is defined by the alignment of streaks of mafic minerals and the elongation of quartz mosaics and some amphibole and plagioclase crystals. This is probably not the regional schistosity, but a product of a strong cleavage superimposed on the schistosity (see 'Structure'; see also Fig. 9).

The southern part of this unit (4b) contains only rare primary features and is generally more strongly foliated than rocks from the outcrop areas of unit 4a in the vicinity of the Main Zone.

The chloritized rocks south of the mine road (unit 4), apparently derived from reworked tuffaceous and other volcaniclastic material, are probably stratigraphically equivalent to the poorly exposed clastic rocks (unit 2) along strike to the west in the Ruby Lake area. The chloritic nature of these rocks is probably related to both alteration associated with the mineralization and intense deformation. Further studies of these chloritic rocks are required to ascertain original lithologies.

INTRUSIVE ROCKS

'Knotted' gabbro (unit 5, Fig. 3)

POIKILITIC 'KNOTTED' GABBRO (unit 5a, Fig. 3).

'Knotted' gabbro is a distinctive fine- to medium-grained, dark green weathering gabbro containing 15-60% hornblende aggregates that weather to produce a surface with 'knotted' relief. It occurs in the northeastern part of the map area (Fig. 2, 3). The knots consist predominantly of 2-7 mm hornblende crystals that can occur with 0.1-0.5 mm plagioclase laths and epidote pseudomorphs after plagioclase. The groundmass consists of very fine grained epidote (6-35%), hornblende (5-15%), plagioclase (4-8%), carbonate (5%), tabular biotite (2-7%), fine grained chlorite (0-15%), polygonal quartz (0-2%), and opaque iron oxide minerals (0-5%) in elongate streaks up to 0.05 x 0.75 mm.

MICROPHYRIC GABBRO (unit 5b, Fig. 3)

The fine grained gabbro (unit 5b, Fig. 3) exposed north of the decline is microphyric with a variable phenocryst content. In one sample (TL-722.1), hornblende (5%) forms optically continuous areas up to 3 mm across that are disrupted internally and at crystal boundaries by chlorite ± quartz ± biotite, and 0.7 mm anhedral to subhedral crystals. Another sample (TL-691.1) contains 40% anhedral, subophitic, polycrystalline clinopyroxene up to 3 mm across that has been altered by epidote and biotite.

The 0.7 mm-sized groundmass contains tabular intergrowths of chlorite (15%), epidote (15-35%) pseudomorphing plagioclase and occurring as subhedral crystals and very fine grained aggregates, and anhedral carbonate (1%). In addition, sample TL-722.1 contains 17% very fine grained, interstitial plagioclase, 2% subhedral pyroxene associated with hornblende and chlorite, and 1% biotite associated with chlorite. Sample TL-691.1 contains fibrous actinolite (5%), pyrite (3%), and quartz (1%) in both interstitial aggregates and associated with chlorite. On the basis of similarities in mineralogy and texture, and despite the finer grain size, this microphyric gabbro is considered to be related to the 'knotted' gabbro (see also 'Geochemistry').

Gabbroic Complex

The gabbroic complex covers the southwestern part of the Tartan Lake area (Fig. 2, 3). This gabbroic complex includes fine- and medium-grained gabbros that have been intruded by aphanitic to fine grained gabbro and feldspar-porphyritic felsic dykes.

MEDIUM GRAINED GABBRO (unit 6a, 6b, 6c, Fig. 3).

This gabbro is apple green to dark green and consists primarily of amphibole, epidote and plagioclase with minor sericite, carbonate, chlorite, and pyrite. The amphiboles, ranging from 40 to 70%, are tremolite-actinolite and uralite pseudomorphs after pyroxene that are up to 3 mm (average 2 mm) in diameter. Tremolite-actinolite forms fibrous aggregates but also occurs as subhedral prisms to anhedral crystals. Smaller prisms of tremolite-actinolite may be included in larger crystals, and up to 2% hornblende may be present as anhedral crystals. Epidote, 20-40%, forms subhedral to anhedral crystals, 0.05-0.07 mm, and very fine grained aggregates that are interstitial to amphibole. In some samples epidote, which can be finely intergrown with plagioclase and carbonate, pseudomorphs plagioclase. Epidotized plagioclase, 10-15%, is present in fine grained intergrowths with epidote and sericite and as relict subhedral crystals. Carbonate or amphibole may form minute overgrowths on plagioclase. Most plagioclase crystals are very fine grained, but form optically continuous areas up to 1.4 mm across. Shreddy aggregates of sericite compose 20% of one sample, but more commonly form less than 2% of the rock as an alteration product of plagioclase. Anhedral carbonate (1%), anhedral pyrite and/or tourmaline (1%), and secondary chlorite associated with pyrite and tourmaline (up to 1%), are minor secondary minerals. Local crosscutting microveinlets consisting of very fine grained epidote (± plagioclase ± carbonate) brecciate the gabbro.

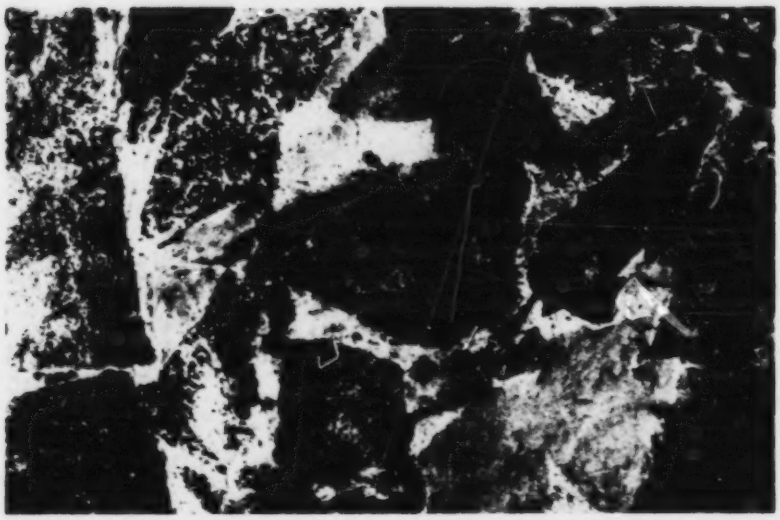

Figure 5: Igneous breccia. Clasts of medium grained gabbro and pyroxenite (dark coloured clasts). Fine grained gabbro matrix constitutes less than one per cent of the rock in this exposure; locally it constitutes more than 50% of an outcrop.

FINE GRAINED GABBRO (units 6d, 6e, Fig. 3).

This gabbro is medium to dark green and fine grained to aphanitic. It consists of plagioclase (30-65%), epidote (20-50%), chlorite (8-30%), and tremolite-actinolite (up to 20%). Accessory minerals include biotite, muscovite, tourmaline, carbonate, sphene, quartz, and pyrite. Epidote forms very fine grained aggregates and 0.05 mm crystals partially to totally pseudomorphing plagioclase. Subhedral plagioclase, up to 0.6 mm, average 0.35 mm, is obscured and pseudomorphed by epidote. Chlorite forms anhedral tabular intergrowths. Tremolite-actinolite, where present, occurs as mono- and polycrystalline poikiloblasts. Up to 7% anhedral to euhedral disseminated pyrite, average 0.1 mm, up to 1.5 mm, is commonly associated with carbonate and/or chlorite. Subhedral biotite, and anhedral carbonate are common accessory minerals. Muscovite, up to 5%, forms anhedral crystals and sericitized feldspar crystals. Subhedral tourmaline (up to 3%), very fine grained anhedral quartz associated with epidote (up to 1%), and euhedral sphene (up to 1%), may also be present.

IGNEOUS BRECCIA (unit 6f, Fig. 3).

A distinctive igneous breccia (Fig. 5) is composed of medium grained angular gabbroic clasts in a fine grained to aphanitic gabbroic matrix. It is a minor component of the southeastern part of the area shown in Figure 3, but it extends to the south and east as part of a large area of igneous breccia (Fig. 2).

ALTERED GABBRO (units 6g, 6h, 6i, Fig. 3).

Areas of well developed schistosity in the southeastern quadrant (South Block) of Figure 3 are characterized by a consistent zonation of altered gabbro. The rock varies from the margins to the centres of these zones, namely: (1) 'unaltered' medium grained gabbro, (2) finer grained gabbro, (3) non- to weakly schistose chloritic gabbro with pink carbonate blastesis, (4) non- to weakly schistose chlorite-carbonate-quartz altered rock; and (5) chlorite-carbonate-quartz-muscovite ± fuchsite ± tourmaline ± pyrite schist (Fig. 7). The non- to weakly schistose chlorite-carbonate-quartz altered gabbro includes a brown weathering chloritic rock that is the carbonatized equivalent of massive fine grained gabbro.

Chlorite, (5-55%, average 20-30%), occurs in very fine grained (0.05-0.15 mm) anhedral aggregates that are locally intimately intergrown with sericite. The chlorite aggregates may be interstitial to plagioclase or epidote pseudomorphs after plagioclase. Chlorite ± sericite aggregates also commonly form bands or lenses and define schistosity. Muscovite forms very fine grained (0.05 mm), tabular and scaly aggregates that may be irregularly oriented or define schistosity. Muscovite, including the variety fuchsite, may constitute 10-50% of the schist, but generally is less than 10 to 15%. Carbonate, highly variable from less than 1% to 60%, forms anhedral crystals and polycrystalline aggregates; grain size ranges from 0.02 to 1 mm. Quartz grains, 2-40%, that average 0.1 mm or less in diameter, may be associated with very fine grained plagioclase, and ranges from anhedral to rounded to prismatic. Tourmaline, 1-3%, occurs as irregularly distributed, euhedral prismatic crystals, 0.03-1.8 mm. Anhedral to cubic pyrite, 0.05-0.35 mm, is present in variable amounts, but generally averages 1-3%. The cubes are associated with chlorite and in many places the larger cubes clearly overgrow the micaceous schist and incorporate chlorite as inclusions. Rarely, the pyrite crystal faces have non-perpendicular interaxial

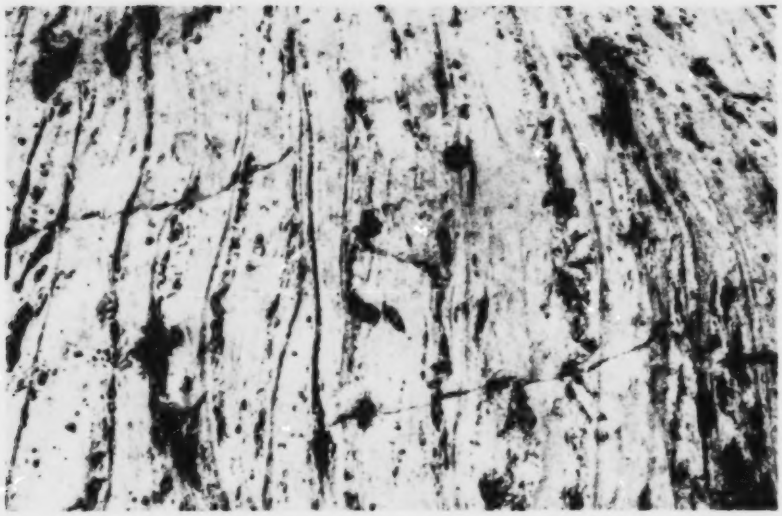

Figure 6: Photograph of pillow lavas, Mine Peninsula.

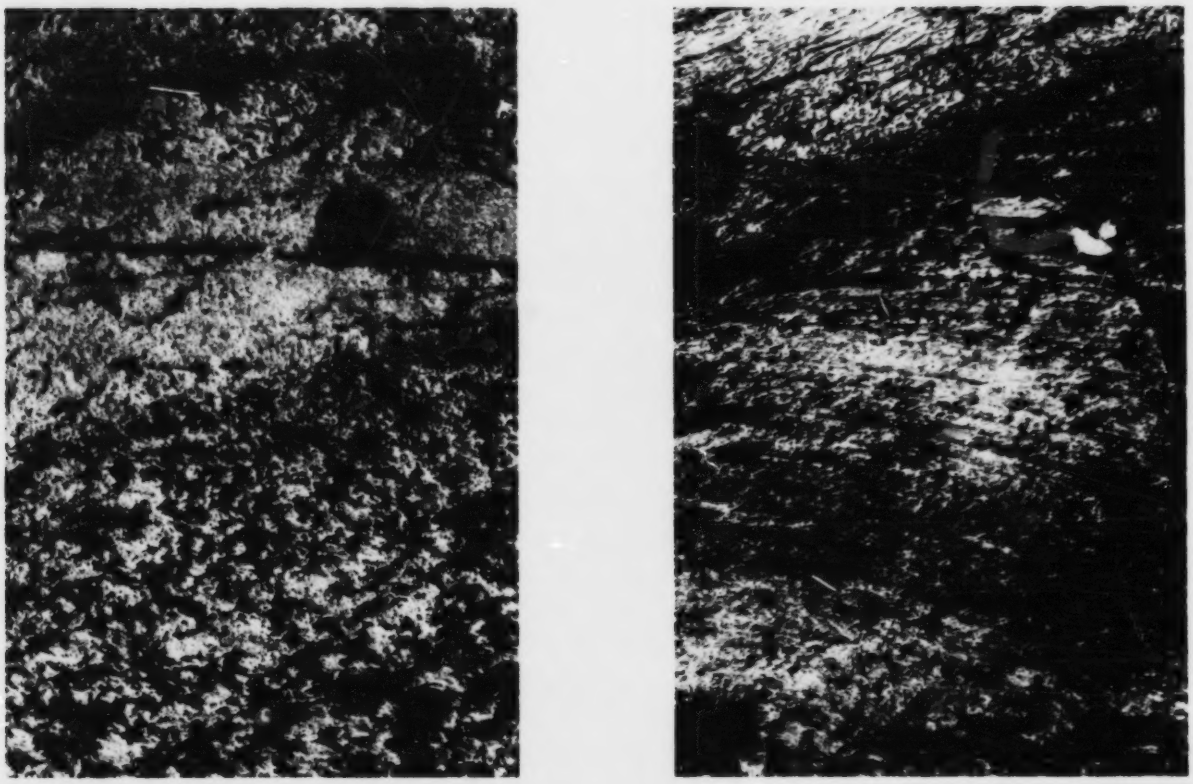

Figure 7: a) Chloritic fine grained gabbro (under lens cap) and non- to weakly schistose chlorite-carbonate-quartz rock; b) same as (a).

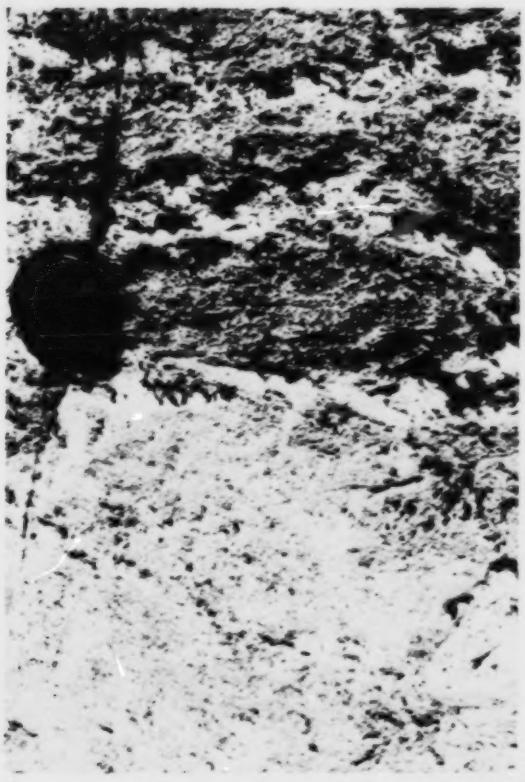

Figure 7: c) non- to weakly schistose chloritic gabbro with pink carbonate blastesis (above) and weakly schistose chlorite-carbonate-quartz altered rock (below); d) chlorite-carbonate-quartz-muscovite ± fuchsite ± tourmaline ± pyrite schist.

angles resulting from stress. Apatite, in 0.07 mm crystals, occurs in only trace amounts.

Schistosities are defined by the alignment of micas. In the less altered rocks, some of the mafic minerals and opaque iron oxide minerals are aligned parallel to schistosity and have been wrapped around plagioclase crystals. Some plagioclase has been granulated and some relict crystals are brecciated with very fine grained sericite infilling the fractures. Crenulation cleavages oblique to the earlier schistosity produce kinking of micas locally in the schist (Fig. 7, 8); other minerals do not readily show the effects of this crenulation cleavage.

Ruby Lake Gabbro (unit 7, Fig. 3)

Gabbroic rocks, although less common in the western half of the map area, occur as minor sills and dykes. Because of their uncertain genetic relationship with mafic intrusive rocks in the eastern part of the map area, these sills/dykes are distinguished here as 'Ruby Lake gabbro'. They are probably related to other mafic magmas in the area (see 'Geochemistry').

The Ruby Lake gabbro consists of 50% hornblende, 20% epidote interstitial to hornblende, 20% plagioclase in fine grained lenses and subhedral, partly epidotized crystals, and 10% opaque iron oxide minerals in anhedral streaks. The average grain size is 0.5 mm. The gabbro has a moderate foliation that is defined by streaks of oxide minerals, plagioclase (± quartz?) and, rarely, the alignment of epidote and hornblende.

A very fine grained (0.1 mm) variety of the Ruby Lake gabbro has phaneritic pyroxene and feldspar.

Porphyritic Felsic Dykes (unit 8, Fig. 3)

Feldspar ± quartz porphyry intrudes the volcanic and sedimentary succession and mafic intrusive rocks to form discontinuous dykes/sills. These felsic intrusive rocks are pink to creamy white and generally contain 20-25% feldspar and/or quartz crystals, up to 8 mm, in a fine grained to aphanitic felsic matrix. There is textural and compositional variability among the porphyritic felsic rocks within the map area.

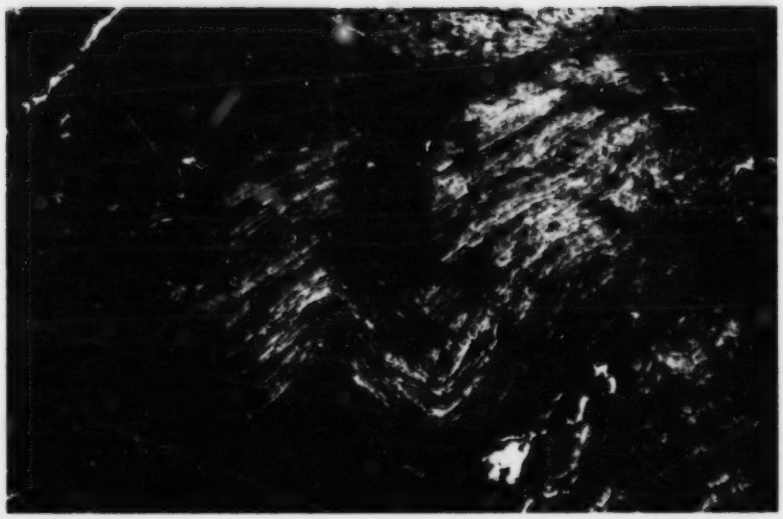

a)

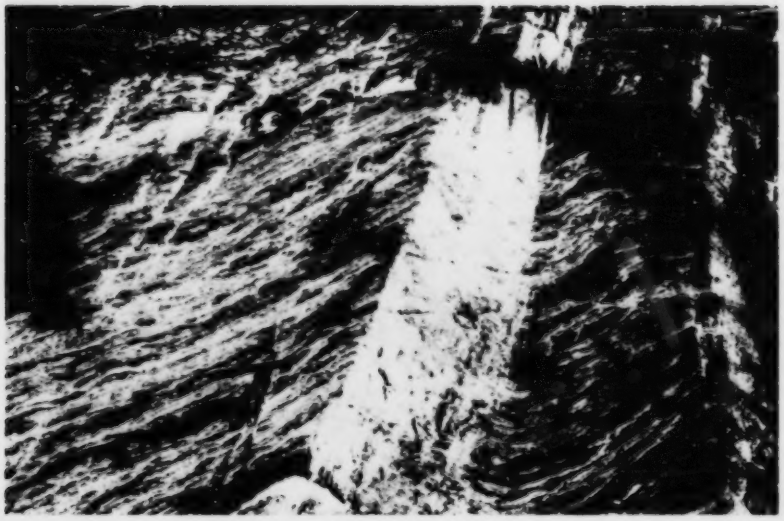

b)

Figure 8 *a, b: Crenulation cleavages and kink-folds in chlorite-quartz schists at South Zone, Tartan Lake.*

MINE PENINSULA

Feldspar ± quartz porphyry resembles intermediate tuff, but locally crosscuts stratigraphic units and intrudes mafic intrusive rocks. Plagioclase phenocrysts, 10-15%, and quartz phenocrysts, up to 10%, are up to 3.5 mm in length. In general, felsic dykes intruding the gabbroic rocks in the northeast part of the map area contain about 5% less plagioclase and quartz phenocrysts than elsewhere. Plagioclase is moderately saussuritized and sericitized. Less than 1% hornblende and trace amounts of apatite are present in some samples. The groundmass is very fine grained (0.02 mm) and comprises quartz + plagioclase + chlorite + epidote ± hornblende ± biotite + partly hematized opaque iron oxide minerals. Alteration includes sericitization, carbonatization, chloritization, tourmalinization, and pyritization. Sericite, up to 10%, overgrows plagioclase. Carbonate, up to 20%, occurs as 0.2 mm crystals and crystal aggregates. Chlorite, up to 25%, is interstitial to phenocrysts and may have very minor associated biotite. Tourmaline (var. schorl), up to 10%, forms very fine grained, disseminated, subhedral to euhedral, prismatic crystals. Pyrite, in variable amounts up to 10%, forms secondary cubic crystals that contain inclusions of muscovite and plagioclase.

SOUTH BLOCK

Feldspar porphyry is found at the northern and western edges of the South Block (Fig. 3). Saussuritized plagioclase phenocrysts constitute 35-50% of the rock, and intense epidotization may obscure additional plagioclase. The crystals are subhedral to euhedral with average phenocryst sizes of 1-2 mm. Some phenocrysts have been brecciated *in situ*. Epidote, up to 30%, commonly replaces the cores of feldspar phenocrysts and mimics the outline of the crystals. The groundmass has an average grain size of 0.2 mm, and comprises quartz + plagioclase + epidote + biotite ± chlorite ± iron oxide minerals. Relict crystal shapes indicate that at least part of this groundmass assemblage, particularly the epidote-rich areas, pseudomorphs plagioclase. Very fine grained epidote microveinlets crosscut the porphyry and are commonly accompanied by very fine grained pyrite and minor tourmaline.

RUBY LAKE AREA

Feldspar ± quartz porphyry sills/dykes intrude sedimentary and volcanic rocks. Although crosscutting intrusive relationships are observed in places, these rocks locally resemble tuffaceous rocks. Subhedral to euhedral plagioclase phenocrysts are up to 3 mm, but have an average length of 0.7 mm. Some phenocrysts are lightly to heavily altered to sericite, chlorite and epidote; both mono- and polycrystalline forms are present. Porphyroblastic overgrowth is indicated by well defined clear feldspar rims surrounding altered plagioclase crystals. Anhedral quartz phenocrysts, 0-7%, are generally 0.5-1.5 mm in diameter. Most quartz phenocrysts are monocrystalline; however, polycrystalline forms that are crosscut by mosaics of quartz and/or carbonate do occur. The groundmass (55%) consists mainly of very fine grained (0.02 mm) anhedral quartz and plagioclase with interstitial muscovite, but also contains fine grained irregular areas consisting of epidote, biotite, chlorite, and disseminated opaque iron oxides. Muscovite, 5-25%, occurs interstitial to feldspar phenocrysts, as well as at the crystal edges and as minute inclusions in feldspar. Muscovite commonly bends around phenocrysts and creates a local foliation. Carbonate averages 15% where present, and forms fine grained anhedral crystals, crystal mosaics and fine grained lenticular aggregates up to 1.5 x 8 mm.

The feldspar and quartz phenocrysts are randomly oriented and some have been brecciated *in situ* with the resulting microfractures infilled by quartz ± carbonate ± muscovite ± epidote. The groundmass is usually non- to weakly foliated. Wherever muscovite is abundant, the foliation is well defined and a late cleavage yields crenulations oblique to the muscovite foliation.

Coarse grained feldspar porphyry dykes are similar to those described above, except that the plagioclase phenocrysts are coarser grained and have an average grain size of 2.5 mm but range up to 8 mm.

Some dykes/sills are notably sheared on outcrop. In these rocks, plagioclase phenocrysts are rarely preserved. Quartz (5%) occurs in grains and rounded to lensoidal mosaic aggregates with an average size of 0.5 mm. Actinolite (up to 5%) can form fibrous aggregates up to 5 mm that are overgrown by biotite. The groundmass is well foliated, commonly streaked due to a rough alignment of mafic minerals, and appears to flow around phenocrysts. In the pressure shadows of quartz phenocrysts, mosaics of carbonate crystals are developed and the grain size increases. Pyrite, possibly intergrown with pyrrhotite, is generally present in amounts up to 3%. It is associated with quartz mosaics or disseminated as cubic to irregularly shaped grains 0.2 mm in diameter.

FELSIC INTRUSIVE VS. EXTRUSIVE ROCKS

It is difficult to distinguish feldspar porphyry intrusive rocks from felsic to intermediate tuffs and volcaniclastic rocks where field relationships with adjacent rock units are unclear or not exposed. Superimposed mylonitic fabrics add to the difficulties in separating these rock types in the field. Rocks that are known to be tuffaceous by field relationships contain some crystals that have been broken irregularly and fragments cannot be visually pieced back together. Lenticular lithic clasts have different compositions from the matrix and a very fine internal grain size. There is usually a large variation in the size of crystals that are larger than the matrix. Compositional and grain size differences may distinguish laminae.

Intrusive relationships were observed for a number of feldspar porphyry dykes. In thin sections of these dykes the fine grained granular groundmass appears to flow around randomly oriented phenocrysts, but pressure shadows are common adjacent to the larger crystals. Some of the phenocrysts have been brecciated *in situ* and the broken fragments are usually less than 1 mm apart, but are separated by granular quartz and feldspar or by mosaics of carbonate ± quartz ± plagioclase ± chlorite ± epidote.

STRUCTURE

As noted previously this project was designed to provide a lithologic map as a basis for undertaking a detailed structural analysis of the deposit. Since the detailed structural analysis is being undertaken as a M.Sc. thesis project at the University of Saskatchewan, this account is presented simply as a documentation of observations made during the mapping program.

THE MINE PENINSULA

Planar Fabrics

The earliest recognized deformation (D_1) produced a well developed regional schistosity (S_1) that is parallel or closely parallel to compositional layering in the metasedimentary rocks east of the mine portal and in the northwest corner of the Mine Peninsula (15+00N to 20+00N/1+00E to 5+00W). Locally, it can be demonstrated that S_1 is axial planar to F_1 isoclinal folds.

Bedding has not been positively identified within the map area. In a number of exposures compositional layers of psammitic and pelitic material probably represent deformed beds, but in other exposures the psammitic layers can be seen to be transposed beds. In addition, felsic tuff layers within more mafic schists exhibit thickening of hinges and thinning of limbs on F_1 folds (e.g. 16+00N/3+00W). Although all compositional layers of D_1 age (S_0) were recorded as bedding planes, it should be noted that many are of tectonic rather than depositional origin (Fig. 9). Younger compositional layers resulting from later deformational events are also present.

Folds

FIRST PHASE (F_1)

Folds related to the D_1 deformation were rarely observed, but it is postulated that a major F_1 fold exists in the area. F_1 minor folds are most easily discernible in the interbedded rhyolitic and intermediate tuffaceous rocks north of base line 14+25N. These are tight to isoclinal

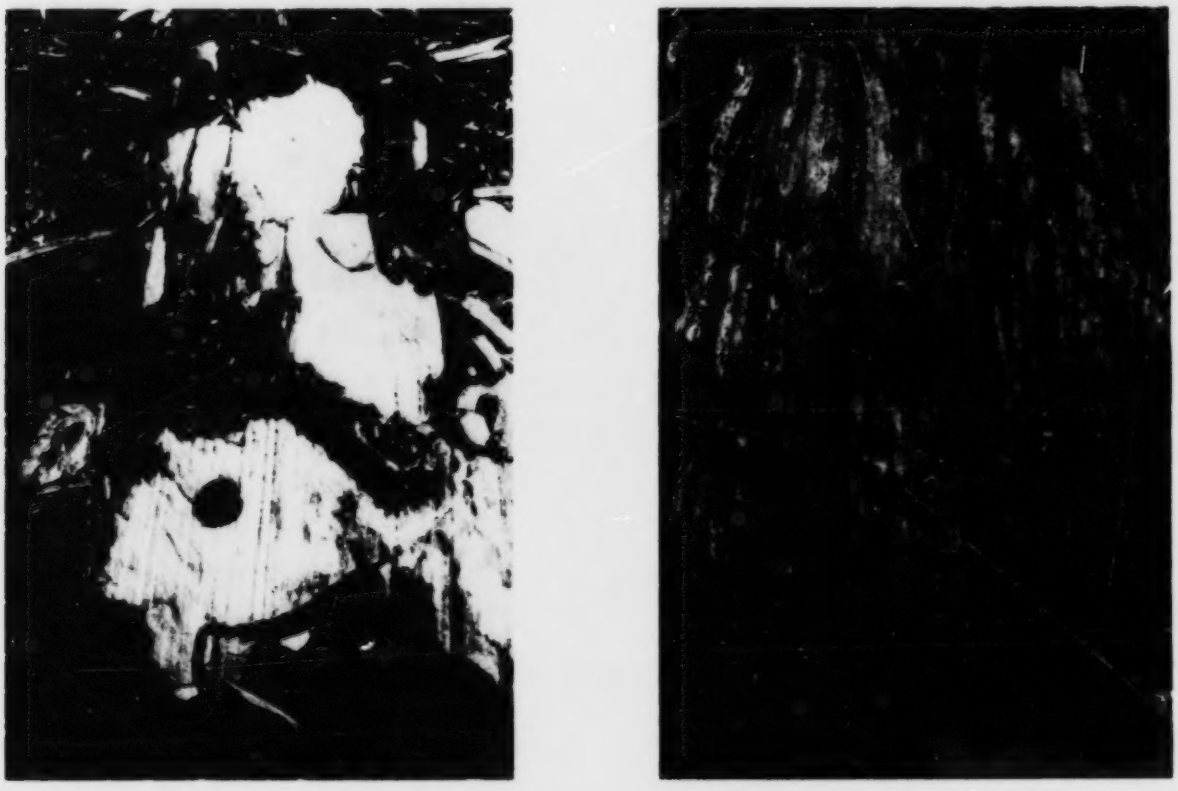

Figure 9 *a,b,c: Compositional layering developed in mafic volcanic rocks (unit 4) immediately north of the Main Zone, Tartan Lake Mine. Note layer discontinuity in (c).*

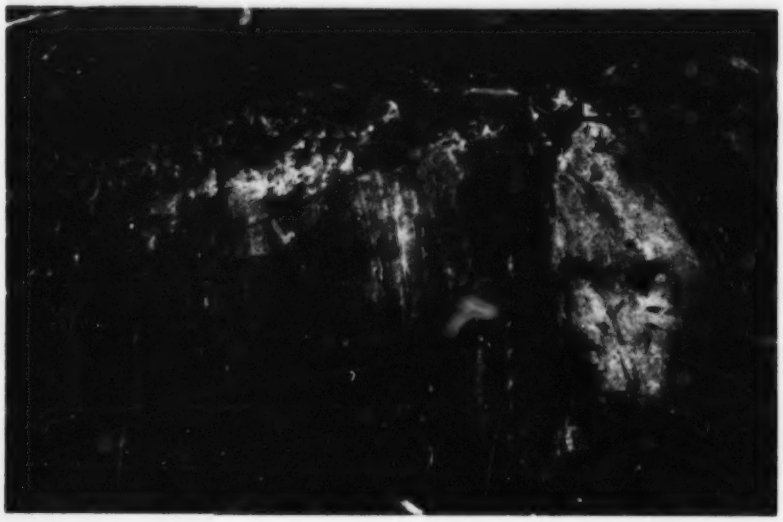

Figure 9c

folds defined by rhyolitic tuff layers (Fig. 10) and S_1 is axial planar to the folds. Although some of the F_1 minor folds were noted to have eastward plunges, no attempts have been made to establish the attitude of the major structure.

The flattening of pillow lavas is considered to be a D_1 event since the pillows appear to be flattened within or close to the plane defining S_1 (see Fig. GS-11-8, Peloquin et al., 1986, p. 64).

The outcrop pattern of pyroxene-phyric pillow lavas in two separate lenses with a central core of aphyric pillow lava (Fig. 3) is determined to some extent by late faults, but it appears also to be controlled by a major early fold structure. Minor folds do not support the presence of an F_2 antiform in the area, therefore the pyroxene-phyric flow outcrop pattern is tentatively explained as a result of the modification of an F_1 structure. The variable plunge on F_2 minor folds in the area north of base line 14 + 25N can also be interpreted as refolding of an earlier major F_1 structure by F_2.

SECOND PHASE (F_2)

The second deformation event (D_2) produced some of the more prominent structural features in the area. Minor fold structures related to this event occur throughout the area, but are most abundant in the greywacke north of base line 14 + 25N and east of the Crusher Fault.

Minor folds (F_2) that deform S_1 and S_0 (Fig. 11), and have a well developed axial planar cleavage are present throughout the map area. The D_2 minor folds are characterized by deformation of S_1 into open to closed S- and Z-type folds with vertical to steeply dipping axial planar cleavages (Fig. 11, 12). Although plunges on the

Figure 10 *a: F_1 fold defined by rhyolite tuff layer in intermediate tuffaceous rock, b) F_1 folds in rhyolite tuff modified by later cleavage.*

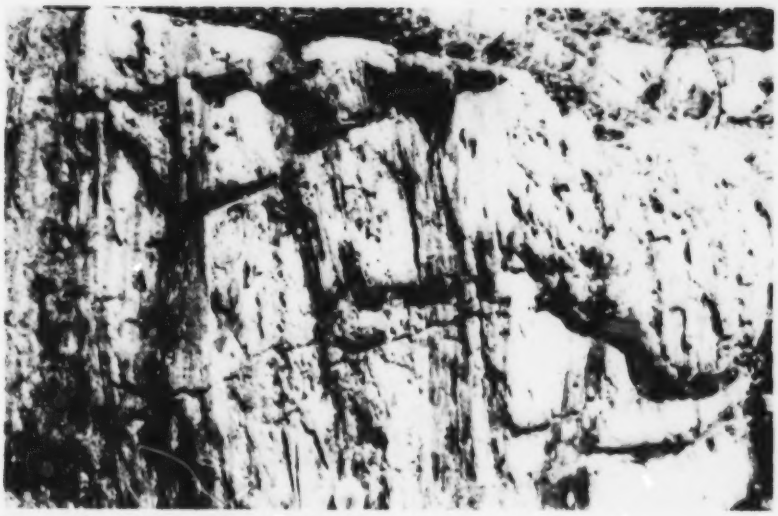

Figure 10 *b: F_1 folds in rhyolite tuff modified by later cleavage.*

Figure 11 *a,b,c: F_2 minor folds in the Tartan Lake area. Note local transformation of S_1 into a younger (S_2) compositional layering.*

a)

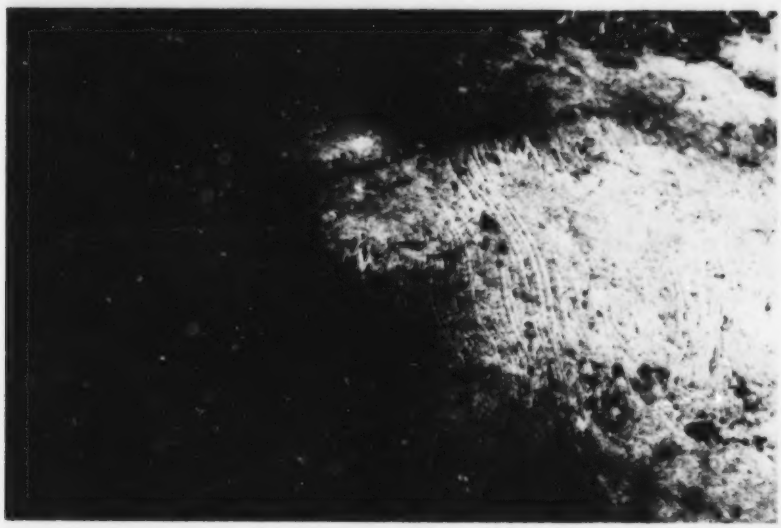

Figure 11b:

Figure 11c

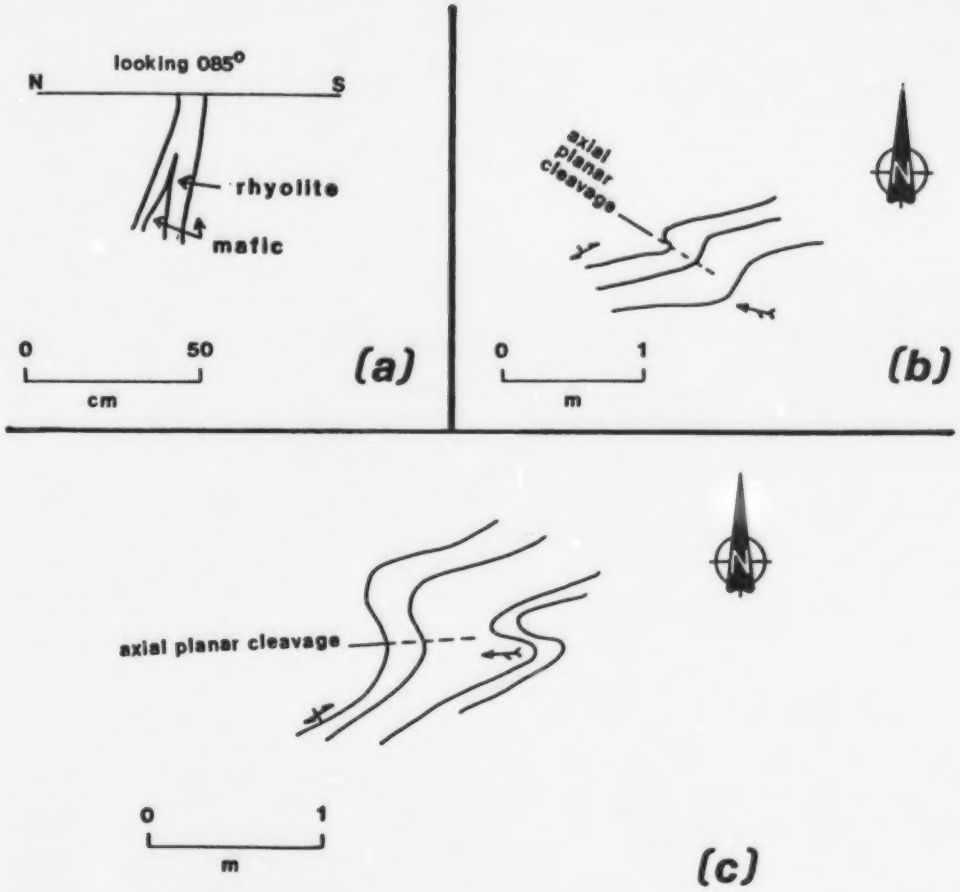

Figure 12: a) Sketch of F_1 minor fold in Figure 11a; b and c) Sketches of F_2 minor folds.

hinges of the F_2 minor folds are variable they have an overall plunge to the west of approximately 50°. In the northern part of the area these minor folds define an open west-plunging F_2 major synform (Fig. 13). A similar F_2 synform with an axis somewhere east of the outcrop area is postulated for the metasedimentary rocks east of the Crusher Fault.

THIRD PHASE

The youngest penetrative deformation event (D_3) recognized in the area produced box-type folds with amplitudes of tens to hundreds of metres; it postdates alteration and mineralization of the gabbro in the South Block. These folds are characterized by gentle to sharp deflections of schistosity, crenulation of schistosity and the local development of a strain-slip (crenulating) cleavage that ranges in strike from NNE to NNW and has dips that range from steep to vertical (Fig. 8, 14).

Post-F_2(?) Cleavage

In the area between the Main Zone and the large area underlain by pyroxene-phyric pillow lavas (i.e., south of base line 14+25N), S. Peloquin (field notes, 1986) recorded a late near vertical cleavage that appears to parallel layering and intersect the schistosity at an angle of 10-15° (Fig. 15). Locally, the compositional layer is interpreted as a transposition of earlier layering by shearing along this cleavage (cf. Fig. 9, 11, 15). The true relationship between these fabrics was not resolved. However, this cleavage does not appear to be the axial planar cleavage of F_2 or F_1 folds (Fig. 15, 12), and appears to be most common in the area immediately north of the Main Zone and its possible extension to the west. This fabric approximates the plane of a postulated fault through the area of the Main Zone and could represent a mylonitic fabric related to faulting and shearing.

The timing of this cleavage is problematic. It appears to be younger than the F_2 axial planar cleavage, but its age relationships were not specifically investigated. It is either a late D_2 event or a younger and separate deformational event.

This late D_2 (post-F_2) structural event could be the same age as a "shear foliation". Locally schistose zones, often denoted by chloritic schist layers, are characterized by a vertical to subvertical cleavage in a zone several centimetres thick (see Fig. 16). Field observations indicate this schist may have developed as a result of minor movements in a fault zone.

Faults

A number of fault zones were detected during routine mapping (Fig. 3). A number of minor (?) shear zones were also noted by S. Peloquin in field notes, but no attempts were made to trace these structures in the field.

Most of the faults north of the Main Zone range from 225 to 245° in strike and approximate the strike directions of two major structures in the South Block, i.e., the Main Zone Fault and the South Zone Fault. The Crusher Fault appears to predate the Main Zone Fault against which it terminates. A number of other regional fault structures are shown from geological data and air-photo lineaments in Figure 17.

SOUTH BLOCK

General Statement

In the early stages of this study the gabbroic rocks south of the Main Zone were considered to be significant in localizing the mineralization. Consequently, the South Block was mapped in detail in order to establish the petrographic and structural characteristics of the gabbro since it is the only mineralized lithology exposed in the vicinity of the mine, e.g., South Zone, Baseline Zone.

During the latter part of the mapping project it was recognized from detailed mapping at the South Zone that zones of alteration and/or deformation could be recognized even where they are only partly exposed, e.g., from a few tens of centimetres of rock exposed at the edge of a covered area. Consequently, the area was re-examined and in addition to the three major zones previously recognized a number of less obvious zones were identified (Fig. 18). Since a number of these zones were identified from a small segment of outcrop and the postulated zones are recessive weathering and drift covered, it is often not certain what type of zone they represent. Some appear to be zones of extensive alteration similar to the Baseline Zone, whereas others appear to be later structural features (faults?) and simple tensional fracture fillings.

Type I Alteration Zones

There are three known major zones (Fig. 18) of chloritic and carbonate rocks with quartz-tourmaline, sulphide and gold mineralization (i.e., South Zone, 5 East Zone and Baseline Zone). These zones locally have a well developed schistosity that is defined by chlorite, and contain folded and deformed quartz and tourmaline veins and large areas of randomly oriented late carbonate and quartz veins and pods; these are referred to as Type I Zones (Fig. 19, 20, 21). The 5 East Zone connects the Baseline and South Zones, but it has been deformed by later faults at its northern end that have distorted the original configuration.

Zone 4, postulated on the basis of several small exposures, occurs at right angles to the 5 East Zone near 1+00N/6+00E. This zone contains similar alteration products and deformation features as the three major

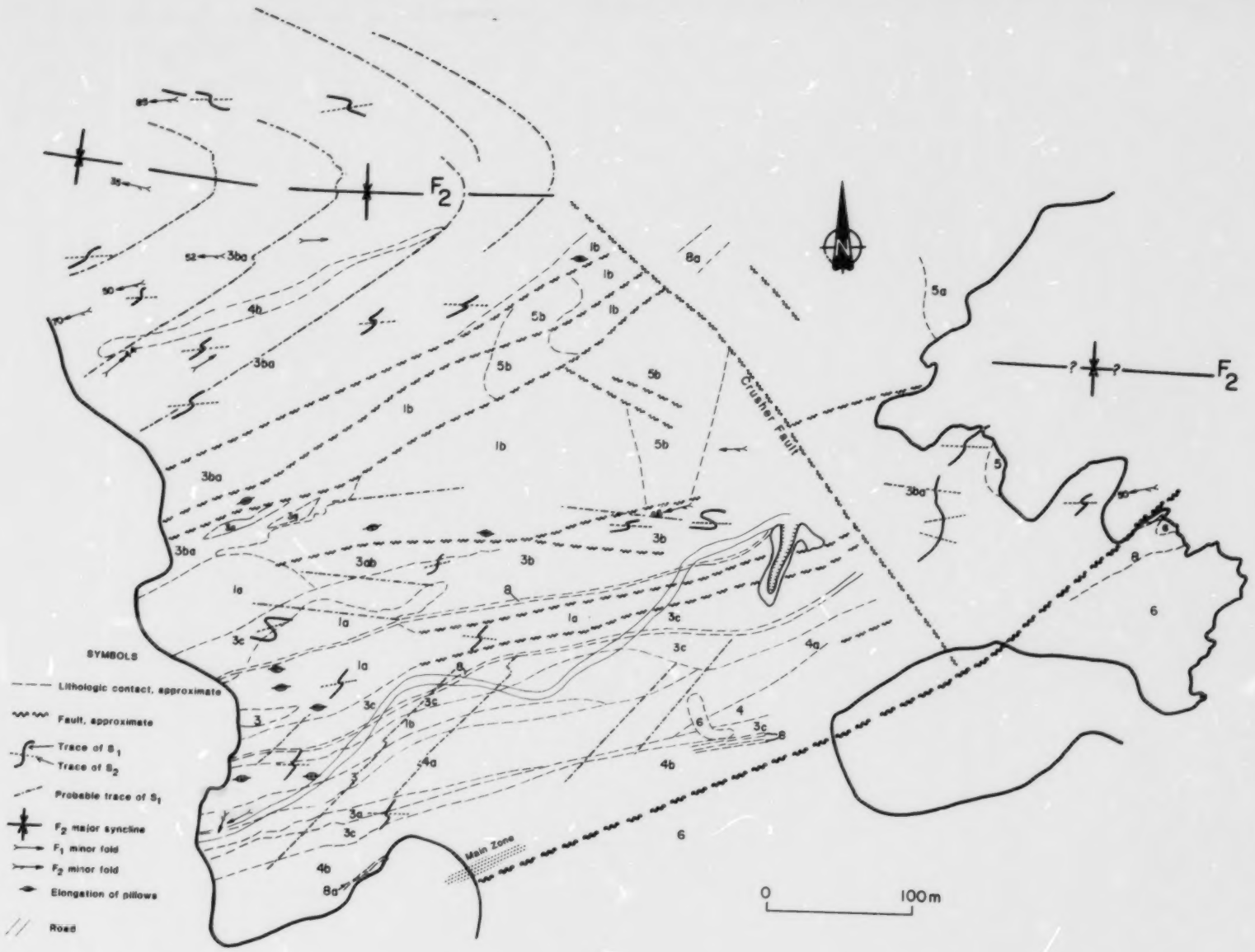

Figure 13: *Major F_2 structure reconstructed from minor F_2 fold observations. Note: north limb of major fold is probably faulted out north of F_2 fold axes shown (area was not mapped in detail).*

Figure 14: Crenulation fold in sheared and altered gabbro.

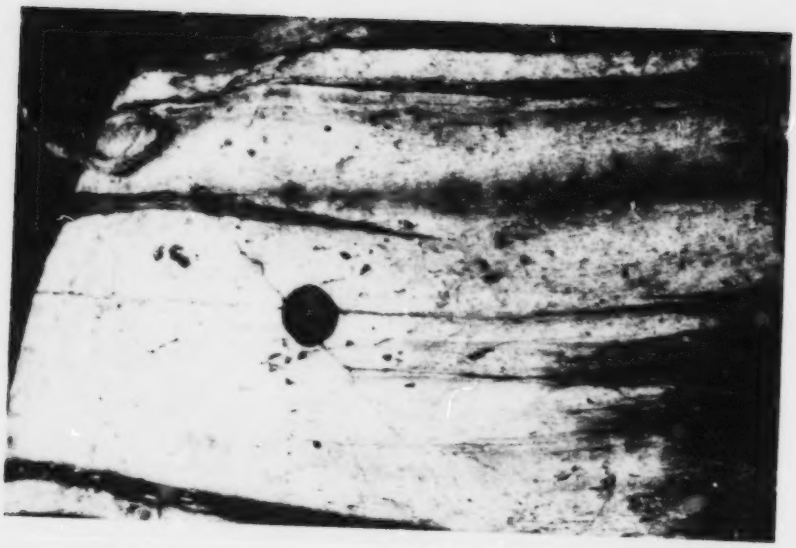

Figure 15: Rhyolitic tuff with well developed cleavage or mylonite fabric.

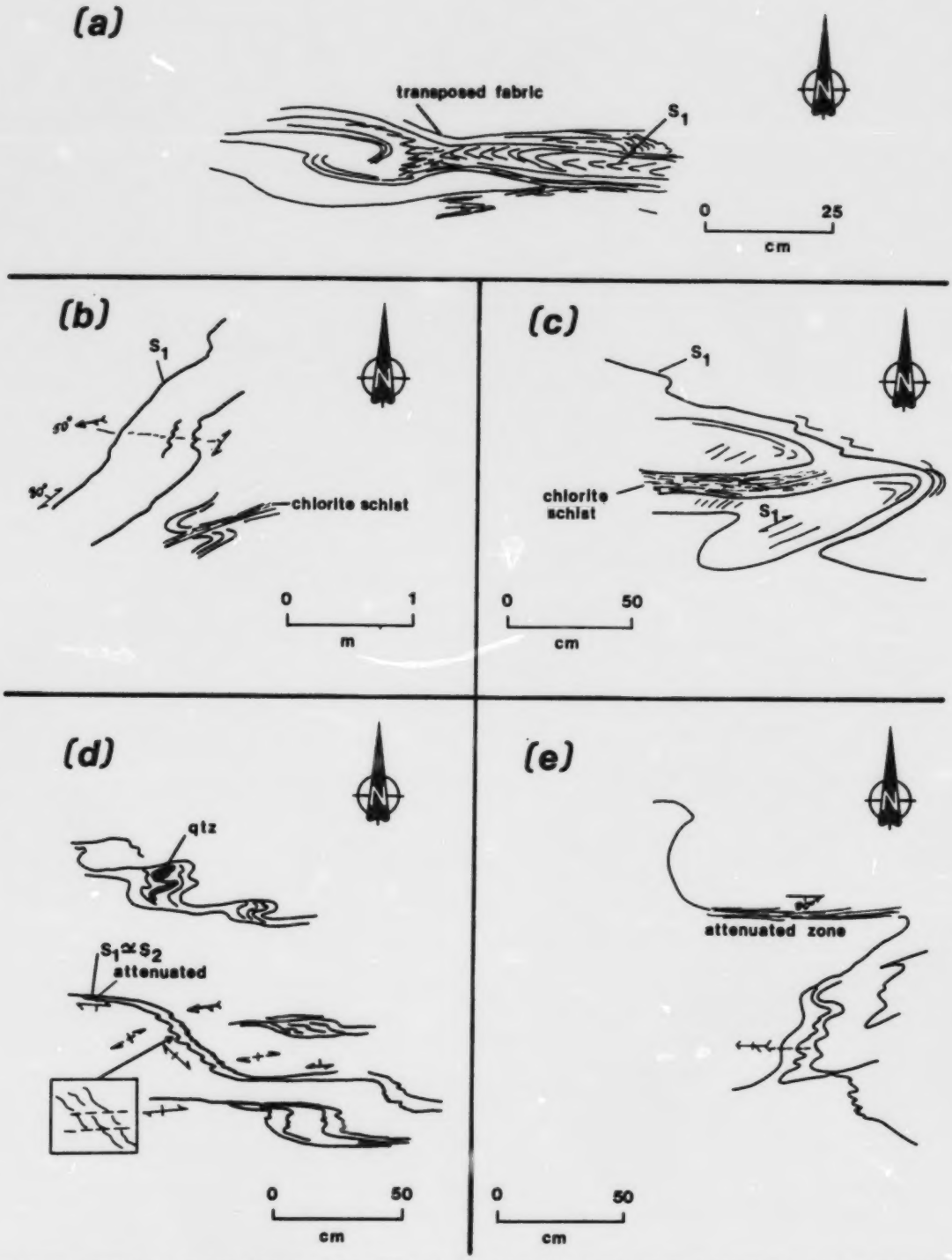

Figure 16: Minor structures in the Tartan Lake area: a) F_2 minor fold with development of zone of alteration sub-parallel to F_2 axial plane; b) Thinning of F_2 minor fold limbs in zones of alteration; c) Minor chlorite schist zone developed in core of F_2 minor fold; d) Minor chlorite schist zone developed adjacent to open F_2 minor fold; e) Transposition of S_1 into S_2(?) in shear zone.

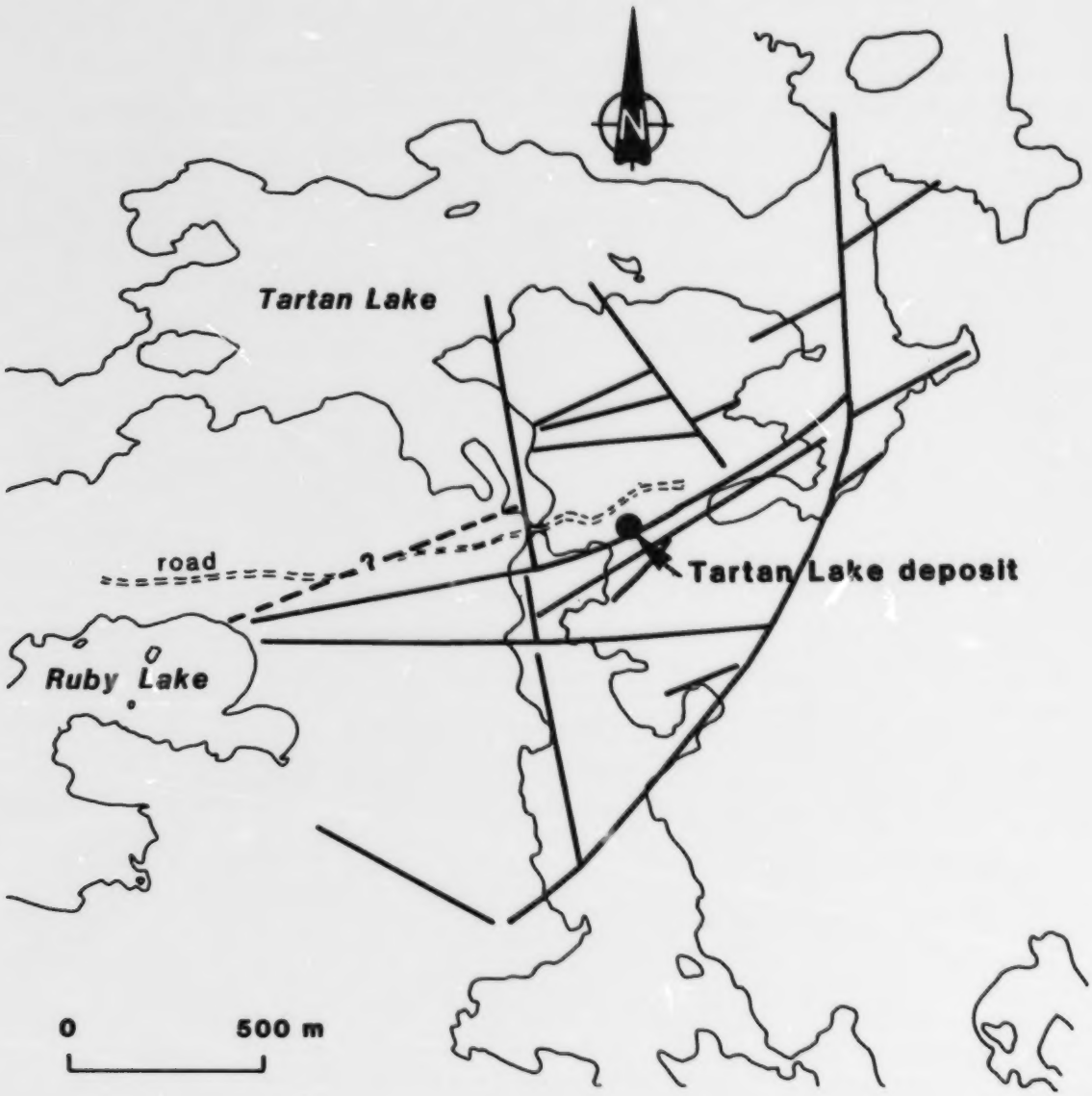

Figure 17: Major faults identified in the Tartan Lake area. Main Zone of the Tartan Lake Mine is identified by the black dot.

zones. Zones 5, 6 and 7 may be of the same age and probably underwent the same alteration as the three major zones (Fig. 18).

Type II Alteration Zones

Zones 8, 9 and 10 contain gold-bearing central quartz veins, surrounded by minor carbonate alteration; these are referred to as Type II Zones. These zones appear to be filled tension fractures that postdate the extensive alteration of Zones 1 to 3. Chlorite schists developed along the margins of the quartz veins are the result of very late shearing in the less competent rocks at the margins of the vein quartz. The quartz, carbonate and gold in these zones are considered to have been derived from the older Type I alteration zones by mobilization. Zones 11 to 15 are probably also Type II zones; however, further studies are required to establish the relative ages of each zone.

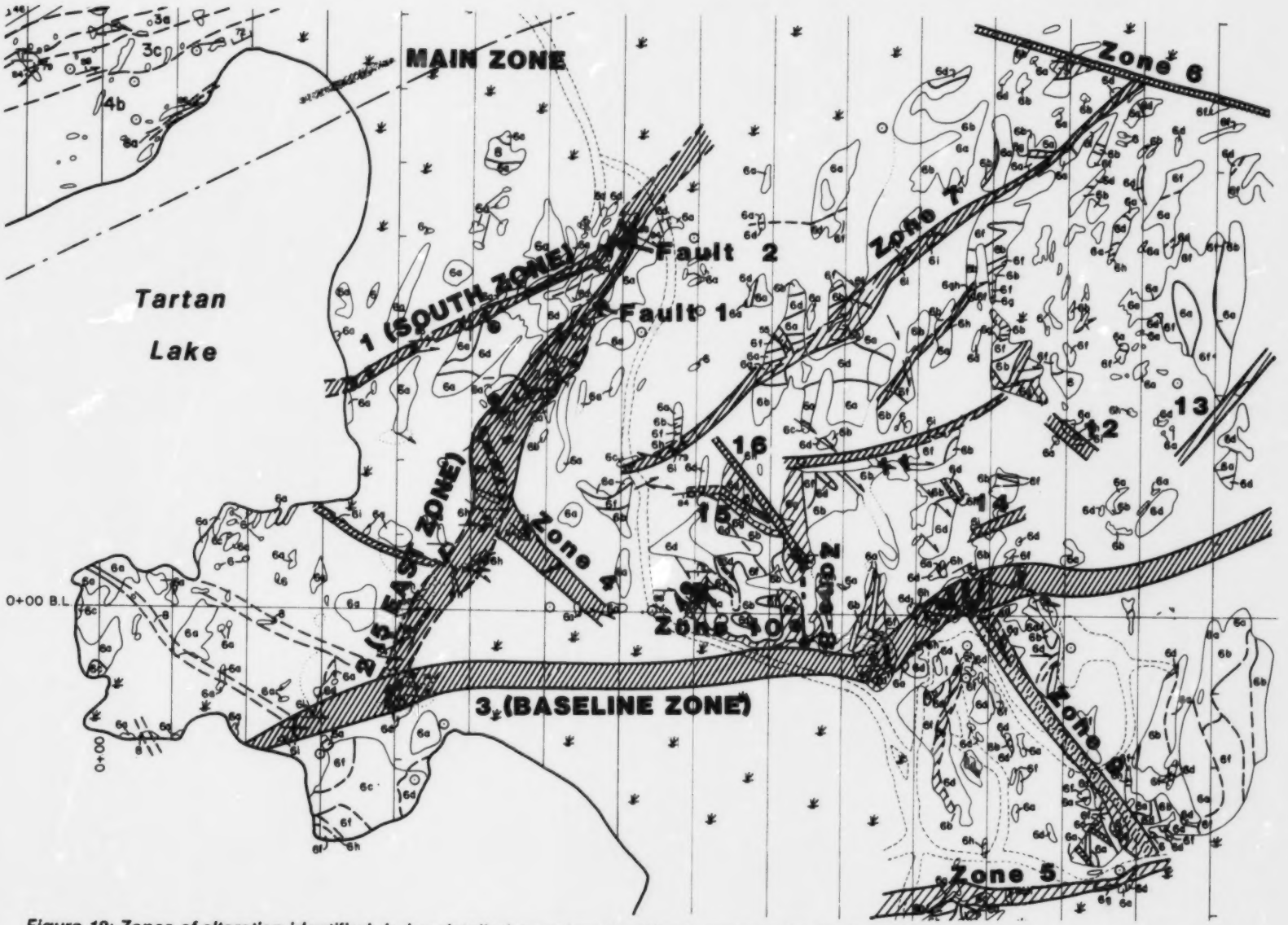

Figure 18: Zones of alteration identified during detailed mapping of gabbroic rocks in the South Block.

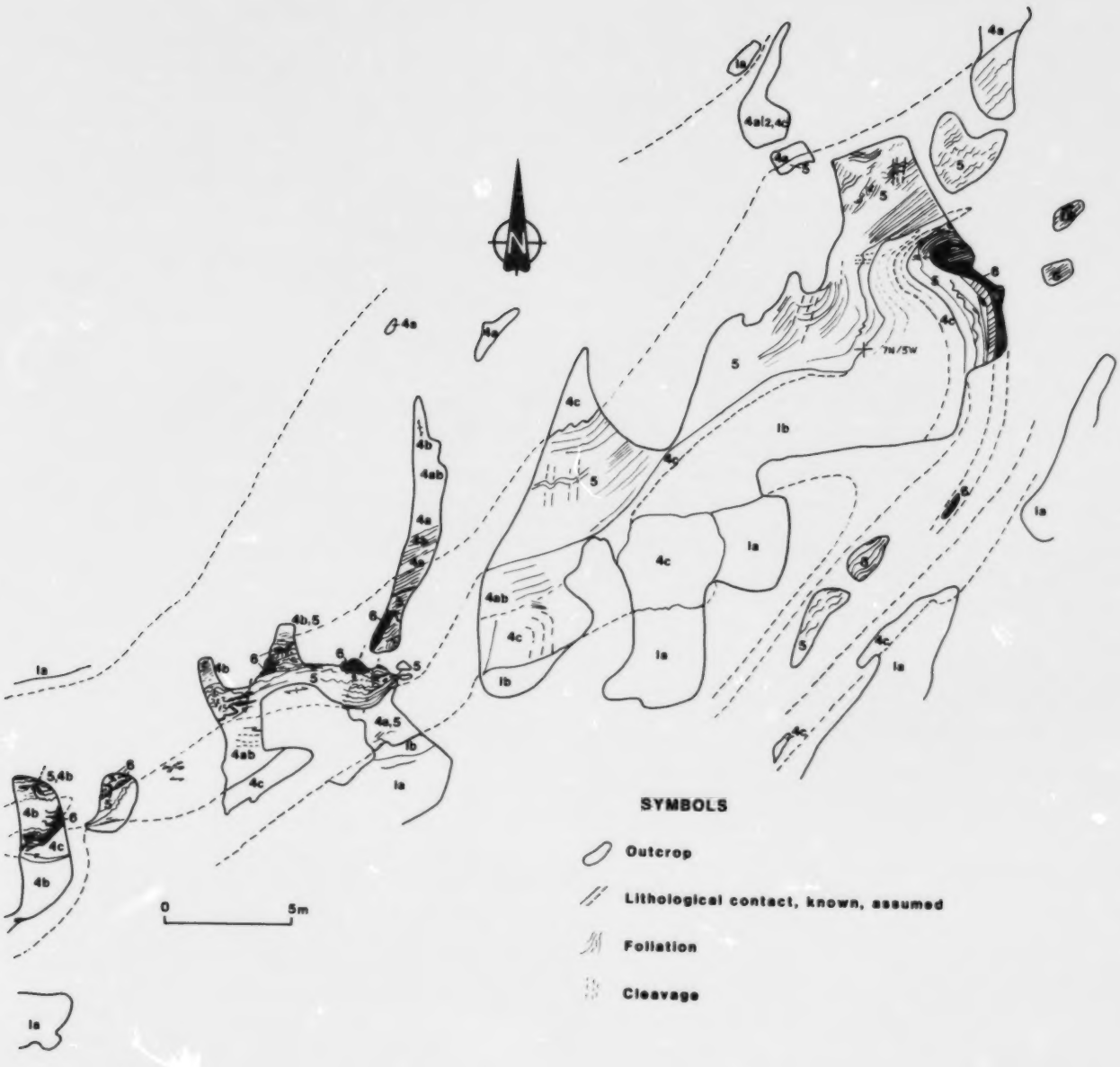

Figure 19: Detailed geology of the surface expression of a part of the South Zone, Tartan Lake Mine. Legend. 1) Gabbroic rocks, 1a) medium- to coarse-grained gabbro, b) medium grained gabbro with minor fine grained gabbro dykes; 2) Fine grained gabbro; 3) Feldspar-rich dyke; 4) chloritic and schistose rocks, 4a) non-schistose carbonatized and chloritic rocks, 4b) weakly schistose carbonatized and chloritic rocks, 4c) chloritic gabbroic rocks; 5) Carbonate-chlorite schist + sulphide + tourmaline + quartz veins + fuchsite; 6) quartz vein. (See also Fig. 6.)

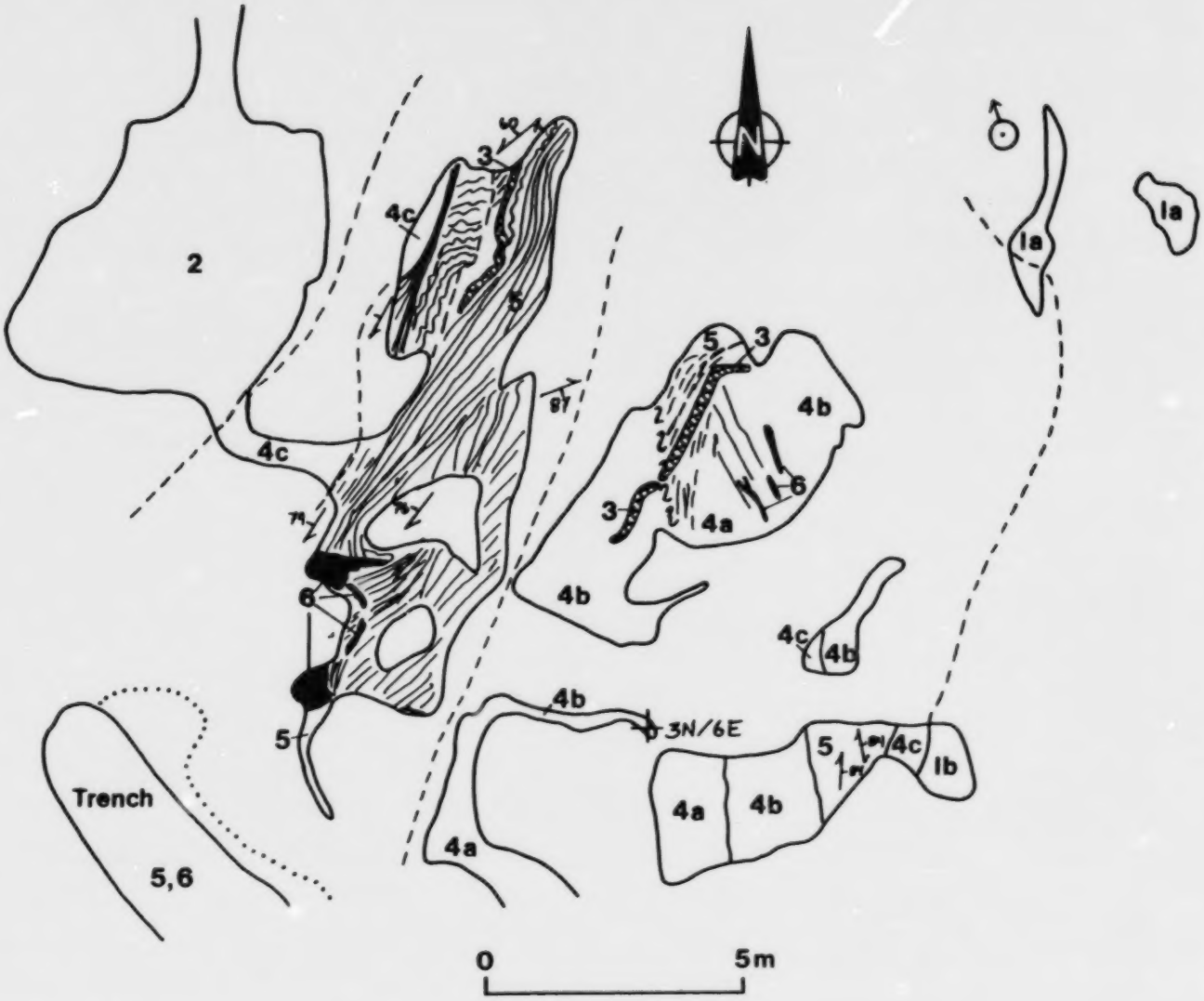

SYMBOLS

- Outcrop
- Lithological contact, known, assumed
- Shear zone
- Foliation
- Cleavage
- Schistosity
- Diamond drillhole

Figure 20: Detailed geology of a part of the 5 East Zone. Symbology as in Figure 19.

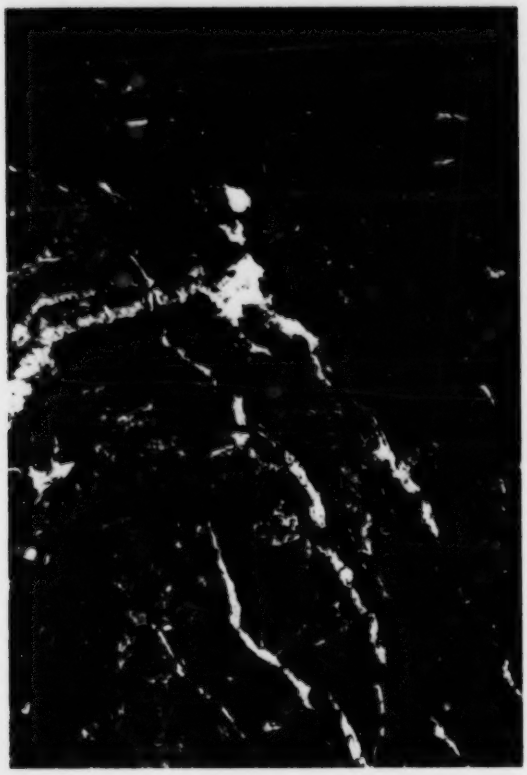

Figure 21: a) Quartz vein mobilizate in altered and schistose rocks of the South Zone and 5 East Zone.

Type III Alteration Zones

A number of zones (e.g., Zone 16) are characterized by the development of a cleavage (but only a weak schistosity, if any), minor chloritization and epidotization, and little carbonate alteration. These zones (Type III) are probably the result of late (post-mineralization and post-mobilization?) faulting of the area (e.g., the Crusher Fault). Most of the Type III zones are indicated only by a cleavage symbol in Figure 3. The late cleavage in Type I zones (e.g., at 1+50N/5+20E) may be related to the same deformation.

Deformational Events

The earliest deformation recognized in the South Block appears to have been a fracturing and/or faulting event that provided the fracture systems for fluid migration to produce the alteration products and mineralization in Zones 1, 2, 3, 4 and their equivalents (Fig. 18). There is no indication in the gabbroic rocks that they were deformed during D_1; i.e., S_1 has not been recognized in unaltered gabbro of the South Block and some altered rocks do not have a well defined schistosity (Fig. 22a).

The second event recognized is a well developed schistosity defined by chlorite and/or sericite (Fig. 22b). The age of this fabric relative to deformational events in the Mine Peninsula area is unknown.

Crenulation folds with an associated strain-slip cleavage deformed the schistosity and produced open folds with amplitudes several tens of metres in length (see Fig. 7, 14). These crenulation folds postdate shearing of the gabbro (e.g., southeast tip of the Mine Peninsula), alteration and probably quartz vein mobilization (Fig. 21), but do not postdate very late strain-slip

Figure 21: b) Quartz vein mobilizate in altered and schistose rocks of the South Zone and 5 East Zone.

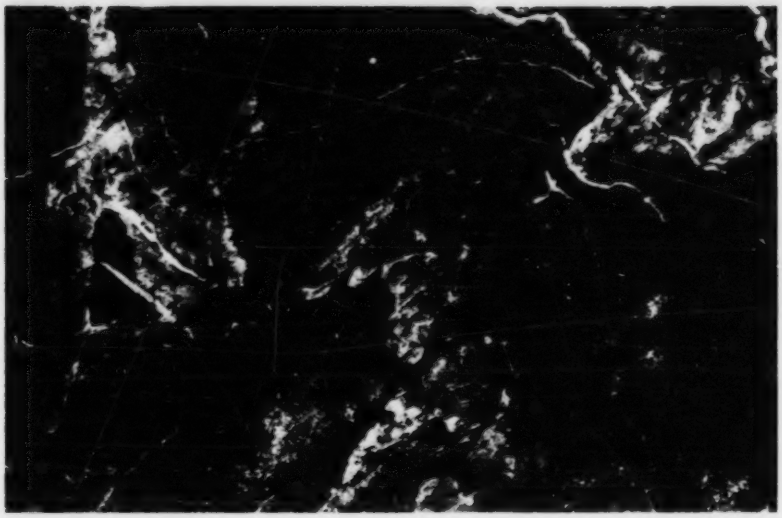

Figure 22: Structural features in alteration zones: a) Carbonatized chloritic rock in 5 East Zone adjacent to fault zone. Note absence of a strong schistosity;

cleavages parallel to the South Zone Fault (Fig. 22d).

The youngest deformation feature recognized during this study is the development of faults along existing zones of alteration, e.g., the South Zone, the 5 East Zone and the Main Zone (observed in underground workings). This faulting postdates the crenulation cleavages in the South Block. Consequently, it postdates and deforms quartz veins and chlorite schists, produces mylonitic zones within the zones of alteration and mineralization, and it shears the gabbro that postdates both crenulation folds and mineralization (Fig. 22b, 22c, 22d).

Structural History of the South Block (Gabbro), Summary

STAGE 1: Fracturing of the gabbro produced northeast- and northwest-striking conjugate fracture sets (5 East Zone). Further failure produces the parallel and subparallel east-west-striking South Zone, Baseline Zone and other subparallel zones (Fig. 23a).

STAGE 2: Extensive alteration of the gabbro along all existing fractures produces alteration zones by chloritization, carbonatization and tourmalization ± auriferous pyritization (Fig. 23b).

STAGE 3: Either (A) a regional deformation (flatten-

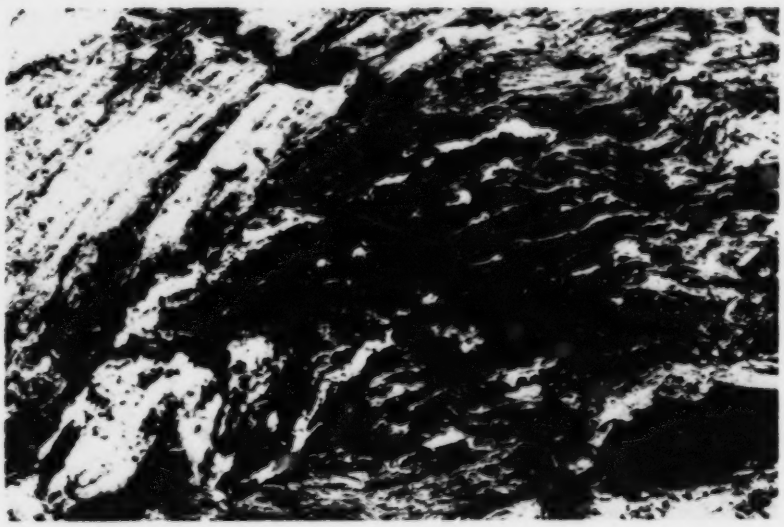

Figure 22: b) Well developed schistosity in carbonatized chlorite schists of South Zone. Change in strike of schistosity is due to later faulting (cf. Fig. 20);

Figure 22: c) Sheared medium grained gabbro developed by late fault at margin of chlorite schists at South Zone.

ing) produces a well developed chlorite-defined schistosity or (B) shearing of the alteration zones under load produces a chlorite-defined fabric (Fig. 23c).

STAGE 4: Deformation of alteration zones. Local deformation includes shearing (S) and folding (F) that produced disruptions of schistosity and mylonitic fabrics (M) in carbonate-chlorite rocks and gabbro. Faults, kink folds (kF), and strain-slip cleavage (C) are also produced by local deformation. Quartz and carbonate are mobilized into veins (V) in both the alteration zones and the adjacent wall rock (Fig. 23d).

STAGE 5: Late faults overprinting earlier fabrics locally produce shearing (S) and strain-slip cleavages and cataclastic fabrics (C) (Fig. 23e).

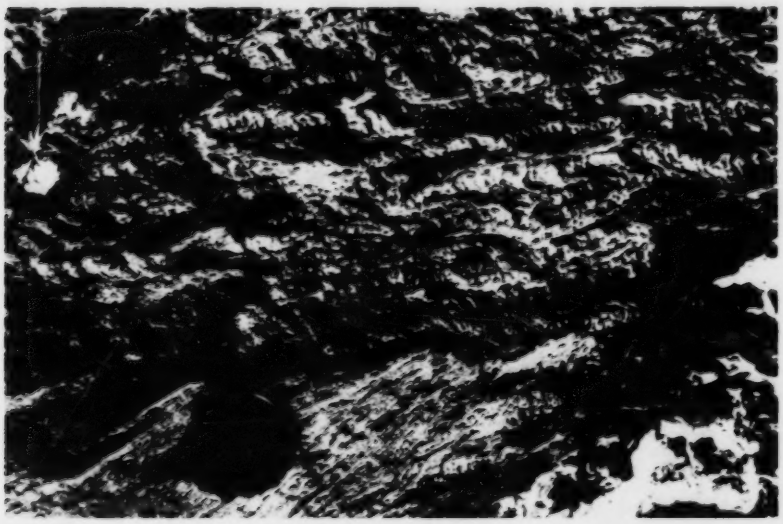

Figure 22: d) Crenulation of chlorite schists by very late cleavage; deformation probably related to faulting shown in B and C.

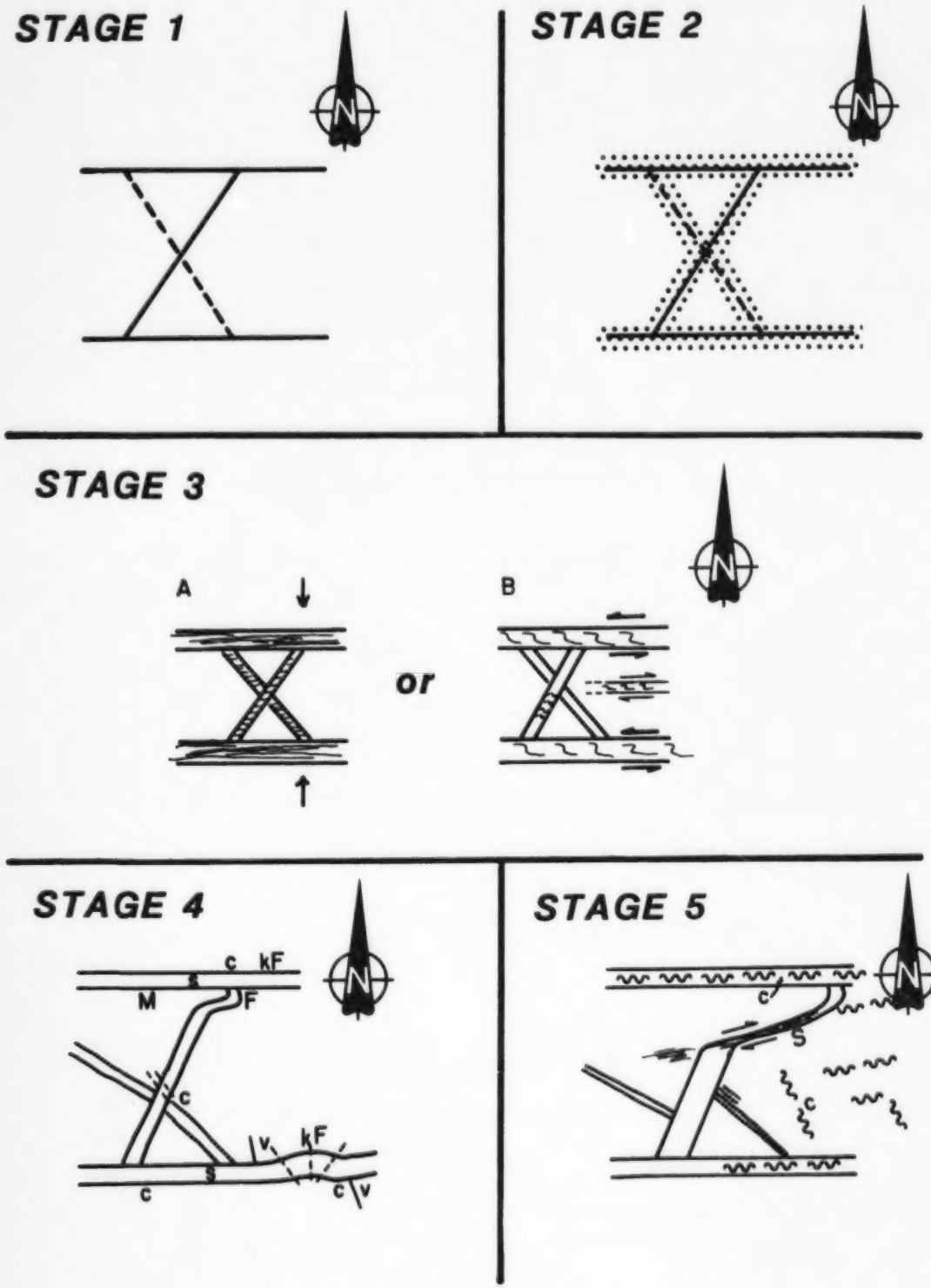

Figure 23: Schematic structural history of the mineralized zones in the South Block gabbro (see text for symbology).

Selected rock types were sampled for major element and trace element analyses in order to establish typical rock compositions and to investigate several rock types as possible sources for the gold. The sampling was of a preliminary nature and the analytical data do not permit definitive statements to be made regarding the rock chemistry, alterations or mineralization. This section of the report is intended solely to present the data obtained to date and provide a summary of conclusions derived from this limited data base.

Samples for major element analyses consisted of 1-3 kg of 2-5 cm-sized rock chips collected with sledge hammers and screened to avoid weathered and atypical material. Samples analyzed only for gold and silver were commonly grab samples and often included weathered and/or atypical material.

The major element analyses (Appendix I) were performed by rapid silicate analytical methods. The 28 element Inductively Coupled Argon Plasma (ICP) analyses (Appendix II) are acid leach partial analyses performed by the Acme Analytical Laboratories Ltd., Vancouver. Gold and silver analyses (Appendix III) were determined by AAS at the Manitoba Energy and Mines Analytical Laboratory, Winnipeg.

VOLCANIC ROCKS

Basalt

The basaltic flows of unit 1 (Fig. 2) were not analyzed for this study. Unpublished analyses of these flows indicate a basaltic composition (H.P. Gilbert, pers. comm., 1987).

Basaltic andesite

Silicate whole rock analyses for three samples of pyroxene-phyric andesite rocks from the Mine Peninsula (Fig. A, Appendix IV) are given in Table 1. Two samples, TL-690.1 and TL-697.1, from the same map unit, have markedly different SiO_2 contents. The higher SiO_2 content in sample TL-697.1 (56.40%) corresponds to lower Na_2O and K_2O values than those in either TL-690.1 (48.5% SiO_2) or TL-606.1 (52.8% SiO_2), and probably represents more extensive alteration in TL-697.1. It is uncertain if these rocks are part of a basaltic or an andesitic suite; consequently they are referred to as basaltic andesite.

Sample TL-52.3 from the south shore of Ruby Lake (Fig. D, Appendix IV) is compositionally similar to analyses of andesite (Carmichael et al., 1974). This rock unit appears to be chemically quite different from the pyroxene-phyric flows (viz., higher SiO_2, Na_2O, K_2O and lower Al_2O_3, CaO, MgO). There are insufficient data at this time to establish whether this 'andesite' is a minor or major component of the volcanic pile in the area: it may represent a fine grained intrusion.

Felsic Volcanic Rocks

Sample TL-87-14 (Table 2) was collected from a thick aphyric rhyolitic tuff or flow. The major element content of this rock clearly indicates a composition quite different from that of the feldspar-porphyritic dykes cutting the gabbro (cf. analyses TL-87-14 and TL-57-3.1; Fig. 24). Consequently, although difficulties were encountered distinguishing between felsic tuffs and felsic dykes in the field, these rocks can be easily dis-

Table 1
Silicate whole rock analyses of basaltic andesite rocks, Tartan Lake.

Sample Number	SiO_2 (%)	Al_2O_3 (%)	FeO(T) (%)	CaO (%)	MgO (%)	Na_2O (%)	K2O (%)	TiO_2 (%)	P_2O_5 (%)	MnO (%)	LOI (%)	TOTAL (%)	CO_2 (%)
TL-690.1	48.50	13.60	5.85	12.72	9.33	1.65	1.14	0.3	0.06	0.13	5.4	98.68	2.82
TL-697.1	56.40	13.40	4.63	13.32	6.41	0.54	0.33	0.2	0.05	0.10	3.3	98.68	1.37
TL-606.1	52.80	15.60	8.64	10.54	5.79	2.09	0.86	0.4	0.13	0.14	2.3	99.29	0.62
TL- 52.3	65.70	12.50	6.33	6.69	2.95	3.51	1.54	0.3	0.09	0.10	3.4	103.11	0.94

TL-690.1 - pyroxene-phyric mafic flow
TL-697.1 - pyroxene-phyric mafic flow
TL-606.1 - pyroxene-phyric mafic flow
TL- 52.3 - massive andesite

Table 2
Silicate whole rock analyses of felsic rocks, Tartan Lake.

Sample Number	SiO_2 (%)	Al_2O_3 (%)	FeO(T) (%)	CaO (%)	MgO (%)	Na_2O (%)	K_2O (%)	TiO_2 (%)	P_2O_5 (%)	MnO (%)	LOI (%)	TOTAL (%)	CO_2 (%)
TL-87-14	78.8	9.3	0.94	1.35	0.17	3.56	1.46	0.2	0.09	0.03	1.4	97.32	-
TL-573.1	60.4	17.0	5.36	4.40	2.47	5.83	1.86	0.6	0.24	0.07	1.8	100.03	0.93
TL-674.1	62.0	16.0	3.58	4.33	2.67	6.48	0.49	0.5	0.13	0.05	3.3	99.53	1.25
TL-669.1a	62.5	16.4	3.33	3.67	1.42	4.25	2.93	0.4	0.15	0.05	3.9	99.00	1.39
TL-669.1b	62.3	15.8	3.39	7.47	1.70	2.38	4.14	0.4	0.15	0.05	4.9	102.68	1.87
TL-687.1	60.0	17.1	5.30	5.08	2.06	5.90	0.59	0.5	0.25	0.09	2.4	99.30	-
RL-586	58.5	17.1	5.84	6.08	2.18	4.88	0.89	0.5	0.30	0.06	1.9	98.27	-
RL-591A	57.7	15.8	4.41	6.27	2.33	2.21	3.84	0.5	0.21	0.12	5.7	99.07	-
RL-627	55.1	17.7	4.57	5.58	3.06	5.61	1.56	0.8	0.39	0.08	4.6	99.03	-
RL-629	66.0	16.2	2.88	2.04	1.11	5.37	2.50	0.3	0.13	0.02	2.6	99.15	-
TL-676.1	55.3	16.4	6.11	4.48	2.20	5.17	2.34	0.5	0.26	0.08	5.7	98.58	-
TL-662.1	61.8	16.4	4.48	4.69	2.57	5.37	2.06	0.5	0.19	0.07	1.3	99.44	-
RL-615	63.0	16.0	3.60	4.72	1.66	6.41	0.42	0.4	0.16	0.03	3.0	99.40	-

- Not determined
TL-87-14 - aphyric rhyolite
TL-573.1 - feldspar (quartz) porphyry
TL-674.1 - feldspar (quartz) porphyry
TL-669.1a - feldspar (quartz) porphyry
TL-669.1b - feldspar (quartz) porphyry
TL-687.1 - feldspar porphyry
RL-586 - feldspar porphyry
RL-591A - feldspar porphyry
RL-627 - feldspar porphyry
TL-629 - feldspar porphyry, sulphide-bearing
TL-676.1 - feldspar porphyry, sulphide-bearing
TL-662.1 - felsic tuff
RL-615 - felsic tuff

criminated on the basis of their SiO_2, Al_2O_3, TiO_2 and MgO contents (Table 2). SiO_2 contents range from 55.1 to 66.0% with an arithmetic mean of 60.0% in feldspar porphyry, compared to 78.8% for the rhyolite sample. Al_2O_3 contents range from 15.8 to 17.1% (mean 16.6%) in feldspar porphyry compared to 9.3% for rhyolite. $FeO_{(T)}$ contents range from 2.88 to 6.11% (mean 4.1%) in feldspar porphyry compared to 0.94% for the rhyolite sample. MgO ranges from 1.11 to 3.06% (mean 2.12%) in feldspar porphyry compared to 0.17% in rhyolite. It is apparent from Table 2 and Figure 24 that analyses TL-662.1 and RL-615 are representative of feldspar-porphyritic dykes rather than felsic tuffs as they had been mapped in the field.

INTRUSIVE ROCKS

Medium- to coarse-grained gabbro

The compositions of three samples from this rock unit are given in Table 3. All of these samples have been epidotized and the sulphide-bearing sample (TL-573.2) is depleted in alkalis. Sample TL-573.2 contains abundant carbonate, but sample TL-553.1 contains higher CO_2 and lower CaO than the other analyses in Table 3; consequently alkali depletion is not directly related to carbonatization.

Analysis TL-574.2 is similar to the analysis of a pyroxene-phyric flow, sample TL-690.1 (Table 1; Fig. 24), which could indicate that the medium grained gabbro

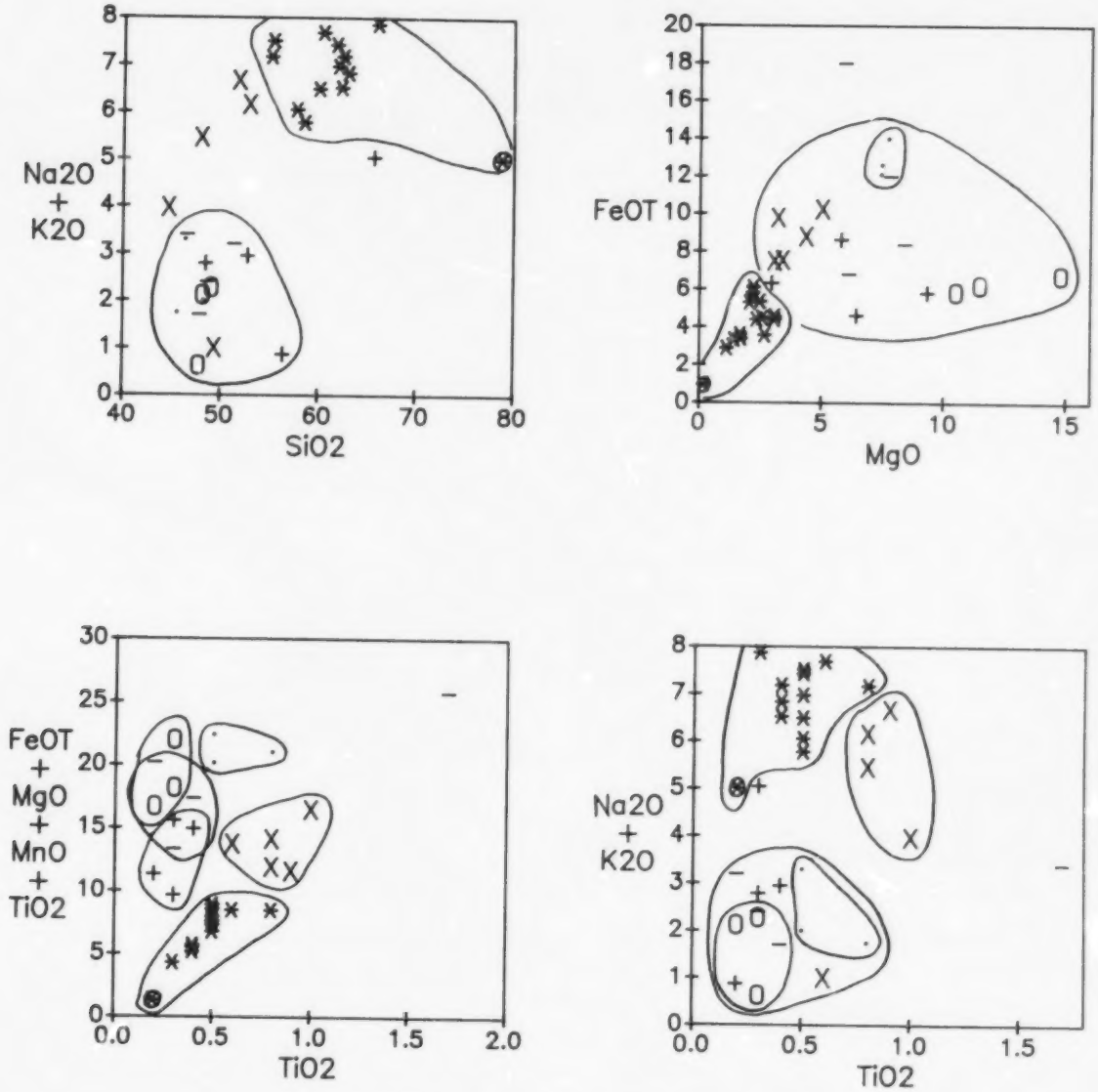

*Figure 24: Silicate whole rock oxide plots for analyses of various rock types from the Tartan Lake area. Symbology: + Basaltic andesite; * Felsic rocks; ⊗ Rhyolite; O medium to coarse grained gabbro; X fine grained gabbro; - knotted gabbro and related(?) rocks.*

was related to the pyroxene-phyric lavas by a common source magma. However, further geochemical studies are required to test this hypothesis.

Fine grained gabbro

Analyses TL-570.3, TL-574.1 and TL-712.1 (Table 4) represent the fine grained gabbro matrix of the 'igneous breccia'. The fine grained gabbro has distinctly higher Al_2O_3, TiO_2, and P_2O_5 and lower MgO than the medium grained gabbroic rocks (cf. Tables 3 and 4). The fine grained gabbro differs from the medium grained gabbroic rocks by distinctly higher Al_2O_3 (ar. mean = 16.4% compared to 12.3%, respectively), TiO_2 (0.8% vs. 0.3%), and P_2O_5 (0.38% vs. 0.02%) and lower MgO (3.80% vs. 12.26%) contents (cf. Tables 3 and 4).

Sample TL-720.1 is problematic in that the exposure was mapped as a volcanic rock (Appendix IV, Fig. A), but it has the composition of the fine grained gabbro and is grouped here with other fine grained gab-

Table 3
Silicate whole rock analyses of medium- to coarse-grained gabbroic rocks, Tartan Lake.

Sample Number	SiO_2 (%)	Al_2O_3 (%)	FeO(T) (%)	CaO (%)	MgO (%)	Na_2O (%)	K_2O (%)	TiO_2 (%)	P_2O_5 (%)	MnO (%)	LOI (%)	TOTAL (%)	CO_2 (%)
TL-574.2	49.1	13.9	6.24	13.56	11.49	1.22	1.05	0.3	0.02	0.16	1.9	98.94	0.34
TL-573.2	47.8	10.8	6.78	14.91	14.78	0.47	0.16	0.3	0.02	0.15	2.4	98.57	0.64
TL-553.1	48.2	12.1	5.88	8.39	10.51	1.31	0.81	0.2	0.03	0.13	11.5	99.06	4.50

TL-574.2 - medium grained gabbro, massive
TL-573.2 - medium grained gabbro, massive, sulphide-bearing
TL-553.1 - medium grained gabbro

Table 4
Silicate whole rock analyses of fine grained gabbroic rocks, Tartan Lake.

Sample Number	SiO_2 (%)	Al_2O_3 (%)	FeO(T) (%)	CaO (%)	MgO (%)	Na_2O (%)	K_2O (%)	TiO_2 (%)	P_2O_5 (%)	MnO (%)	LOI (%)	TOTAL (%)	CO_2 (%)
TL-570.3	48.0	18.0	8.81	7.65	4.35	5.03	0.43	0.8	0.35	0.17	5.7	99.29	2.58
TL-574.1	44.7	19.1	10.25	11.28	5.02	2.59	1.38	1.0	0.49	0.21	2.5	98.52	0.07
TL-712.1	52.9	18.6	7.55	7.71	3.39	3.27	2.89	0.8	0.35	0.18	1.5	99.14	0.14
TL-720.1	51.8	17.0	7.50	5.53	3.05	3.73	2.94	0.9	0.38	0.14	6.3	99.27	2.92
TL-23-G-1	49.4	19.4	9.80	12.80	3.20	0.70	0.30	0.6	0.35	0.14	2.9	99.59	-

TL-570.3 - gabbro, fine grained
TL-574.1 - gabbro, fine grained, massive
TL-712.1 - gabbro, fine grained, epidotized, sulphide-bearing
TL-720.1 - gabbro, fine grained
TL-23-G-1 - gabbro, fine grained

bros. Furthermore, TiO_2, P_2O_5 and MgO distinguish analysis TL-720.1 from that of the microphyric 'knotted' gabbro (see analysis TL-691.1, Table 5) and the rock probably should not be considered part of the nearby 'knotted' gabbro bodies.

Sample TL-23-G-1 from the Ruby Lake area has a composition similar to that of the fine grained gabbro matrix in the igneous breccia. This analysis provides further evidence that the fine grained gabbro is distinct from the main gabbro body in the southeastern part of the area (Fig. 2) that consists of the same medium- to coarse-grained gabbro as the breccia clasts.

'Knotted' gabbro

Analyses TL-162C and TL-162A (Table 5) represent the texturally distinctive 'knotted' gabbro (Appendix IV, Fig. D). Analysis TL-691.1, from the microphyric gabbro (Appendix IV, Fig. A), is chemically similar to the 'knotted' gabbro and all three analyses differ from the fine grained gabbros, particularly in Al_2O_3, $FeO_{(T)}$, MgO and P_2O_5 contents (Fig. 24, 25). 'Knotted' gabbro has an arithmetic mean of 14.9% Al_2O_3, similar to 15.2% Al_2O_3 for microphyric gabbro, but different from a mean of 18.4% Al_2O_3 for fine grained gabbro. FeO(T) contents have a mean of 13.1% for 'knotted' gabbro and 12.6% for microphyric gabbro, but a mean of 8.8% for fine grained gabbro. MgO has a mean of 7.6% for 'knotted' gabbro and 7.43% for microphyric gabbro, compared with a mean of 3.8% for fine grained gabbro. P_2O_5 has a mean of 0.05% for 'knotted' gabbro and 0.07% for microphyric gabbro, but 0.38% for fine grained gabbro.

The 'knotted' gabbro plots compositionally on variation diagrams midway between the other two gab-

Table 5
Silicate whole rock analyses of 'knotted' gabbro and related(?) fine- to medium-grained gabbroic rocks.

Sample Number	SiO_2 (%)	Al_2O_3 (%)	FeO(T) (%)	CaO (%)	MgO (%)	Na_2O (%)	K_2O (%)	TiO_2 (%)	P_2O_5 (%)	MnO (%)	LOI (%)	TOTAL (%)	CO_2 (%)
TL-162C	46.4	15.3	12.10	9.70	7.40	3.00	0.30	0.5	0.05	0.18	5.0	99.93	-
TL-162A	48.3	14.4	14.00	10.00	7.70	1.80	0.20	0.5	0.05	0.22	2.2	99.37	-
TL-691.1	45.6	15.2	12.60	11.07	7.43	1.56	0.18	0.8	0.07	0.20	3.4	98.11	0.84
TL-31-G-1	47.9	17.0	8.40	13.50	8.40	1.60	0.10	0.4	0.03	0.15	2.4	99.88	-
TL-25-G-1	46.6	13.4	18.00	8.30	5.90	3.30	0.10	1.7	0.05	0.18	2.8	100.33	-
TL-23-G-2	48.7	20.5	6.80	13.20	6.10	2.30	0.10	0.3	0.04	0.11	2.4	100.55	-
TL-27-G-5	51.4	13.2	12.00	8.80	7.80	1.80	1.40	0.2	0.11	0.19	2.0	98.90	-

TL-162C - 'knotted' gabbro
TL-162A - fine- to medium-grained gabbro
TL-691.1 - microphyric gabbro
TL-31-G-1 - gabbro
TL-25-G-1 - gabbro
TL-23-G-2 - gabbro
TL-27-G-5 - gabbro

bros (Fig. 8, 9). The higher Na_2O content (3.0%) in sample TL-162C probably represents feldspar accumulations in the 'knots' relative to the microphyric variety (1.56%) of the same rock.

Ruby Lake Gabbro

Four rocks mapped as gabbro in the Ruby Lake area (Appendix IV, Fig. D) have variable compositions (Table 5, samples TL-31-G-1, TL-25-G-1, TL-23-G-2, TL-27-G-5). Sample TL-31-G-1 resembles the 'knotted' gabbro. The distinctly higher TiO_2 and FeO in sample TL-25-G-1 may represent anomalous ilmenite concentrations. Samples TL-23-G-2 and TL-27-G-5 are problematic; they may represent other fine grained gabbros or mafic flows (cf. analyses TL-553.1, Table 3, and TL-690.1, Table 1).

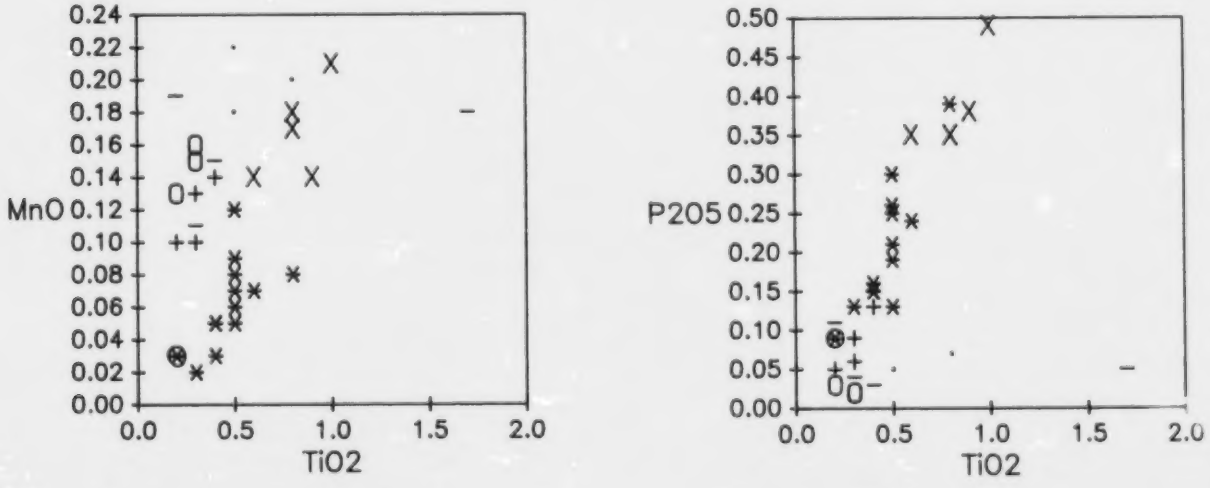

Figure 25: TiO_2 vs MnO and TiO_2 vs P_2O_5 variation diagrams for analyses of Tartan Lake rocks. Symbology as in Figure 8.

Table 6
Silicate whole rock analyses of chloritized mafic rocks, Tartan Lake.

Sample Number	SiO_2 (%)	Al_2O_3 (%)	FeO(T) (%)	CaO (%)	MgO (%)	Na_2O (%)	K_2O (%)	TiO_2 (%)	P_2O_5 (%)	MnO (%)	LOI (%)	TOTAL (%)	CO_2 (%)
TL-689.3	49.6	12.1	15.25	6.04	6.82	2.78	1.04	2.3	0.16	0.27	2.3	98.66	0.15
TL-689.4	46.5	12.9	8.11	14.58	9.14	1.29	0.79	0.6	0.07	0.17	3.9	98.05	1.52
TL-731.1	54.3	11.4	9.28	7.84	9.97	3.12	0.72	0.3	0.11	0.16	1.7	98.90	0.12

TL-689.3 - chloritized mafic rock
TL-689.4 - chloritized mafic rock with carbonate alteration
TL-731.1 - schistose chloritic rock

Feldspar-porphyritic felsic intrusions

Analyses of these rocks are given in Table 2. Samples TL-573.1 and TL-674.1 were collected from dykes cutting gabbro (Appendix IV, Fig. B). Samples TL-669.1a and TL-669.1b were collected from the same sheared dyke in a zone of alteration and deformation (Appendix IV, Fig. A). The analyses of these rocks are different from that of the rhyolite (Table 2) and represent a dacitic composition. It is readily apparent from analysis TL-669.1b, the more altered of the two samples from locality 669, that there has been a significant decrease in Na_2O with the concomitant increase in CaO and K_2O. This confirms thin section observation of a general increase in muscovite with increases in pyrite, chlorite and carbonate, and probably represents an overall potassium metasomatism accompanying the gold mineralization.

CHLORITIC ROCKS

Three samples were analyzed from unit 4 (Appendix IV, Fig. A) in an attempt to establish the origins of these rocks. The analyses (Table 6) indicate highly variable compositions, of which some of the variability is probably due to alteration; further work is required to determine the original nature of these rocks.

Table 7 contains analyses of volcaniclastic sedimentary rocks (Appendix IV, Fig. A) that are probably greywacke. A comparison of analyses in Tables 6 and 7 suggests that the chloritic rocks are not the altered equivalents of the metasedimentary rocks. Although caution must be used in describing the chloritic rocks in terms of statistical averages because of the high variability and limited sample population, there are notable differences in SiO_2, CaO, MgO and P_2O_5 contents. SiO_2 averages 60.7% in volcaniclastic rocks compared with 50.2% in chloritic rocks. CaO averages 4.1% in volcaniclastic rocks compared with a range of 6.04 to 14.58% in chloritic rocks. MgO averages 2.4% in volcaniclastic rocks compared with 8.6% in chloritic rocks. P_2O_5 averages 0.24% in volcaniclastic rocks compared with 0.11% in chloritic rocks. The chloritic rocks probably represent altered volcanic and gabbroic rocks instead.

TRACE ELEMENT GEOCHEMISTRY

Fifty seven samples were analyzed by ICP methods to determine if pathfinder elements were present and to investigate if a source rock for the gold could be identified.

Analyses of basaltic andesites from the Ruby Lake area (Table 8) reveal low Au (1-6 ppb) and Ag (0.1-0.2 ppm) values. Cu ranges from 3 to 480 ppm and Fe ranges from 1.04 to 6.12% with no significant correlation among the analyses.

Since the gabbro is spatially associated with the Main Zone and is host to several zones of gold-bearing schists derived in part from the gabbro, samples of the moderately and extensively altered gabbro were analyzed. As noted earlier the variable alkali contents of the massive gabbros (Tables 3, 4) indicate an alteration that was not detected during field mapping. Two major element analyses (Table 9) from chlorite schist zones developed in the gabbro indicate a depletion in SiO_2 from approximately 48% in the relatively unaltered gabbro to approximately 38% in the extensively altered gabbro (cf. Tables 3 and 4). The extensively altered gabbro contains less than 1% Na_2O but up to 3.3% K_2O (Table 9).

The nine ICP analyses from altered and schistose gabbro (chlorite schist zones) are presented in Tables 10a and 10b. Although most of the analyses presented in Table 10 are from samples collected from outcrops containing visible gold, the highest gold analysis is only 10 ppb and probably reflects nugget-type gold concentrations. Analysis TL-588.4 (Table 10a) is problematic since the sample site could not be confirmed by a field check and may represent a mislabelled sample. The higher gold content of this sample (24 ppb) correlates with high Ca

Table 7
Silicate whole rock analyses of mafic volcaniclastic and sedimentary rocks, Tartan Lake.

Sample Number	SiO_2 (%)	Al_2O_3 (%)	FeO(T) (%)	CaO (%)	MgO (%)	Na_2O (%)	K_2O (%)	TiO_2 (%)	P_2O_5 (%)	MnO (%)	LOI (%)	TOTAL (%)	CO_2 (%)
TL-667.1	65.6	13.5	8.21	3.55	1.77	2.40	2.68	0.5	0.25	0.17	1.0	99.63	0.12
RL-622	55.3	16.5	8.29	4.35	2.59	5.47	2.44	0.7	0.31	0.16	2.7	98.82	-
RL-623	62.2	15.2	7.27	4.89	2.16	1.46	3.65	0.7	0.22	0.14	1.3	99.18	-
RL-638	53.8	16.5	9.85	5.89	3.12	4.55	2.34	0.8	0.44	0.16	1.4	98.85	-
RL-617B	52.4	13.1	9.99	5.34	5.56	1.80	0.97	0.9	0.12	0.18	7.6	97.98	-
TL-678.1	57.6	16.7	5.76	5.09	2.26	4.46	2.99	0.6	0.25	0.11	3.0	98.78	-
TL-682.1	62.0	16.4	4.39	4.86	2.47	5.20	1.91	0.5	0.19	0.06	0.9	98.90	-
TL-696.1	63.8	12.6	8.82	3.43	2.10	2.73	1.17	0.4	0.28	0.17	2.8	98.29	-
TL-699.1	64.4	13.4	9.67	0.85	2.56	2.07	2.11	0.3	0.10	0.18	3.2	98.85	-
TL-727.1	67.3	13.7	5.65	3.55	1.25	3.60	2.38	0.4	0.28	0.13	1.1	99.33	-
TL-728.1	63.7	12.8	9.13	3.64	1.98	2.58	2.12	0.4	0.25	0.19	2.7	99.44	-
TL-729.2	62.1	13.2	9.28	4.70	2.03	2.63	1.69	0.4	0.34	0.26	2.6	99.24	-
TL-730.1	63.7	13.5	8.18	4.46	1.72	3.10	1.28	0.3	0.24	0.24	2.3	99.10	-
RL-617A	59.6	16.1	5.13	3.96	2.26	4.77	2.14	0.5	0.23	0.05	4.8	99.58	-
TL-672.1	56.3	12.9	16.88	2.22	2.91	0.56	2.73	0.4	0.22	0.09	2.6	97.82	-

TL-667.1 - sulphide-bearing mafic volcaniclastic sedimentary rock
RL-622 - mafic siltstone
RL-623 - mafic fine siltstone
RL-638 - mafic volcanic-derived wacke
RL-617B - intermediate tuff
TL-678.1 - intermediate tuff
TL-682.1 - intermediate tuff
TL-696.1 - intermediate tuff
TL-699.1 - intermediate tuff
TL-727.1 - intermediate tuff
TL-728.1 - intermediate tuff
TL-729.2 - intermediate tuff
TL-730.1 - intermediate volcaniclastic rock
RL-617A - intermediate tuff
TL-672.1 - intermediate tuff

(13.75%), high Sr (292 ppm) and high Cu (709 ppm). In general there appears to be some relationship, albeit not consistent, between the presence of gold and Ag, Ni, Cr, As, Sb, B, pyrite and chalcopyrite.

Four samples of chloritic schists from the Mine Peninsula were analyzed by ICP methods (Table 11) in order to compare the analyses with those of the chloritic schists derived from the gabbros (Table 10b). Spurious values in the La, B, and Cr were obtained but the highest gold value is only 4 ppb and other potential indicators (e.g., Cu, Ag) are also low.

It is clear from these analyses that a more extensive trace and major element study of the schists is warranted. Total digestion methods for the trace element analyses (e.g., REE, large ion lithophile elements) might prove useful in petrogenetic modelling.

A number of samples of tuffaceous rocks from the Mine Pensinsula also were analyzed by ICP to determine if they contain elevated Au or other elements normally associated with mineralization in this area (viz., Cu, Cr, Fe, B, Ag). Sample TL-672.1 (Table 12) contains elevated Au (36 ppb), Cu (436 ppm), As (26 ppm), Fe (12.64%), Al (4.35%) and B (7 ppm) relative to other samples in Table 12, but the sample was collected in proximity to the Main Zone. The Al and B probably reflect alteration of the host rocks by the mineralizing event. The As-Fe-Cu correlation suggests a relationship between sulphides and Au. The remaining analyses do not contain any data to indi-

Table 8
Partial chemical analyses of basaltic andesite volcanic rocks, Ruby Lake area.

Sample Number	Mo (ppm)	Cu (ppm)	Pb (ppm)	Zn (ppm)	Ag (ppm)	Ni (ppm)	Mn (ppm)	Fe (%)	As (ppm)	U (ppm)	Th (ppm)	Sr (ppm)	Cd (ppm)	Sb (ppm)
RL-501	1	18	2	79	0.1	32	705	4.28	2	5	1	13	1	2
RL-504	1	163	2	22	0.2	12	208	1.04	35	5	1	32	1	2
RL-516	1	480	3	49	0.1	5	423	2.80	2	5	1	43	1	2
RL-523	1	129	4	74	0.1	29	630	4.51	2	5	1	23	1	2
RL-533	1	205	3	21	0.1	21	226	1.93	8	5	1	35	1	2
RL-551	1	411	7	43	0.2	31	950	3.56	6	5	1	125	1	2
RL-569	1	25	2	24	0.2	17	375	1.99	33	5	1	44	1	3
RL-576	1	8	4	77	0.1	36	930	6.12	40	5	1	39	1	2
RL-597	1	3	2	15	0.1	32	331	1.24	12	5	1	61	1	2

Sample Number	Bi (ppm)	Ca (%)	P (%)	La (ppm)	Cr (ppm)	Mg (%)	Ba (ppm)	Ti (%)	B (ppm)	Al (%)	Na (%)	K (%)	Au (ppb)
RL-501	2	0.38	0.044	2	123	3.81	149	0.11	2	2.94	0.08	0.52	1
RL-504	2	0.66	0.035	2	10	0.52	44	0.10	4	0.81	0.13	0.18	1
RL-516	2	2.27	0.022	2	5	1.29	139	0.14	3	1.80	0.13	1.14	1
RL-523	2	4.09	0.055	2	59	3.59	56	0.11	2	3.02	0.13	0.30	1
RL-533	2	0.79	0.032	2	82	0.78	48	0.07	6	0.81	0.12	0.13	1
RL-551	2	12.14	0.018	2	98	2.18	68	0.04	2	2.15	0.15	0.30	2
RL-569	2	1.84	0.043	2	38	0.93	165	0.08	3	1.27	0.10	0.57	4
RL-576	2	2.03	0.046	2	89	3.74	22	0.08	2	3.63	0.10	0.07	6
RL-597	2	8.16	0.026	5	123	0.94	28	0.09	3	1.27	0.11	0.14	1

RL-501 - pyroxene-phyric basaltic andesite, sheared
RL-504 - pyroxene-phyric basaltic andesite, pillowed
RL-516 - aphanitic basaltic andesite, massive, amygdaloidal
RL-523 - basaltic andesite, pillowed (?), schistose, with carbonate alteration
RL-533 - basaltic andesite, pillowed, schistose, amygdaloidal
RL-551 - pyroxene-phyric basaltic andesite, pillowed, schistose
RL-569 - pyroxene-phyric basaltic andesite
RL-576 - basaltic andesite, altered
RL-597 - pyroxene-phyric basaltic andesite with carbonate alteration

Table 9
Silicate whole rock analyses of schistose gabbroic rocks, Tartan Lake.

Sample Number	SiO_2 (%)	Al_2O_3 (%)	FeO(T) (%)	CaO (%)	MgO (%)	Na_2O (%)	K_2O (%)	TiO_2 (%)	P_2O_5 (%)	MnO (%)	LOI (%)	TOTAL (%)	CO_2 (%)
TL-586.1	37.2	15.5	13.51	10.86	7.64	0.85	0.53	1.6	1.10	0.15	7.3	96.24	3.04
TL-563.1	39.1	12.6	4.96	11.10	7.62	0.57	3.31	0.2	0.03	0.13	19.0	98.62	14.74

TL-586.1 - schistose gabbro, chlorite schist
TL-563.1 - schistose gabbro, chlorite schist

Table 10a
Partial chemical analyses of altered gabbroic rocks, Tartan Lake.

Sample Number	Mo (ppm)	Cu (ppm)	Pb (ppm)	Zn (ppm)	Ag (ppm)	Ni (ppm)	Mn (ppm)	Fe (%)	As (ppm)	U (ppm)	Th (ppm)	Sr (ppm)	Cd (ppm)	Sb (ppm)
TL-513A	2	9	7	68	0.1	7	700	5.60	4	5	2	65	1	2
TL-528.2	1	22	2	31	0.1	129	807	3.89	7	5	2	88	1	2
TL-553.1	2	5	5	47	0.2	112	815	3.56	5	5	3	109	1	2
TL-570.2	1	69	2	73	0.1	7	544	5.68	2	5	2	21	1	4
TL-588.4	1	709	2	19	0.2	34	908	1.77	2	10	3	292	1	2
RL-616	1	128	3	50	0.1	22	561	4.42	37	5	1	35	1	2

Sample Number	Bi (ppm)	Ca (%)	P (%)	La (ppm)	Cr (ppm)	Mg (%)	Ba (ppm)	Ti (%)	B (ppm)	Al (%)	Na (%)	K (%)	Au (ppb)
TL-513A	2	1.95	0.188	5	3	2.12	126	0.16	2	2.68	0.14	0.30	1
TL-528.2	3	8.16	0.004	2	419	6.69	5	0.01	2	2.26	0.14	0.01	1
TL-553.1	3	6.63	0.007	2	346	5.59	9	0.01	2	3.61	0.12	0.02	3
TL-570.2	2	3.92	0.118	6	3	3.85	50	0.03	2	2.83	0.13	0.09	10
TL-588.4	3	13.75	0.023	3	92	1.24	26	0.01	2	1.14	0.17	0.06	24
RL-616	2	0.77	0.018	2	2	1.70	266	0.43	5	2.00	0.10	0.74	2

TL-513A gabbro, altered
TL-528.2 gabbro, altered, chlorite-carbonate
TL-563.1 gabbro, altered, schistose
TL-570.2 gabbro, altered
TL-588.4 gabbro, altered with pale green feldspar clots
RL-616 amphibole-bearing gabbro

Table 10b
Partial chemical analyses of schistose gabbroic rocks, Tartan Lake.

Sample Number	Mo (ppm)	Cu (ppm)	Pb (ppm)	Zn (ppm)	Ag (ppm)	Ni (ppm)	Mn (ppm)	Fe (%)	As (ppm)	U (ppm)	Th (ppm)	Sr (ppm)	Cd (ppm)	Sb (ppm)
TL-513C	1	75	3	60	0.1	22	502	4.21	7	5	1	101	1	2
TL-563.1	1	5	4	25	0.1	74	857	3.10	3	6	2	153	1	2
TL-586.1	1	215	2	80	0.2	8	833	8.15	21	5	3	103	1	2
TL-589.1	1	267	5	94	0.1	7	741	8.54	8	5	2	91	1	2

Sample Number	Bi (ppm)	Ca (%)	P (%)	La (ppm)	Cr (ppm)	Mg (%)	Ba (ppm)	Ti (%)	B (ppm)	Al (%)	Na (%)	K (%)	Au (ppb)
TL-513C	2	1.67	0.047	2	22	2.46	85	0.25	2	2.63	0.13	0.30	7
TL-563.1	3	8.88	0.009	2	41	4.31	25	0.01	2	1.06	0.14	0.15	1
TL-586.1	2	4.80	0.526	6	1	4.57	15	0.13	2	4.26	0.12	0.04	1
TL-589.1	2	3.67	0.194	3	1	4.31	48	0.04	2	4.56	0.11	0.15	9

TL-513C gabbro, altered, schistose
TL-563.1 gabbro, altered
TL-586.1 gabbro, altered, schistose, sulphide-bearing
TL-589.1 gabbro, altered, schistose, sulphide-bearing

Table 11
Partial chemical analyses of chloritic and schistose rocks, Tartan Lake.

Sample Number	Mo (ppm)	Cu (ppm)	Pb (ppm)	Zn (ppm)	Ag (ppm)	Ni (ppm)	Mn (ppm)	Fe (%)	As (ppm)	U (ppm)	Th (ppm)	Sr (ppm)	Cd (ppm)	Sb (ppm)
TL-689.3	1	52	6	89	0.1	13	845	6.33	4	5	1	9	1	2
TL-689.4	1	28	3	31	0.1	53	423	2.01	16	5	2	55	1	2
TL-720.2	1	2	2	90	0.1	7	619	6.18	6	5	5	113	1	2
TL-731.1	1	10	3	30	0.3	21	350	2.78	2	5	1	12	1	2

Sample Number	Bi (ppm)	Ca (%)	P (%)	La (ppm)	Cr (ppm)	Mg (%)	Ba (ppm)	Ti (%)	B (ppm)	Al (%)	Na (%)	K (%)	Au (ppb)
TL-689.3	2	0.97	0.053	2	1	2.01	271	0.64	2	2.43	0.16	0.62	1
TL-689.4	3	3.26	0.023	2	202	1.58	84	0.15	3	1.61	0.10	0.31	4
TL-720.2	2	2.39	0.181	23	3	2.66	85	0.04	32	3.33	0.09	0.37	1
TL-731.1	2	0.56	0.036	2	144	1.94	176	0.09	2	1.56	0.12	0.42	1

TL-689.3 chloritic rock
TL-689.4 chloritic rock with carbonate alteration
TL-720.2 chloritic rock
TL-731.1 chloritic rock, schistose

cate that the tuffaceous rocks were the source rocks for the concentrations of gold and other elements found in the Tartan Lake ore deposits.

Gold values ranging from 40 to 90 ppb were obtained in three samples of feldspar-quartz porphyritic felsic rocks (Table 13). Sample TL-676.1 was collected from an old trench in the hanging wall of the Main Zone (Appendix IV, Fig. A) and may represent a leakage halo. Samples RL-519 and RL-627 are from areas that have been faulted and sheared. Analysis RL-519 with 94 ppb Au correlates with high As and Cu suggesting a sulphide control on mineralization. RL-627 with 45 ppb Au correlates with high K, Al, Tl, Mg, Ca, Fe and Cu suggesting a lithologic control on mineralization rather than a sulphide control. The remainder of the feldspar-porphyritic felsic intrusions analyzed (Table 13) did not contain more than 10 ppb Au even where the samples contained abundant pyrite.

One hundred and six grab samples were analyzed for gold and silver by fire assay and atomic absorption methods (Tables 14-17). The highest gold values were obtained from quartz veins, but not all quartz veins contained gold. Trace amounts of gold occur in some schistose rocks, but analyses from several schistose zones with visible gold did not yield anomalous gold values; this may reflect either a nugget effect or inadequate sample size.

Table 12
Partial chemical analyses of intermediate tuffaceous and sedimentary rocks, Tartan Lake.

Sample Number	Mo (ppm)	Cu (ppm)	Pb (ppm)	Zn (ppm)	Ag (ppm)	Ni (ppm)	Mn (ppm)	Fe (%)	As (ppm)	U (ppm)	Th (ppm)	Sr (ppm)	Cd (ppm)	Sb (ppm)
RL-622	1	144	6	96	0.1	7	1057	5.68	9	5	2	62	1	2
RL-623	1	96	2	117	0.1	5	787	4.46	5	5	2	28	1	2
RL-638	1	235	5	67	0.2	4	789	5.47	8	5	3	44	1	2
RL-617B	1	89	3	76	0.1	29	1068	6.64	5	5	1	132	1	2
TL-656.1	2	108	2	222	0.1	1	1191	5.23	34	5	2	25	1	2
TL-660.1	1	90	8	108	0.1	3	974	5.94	2	5	2	32	1	2
TL-667.1	2	79	4	79	0.1	1	755	5.78	4	5	1	16	1	2
TL-672.1	1	436	9	177	0.1	5	553	12.64	26	5	2	13	1	2
TL-678.1	1	16	3	60	0.1	4	717	3.77	7	5	6	64	1	2
TL-682.1	1	2	4	36	0.1	21	288	2.18	2	5	4	97	1	2
TL-696.1	1	159	9	249	0.1	4	1252	6.55	6	5	2	29	1	2
TL-699.1	1	4	3	199	0.1	1	1249	7.04	3	5	2	22	1	2
TL-727.1	1	125	2	83	0.2	1	742	3.41	2	5	2	34	1	2
TL-728.1	1	74	2	143	0.1	1	1297	6.64	6	5	2	26	1	2
TL-729.2	1	173	6	180	0.2	1	1756	6.51	2	5	2	64	1	2
TL-730.1	1	68	6	263	0.1	2	1541	5.60	2	5	2	48	1	2

Sample Number	Bi (ppm)	Ca (%)	P (%)	La (ppm)	Cr (ppm)	Mg (%)	Ba (ppm)	Tl (%)	B (ppm)	Al (%)	Na (%)	K (%)	Au (ppb)
RL-622	2	1.66	0.111	5	18	1.52	440	0.28	2	2.60	0.15	1.57	2
RL-623	3	0.50	0.076	5	4	1.15	310	0.25	3	2.39	0.08	1.79	6
RL-638	2	0.99	0.156	9	1	1.40	617	0.28	2	2.39	0.14	1.62	2
RL-617B	2	4.85	0.041	6	43	3.38	46	0.05	2	3.44	0.12	0.06	3
TL-656.1	2	0.89	0.028	9	2	1.21	97	0.14	2	2.39	0.10	0.96	1
TL-660.1	2	1.46	0.072	8	1	1.75	63	0.08	2	2.70	0.10	0.46	1
TL-667.1	2	0.44	0.089	3	3	0.93	581	0.20	2	2.58	0.11	1.67	1
TL-672.1	2	0.26	0.070	3	1	1.76	391	0.21	7	4.35	0.07	1.65	36
TL-678.1	2	2.25	0.091	22	4	1.30	534	0.23	4	2.18	0.16	1.44	1
TL-682.1	2	0.78	0.070	13	13	1.10	405	0.19	3	1.58	0.18	0.83	1
TL-696.1	2	1.31	0.097	3	2	1.27	105	0.13	2	2.65	0.11	0.50	2
TL-699.1	2	0.45	0.034	9	1	1.52	76	0.07	2	2.88	0.08	0.43	3
TL-727.1	3	0.67	0.097	5	1	0.68	349	0.18	2	1.64	0.12	1.14	4
TL-728.1	2	1.44	0.084	3	1	1.12	349	0.19	2	2.75	0.12	1.25	1
TL-729.2	2	1.52	0.121	4	1	1.20	433	0.20	2	2.75	0.11	1.09	2
TL-730.1	2	1.21	0.079	4	3	0.93	188	0.16	2	2.34	0.12	0.74	1

RL-622 - mafic siltstone
RL-623 - mafic fine siltstone
RL-638 - mafic volcanic-derived wacke
RL-617B Intermediate tuff
TL-656.1 Intermediate tuff
TL-660.1 Intermediate tuff
TL-667.1 Intermediate tuff, sulphide-bearing
TL-672.1 Intermediate tuff
TL-678.1 Intermediate tuff
TL-682.1 Intermediate tuff
TL-696.1 Intermediate tuff
TL-699.1 Intermediate tuff
TL-727.1 Intermediate tuff
TL-728.1 Intermediate tuff
TL-729.2 Intermediate tuff
TL-730.1 Intermediate volcaniclastic rock

Table 13
Partial chemical analyses of feldspar and feldspar-quartz porphyritic felsic rocks.

Sample Number	Mo (ppm)	Cu (ppm)	Pb (ppm)	Zn (ppm)	Ag (ppm)	Ni (ppm)	Mn (ppm)	Fe (%)	As (ppm)	U (ppm)	Th (ppm)	Sr (ppm)	Cd (ppm)	Sb (ppm)
TL-17.2					<1									
TL-18.X					<1									
TL-27C-1					<1									
TL-71.1A					<1									
TL-72.2					<1									
TL-157A-1					<1									
TL-425					<1									
TL-573.1	1	20	48	253	0.2	4	371	3.21	3	5	5	77	1	2
TL-576.1														
TL-577.1	1	12	6	34	0.1	3	223	2.15	3	5	6	84	1	2
TL-579.1														
TL-592.1	1	18	2	73	0.1	4	578	3.05	4	5	5	74	1	2
TL-662.1	1	1	4	40	0.3	24	363	2.36	2	5	4	90	1	2
TL-676.1														
TL-687.1	3	135	2	71	0.2	8	541	3.29	17	5	4	60	1	2
RL-502	1	1	2	44	0.1	5	368	2.99	2	5	6	98	1	2
RL-506	1	200	17	44	0.4	22	389	3.04	5	5	3	45	1	2
RL-515	1	4	6	64	0.2	8	503	2.13	2	5	9	162	1	2
RL-519	1	81	4	31	0.1	7	274	2.79	30	5	6	80	1	2
RL-548	1	1	2	57	0.2	7	611	3.04	7	5	5	102	1	2
RL-573	1	5	2	64	0.1	50	1011	5.42	35	5	1	86	1	164
RL-579A	1	12	3	50	0.1	10	481	3.04	2	5	4	62	1	2
RL-586	1	32	2	36	0.1	4	329	3.24	10	5	7	56	1	4
RL-591A	1	14	8	84	0.2	6	725	1.99	3	5	5	105	1	2
RL-615	1	12	2	18	0.1	6	227	2.00	2	5	3	46	1	2
RL-617A	1	3	6	50	0.2	4	351	3.15	2	5	7	96	1	2
RL-627	1	34	2	36	0.1	8	526	3.02	4	5	7	51	1	2
RL-629	1	7	3	17	0.1	1	127	1.56	3	5	8	40	1	2

Sample Number	Bi (ppm)	Ca (%)	P (%)	La (ppm)	Cr (ppm)	Mg (%)	Ba (ppm)	Tl (%)	B (ppm)	Al (%)	Na (%)	K (%)	Au (ppb)
TL-17.2													<12
TL-18.X													<12
TL-27C-1													<12
TL-71.1A													<12
TL-72.2													<12
TL-157A-1													<12
TL-425													<12
TL-573.1	2	1.28	0.092	18	1	1.36	358	0.17	2	1.77	0.17	0.73	1
TL-576.1													<12
TL-577.1	2	0.91	0.094	22	3	0.84	294	0.22	5	1.29	0.17	0.55	9
TL-579.1													<12
TL-592.1	2	0.83	0.094	21	4	1.42	90	0.18	2	1.81	0.16	0.23	1
TL-662.1	2	0.99	0.068	13	12	1.37	390	0.19	2	1.81	0.18	1.07	1

Table 13 (cont'd.)

Sample Number	Bi (ppm)	Ca (%)	P (%)	La (ppm)	Cr (ppm)	Mg (%)	Ba (ppm)	Tl (%)	B (ppm)	Al (%)	Na (%)	K (%)	Au (ppb)
TL-676.1													40
TL-687.1	2	1.65	0.089	14	8	1.26	68	0.17	2	1.75	0.15	0.18	3
RL-502	2	1.57	0.092	25	2	1.13	281	0.12	4	1.88	0.13	0.64	1
RL-506	2	0.89	0.100	12	35	1.58	49	0.15	2	1.57	0.13	0.09	1
RL-515	2	1.64	0.087	32	6	1.11	127	0.13	3	1.53	0.15	0.26	1
RL-519	2	1.59	0.092	24	5	1.11	126	0.04	4	1.62	0.14	0.28	94
RL-548	2	3.14	0.094	23	11	1.27	120	0.09	5	1.85	0.12	0.23	1
RL-573	2	10.02	0.038	6	309	3.24	5	0.03	2	3.18	0.13	0.03	2
RL-579A	2	1.16	0.089	18	8	1.57	108	0.16	3	1.99	0.16	0.53	3
RL-586	2	1.13	0.113	28	3	1.18	78	0.14	3	1.49	0.15	0.19	2
RL-591A	2	4.85	0.074	16	5	1.01	132	0.09	8	1.46	0.11	0.57	1
RL-615	2	2.58	0.059	13	10	0.81	44	0.10	10	1.12	0.18	0.11	1
RL-617A	2	3.46	0.088	30	8	1.21	166	0.04	3	1.76	0.15	0.29	1
RL-627	2	3.63	0.148	32	10	1.86	103	0.15	2	2.04	0.16	0.51	45
RL-629	2	1.08	0.047	28	3	0.47	186	0.02	6	0.78	0.12	0.27	3

TL-17.2
TL-18.X
TL-27C-1
TL-71.1A
TL-72.2
TL-157A-1
TL-425
TL-573.1 feldspar porphyry
TL-576.1
TL-577.1 feldspar porphyry, dyke, sulphide-bearing
TL-579.1
TL-592.1 feldspar porphyry
TL-662.1 felsic tuff
TL-676.1 feldspar porphyry
TL-687.1 feldspar porphyry
RL-502 feldspar porphyry
RL-506 feldspar porphyry
RL-515 feldspar porphyry
RL-519 feldspar porphyry, sulphide-bearing
RL-548 feldspar porphyry
RL-573 feldspar porphyry(?) schistose, chloritic
RL-579A feldspar porphyry
RL-586 feldspar porphyry
RL-591A feldspar porphyry
RL-615 felsic tuff
RL-617A Intermediate tuff
RL-627 feldspar porphyry
RL-629 feldspar porphyry, sulphide-bearing

Table 14
Gold and silver analyses for grab samples of vein quartz and some quartz-rich rocks.

Sample Number	Au (ppb)	Ag (ppm)	Sample Location	Field Description	
TL-1.2	< 12	< 1	26 + 00N/ 19 + 00W	RLE	Quartz from small shear
TL-4.4	45	< 1	17 + 80S/ 20 + 50W	RLE	Quartz-tourmaline vein
TL-4.5A	< 12	< 1	17 + 80S/ 20 + 50W	RLE	Quartz-tourmaline vein, from shear
TL-4.5B	< 12	< 1	17 + 80S/ 20 + 50W	RLE	Quartz-tourmaline vein, not from shear
TL-5.1	17	< 1	14 + 70S/ 22 + 30W	RLE	Quartz vein
TL-5.5	< 12	< 1	14 + 70S/ 22 + 30W	RLE	Quartz vein
TL-13.1	45	< 1	14 + 50S/ 21 + 25W	RLE	Quartz vein, from shear
TL-22.2	< 12	< 1	21 + 00N/ 18 + 30W	RLE	Quartz vein
TL-27-G-2	< 12	< 1	10 + 00N/ 27 + 20W	RLE	Quartz and gossan
TL-49.1	< 12	< 1	14 + 80S/ 6 + 70W	RLE	Quartz vein
TL-59.1	< 12	< 1	11 + 80S/ 28 + 30W	RLE	Quartz vein, from shear
TL-74-A-1	< 12	< 1	22 + 00S/ 22 + 50E	TL	Quartz
TL-141-A-1	< 12	< 1	23 + 70N/ 0 + 20E	TL	Quartz vein
TL-153.2	< 12	< 1	32 + 00N/ 34 + 20E	TL	Quartz vein
TL-156.6	< 12	< 1	24 + 00N/ 31 + 50E	TL	Quartz
TL-159.1	< 12	< 1	30 + 50N/ 27 + 50E	TL	Quartz from pit
TL-161.3	< 12	< 1	35 + 00N/ 34 + 00E	TL	Quartz from trench
TL-162.5	< 12	< 1	36 + 20N/ 31 + 00E	TL	Quartz-rich zone from trench
TL-162.7	< 12	< 1	36 + 20N/ 31 + 00E	TL	Quartz, talc and gossan, from trench
TL-162.8	17	< 1	36 + 20N/ 31 + 00E	TL	Quartz in gossan, from trench
TL-162.9	< 12	< 1	36 + 20N/ 31 + 00E	TL	Quartz in gossan, from trench
TL-176.2	< 12	< 1	15 + 60N/ 16 + 50E		Quartz vein
TL-193.1	< 12	< 1	6 + 55N/ 2 + 00E		Quartz from main zone
TL-378.1	< 12	< 1	25 + 00S/ 33 + 25E	TL	Quartz
TL-RLG-414	< 12	< 1	4 + 00S/ 15 + 40W	RL	Quartz vein
TL-420	< 12	< 1	3 + 00N/ 5 + 00W	RL	Quartz from trench
TL-422	162	< 1	3 + 00N/ 5 + 00W	RL	Quartz from trench
TL-424	508	< 1	3 + 00N/ 8 + 00W	RL	Quartz from trench
TL-446	214	< 1	17 + 00S/ 20 + 00E	TL	Quartz from shear
TL-526.0	< 12		3 + 35N/ 9 + 15E	TL	Quartz
TL-533.1	17		1 + 40S/ 3 + 90E	TL	Quartz
TL-551.1	> 8500		0 + 30N/ 8 + 00E	TL	Quartz
TL-585.1	> 20000		0 + 20S/ 9 + 50E	TL	Feldspar-quartz vein
TL-669.4	1079		14 + 20N/ 17 + 40E	TL	Quartz and schist
TL-674.2	1020		6 + 75N/ 1 + 15E	TL	Chlorite schist and quartz
TL-676.3	> 6000		5 + 95N/ 0 + 50E	TL	Quartz rubble

Table 15
Gold and silver analyses for grab samples of schistose rocks.

Sample Number	Au (ppb)	Ag (ppm)	Sample Location	Field	Description
TL-162B	< 12	6	36 + 50N/31 + 00E	TL	Rusty weathering schist from shear zone
TL-13.2	< 12	< 1	14 + 50S/21 + 25W	RLE	Shear zone
TL-162.1	< 12	< 1	36 + 20N/31 + 00E	TL	Grey schist
TL-415	< 12	< 1	4 + 75S/15 + 00E	RL	Chlorite schist from shear zone
TL-529.2	46		3 + 40N/ 4 + 20E	TL	Schist
TL-528.4	63		3 + 75N/ 4 + 90E	TL	Schist
TL-530.2	< 12		2 + 35N/ 4 + 35E	TL	Schist
TL-531.1	51		1 + 20N/ 3 + 20E	TL	Schist
TL-551.2	< 12		0 + 30N/ 8 + 00E	TL	Schist
TL-566.2	< 12		5 + 00N/ 7 + 00E	TL	Chlorite-carbonate schist
TL-570.1	< 12		3 + 80N/ 6 + 00E	TL	Shear zone
TL-581.2	17		1 + 25N/ 5 + 30E	TL	Schist and quartz
TL-589.1	405		4 + 70N/10 + 75E	TL	Chlorite schist
TL-591.1	< 12		7 + 30N/13 + 00E	TL	Schist and quartz
TL-663.1	< 12		12 + 35N/10 + 95E	TL	Chlorite schist and quartz
TL-685.1	13		8 + 45N/ 3 + 40E	TL	Chlorite schist
TL-720.2	< 12		19 + 30N/ 4 + 20E	TL	Chlorite schist
TL-721.1	< 12		17 + 55N/ 5 + 60E	TL	Quartz-chlorite schist

Table 16
Gold and silver analyses for grab samples of sulphide- and graphite-rich rocks.

Sample Number	Au (ppb)	Ag (ppm)	Sample Location	Field	Description
TL-159.2	< 12	< 1	30 + 50N/27 + 50N	TL	Gossan from pit
TL-161.2	17	< 1	35 + 00N/34 + 00E	TL	Gossan zone from trench
TL-162.2	69	1	36 + 20N/31 + 00E	TL	Clinker or cinder graphite
TL-162.3	< 12	< 1	36 + 20N/31 + 00E	TL	Gossan zone
TL-162.4	17	< 1	36 + 20N/31 + 00E	TL	Graphite (clinker) with talc?
TL-385-A	29	< 1	33 + 30N/33 + 80N	TL	Pyrite zone
TL-385-B	75	2	33 + 30N/33 + 80N	TL	Graphite zone
TL-385-C	57	3	33 + 30N/33 + 80N	TL	Graphite zone

Table 17
Gold and silver analyses for grab samples of various rock types, Tartan Lake.

Sample Number	Au (ppb)	Ag (ppm)	Sample Location	Field Description	
TL-162C	< 12	3	36 + 50N/31 + 00E	TL	Knotted gabbro
TL-162A	< 12	< 1	36 + 50N/31 + 00E	TL	Gabbro
TL-31-G-1	< 12	< 1	23 + 70N/25 + 80W	RLE	Gabbro
TL-27-G-5	< 12	< 1	10 + 00N/27 + 20W	RLE	Pyroxene-phyric breccia
TL-25-G-1	< 12	< 1	16 + 00N/26 + 80W	RLE	Gabbro
TL-23-G-2	< 12	< 1	20 + 70N/24 + 00W	RLE	Gabbro
TL-23-G-1	< 12	3	20 + 70N/24 + 00W	RLE	Intermediate dyke
TL-162	101	< 1	36 + 50N/31 + 00E	TL	Gabbro
TL-18.1	< 12	< 1	16 + 20S/15 + 30W	RLE	Massive basalt flow
TL-26-A-G.1	< 12	< 1	12 + 50N/26 + 30W	RLE	Layered volcaniclastic rocks
TL-26-A-G-1	< 12	< 1	12 + 50N/26 + 30W	RLE	Layered volcaniclastic rocks
TL-27-G-3	< 12	< 1	10 + 00N/27 + 20W	RLE	Volcaniclastic rock
TL-74-A-A	< 12	< 1	22 + 00S/22 + 50E	TL	Gabbro
TL-74-B-3	< 12	< 1	21 + 20S/21 + 30E	TL	Aphanitic intermediate dyke, gossan
TL-145.1	< 12	< 1	14 + 00N/ 0 + 00E		Pyroxene-phyric andesite
TL-157-A-3	< 12	< 1	26 + 00N/29 + 00E		Fine grained intermediate dyke, gossan
TL-157-A-4	< 12	< 1	26 + 00N/29 + 00E		Shear zone
TL-421	17	< 1	3 + 00N/ 5 + 00W	RL	Feldspar porphyry from trench
TL-423	< 12	< 1	3 + 00N/ 5 + 00W	RL	Volcanic rock
TL-528.3	55		3 + 75N/ 4 + 90E	TL	Intermediate dyke
TL-556.2	< 12		0 + 25S/ 8 + 15E	TL	Diorite, altered
TL-566.1	< 12		5 + 00N/ 7 + 00E	TL	Diorite, altered
TL-566.3	38		5 + 00N/ 7 + 00E	TL	Intermediate rock, fine grained, non-poorly schistose
TL-570.2	< 12		3 + 80N/ 6 + 00E	TL	Diorite, altered, fine grained
TL-575.1	< 12		0 + 55S/ 0 + 20E	TL	Intermediate dyke, fine grained

RL = Ruby Lake Grid
TL = Tartan Lake Grid
RLE = extrapolated from Ruby Lake grid coordinates

MINERALIZATION

SUMMARY OF EXPLORATION HISTORY

A summary of the exploration history for the area including the Tartan Lake deposit is given in Table 18.

TABLE 18
EXPLORATION HISTORY OF THE TARTAN LAKE DEPOSIT
(after Mineral Inventory Card 63K/13 Au2, Manitoba Energy and Mines)

1931	Monica 2 claim staked by Ed Fahey. Killarney claims staked by Thomas Creighton.
1932	Surface work on the Killarney claim yielded assays from 0.09 oz/ton Au over 15 feet to 5.01 oz/ton Au over 1 foot (Brownell, 1932, unpublished report, Manitoba Energy and Mines, Minerals Division). The Monica 2 claim was optioned to Consolidated Mining and Smelting Co. of Canada. Assays of 0.11 to 0.14 oz/ton Au over 7 feet were obtained from surface trenches.
1939	Thomas Creighton and Edmund Patton were issued a mining lease for the Killarney claim.
1945-1947	Killarney claim optioned to Nesnah Mining and Exploration Co. Ltd. At least 37 diamond drillholes (3600 ft. total) were drilled in the general vicinity of the Baseline Zone. The mineralization was traced for 1200 feet along strike. The best section obtained was 0.847 oz/ton Au over 7.8 feet including one foot of 7.58 oz/ton Au.
1960	Killarney claim cancelled.
1961	Area of Killarney claim staked as Lin claim by J. Murray.
1971	Monica claim cancelled.
1972	Area of Monica claim restaked by A. Jacobson as C.B. 4885.
1974	C.B. 4885 cancelled.
1976	Lin claim cancelled.
1977-1981	C.B. 8525, Veb, Tort claims staked by Granges Exploration Aktiebolag.
1981-1987	Diamond drilling outlined deposit with ore reserves of 513 000 tons of 0.349 oz/ton Au to a depth of 1150 feet.
1987	Mill construction completed and production commenced at 500 ton/day mill capacity.

ZONES OF MINERALIZATION

Gold has been identified in three geological settings in the Tartan Lake area, namely: 1) the Main Zone of the mine; 2) the South Zone and similar areas of carbonate and chlorite alteration in the 5 East and Baseline Zones; and, 3) in quartz veins of Zone 10 ('glory hole') and Zone 8 type (see Fig. 18).

Main Zone

The Main Zone of the mine was not investigated during the field aspect of this project. A brief examination of the underground workings was made during a mine visit in August, 1987. The upper portions of the deposit (Fig. 26) contain abundant late veins of white quartz ± gold and disrupted schistose, auriferous, pyritic lenses of altered feldspar porphyry dyke and chlorite schist. The lower levels of the orebody contain only minor vein quartz and consist mainly of a pyritic and sericitic schistose feldspar porphyry that in thin section resembles the felsic dykes from the Mine Peninsula.

South Zone, 5 East Zone, Baseline Zone

The South Zone, 5 East and Baseline Zones are major zones of extensive alteration, and visible gold has been recorded from a number of places within each of these zones. An ore zone has been delineated by drilling and underground workings at the South Zone. These zones are characterized by chloritic schists that have been disrupted by extensive carbonatization, minor pyritization, as well as veins, lenses and pods of quartz and tourmaline. Some of the carbonate, quartz and tourmaline are deformed within the chlorite schist fabric; some fill later tension fractures (Fig. 26, 22).

The timing of carbonatization events in these alteration zones is not certain since the carbonate rarely exhibits a planar fabric except in late fault zones. Apparently undeformed pods and lenses of Fe-carbonate are common and carbonatized mafic rocks at the margins of the alteration zones commonly do not exhibit a chlorite-defined schistosity. Visible gold in quartz veins within these zones is interpreted as mobilization of gold (± sulphide) and quartz from within the alteration zone itself by post-deposition mobilization.

Other Zones

Narrow (15-30 cm) quartz veins at Zone 10 (glory hole') and Zone 8 contain abundant visible gold. These are simple quartz veins that are interpreted as fracture fillings. Minor carbonatization of the host rocks resulted in a pale straw coloured altered gabbro on fresh surfaces that differs from earlier alteration in that chlorite is not developed. The timing of the gold-quartz mobilization is

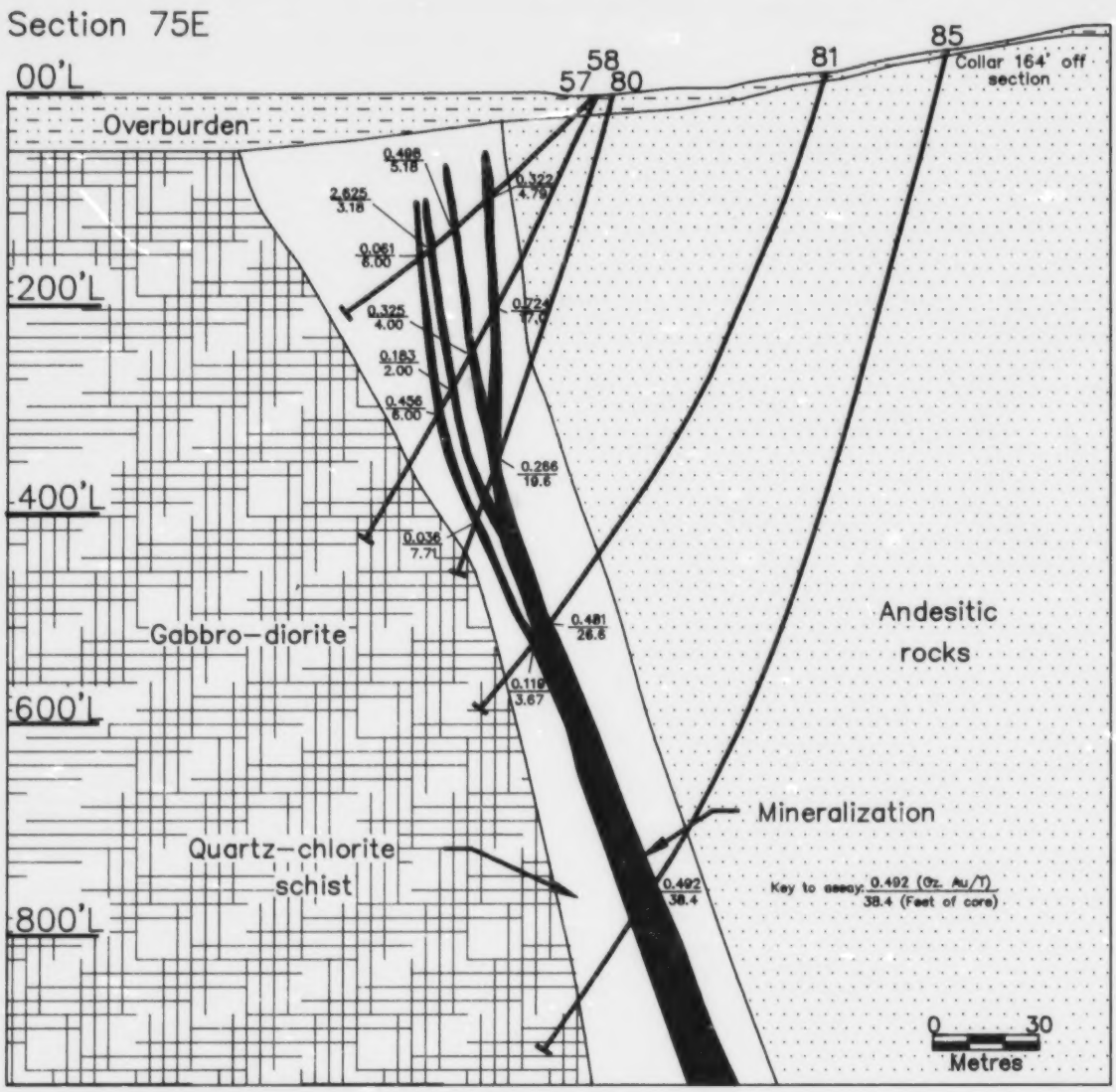

Figure 26: Cross-section of the Tartan Lake Main Zone. Compliments of Granges Exploration Ltd., September, 1987.

probably the same in both the tension veins and the major altered zones. This mobilization preceded the late faults identified in the South Zone and the north end of the 5 East Zone.

EXPLORATION POTENTIAL

Only limited conclusions can be drawn from this study since the surface exposures examined represent different geological environments from that of the Main Zone deposit.

The geological data indicate: (1) the gold mineralization did not accompany the felsic intrusive magma, but was superimposed upon the dykes after their emplacement; (2) the presence of pyrite in the feldspar porphyry dykes is not an indication of gold content; and (3) sericite and sulphide minerals accompany the gold mineralization, but there is not an apparent one-to-one correlation.

Within the gabbro body ore zones will probably be restricted to thick zones of carbonate-chlorite-sericite-pyrite-tourmaline alteration with strikes of approximately 250° and 025°. Narrow quartz-carbonate tension veins are late leakage haloes and although they may have high Au contents, their greatest value is as indicators of gold in nearby source rocks.

One procedure that could be adopted is to delineate all zones of schistose and altered rocks within the gabbro using the same techniques as used here in the South Block. This would be followed by gold analyses of rock samples and tills from topographic depressions that correspond to the defined structures. It

appears from the work done to date that the gold mineralization is:

- 1. younger than the feldspar porphyry dykes;
- 2. older than the late faults and shears;
- 3. the same age as sericitization of feldspar dykes, and therefore was not introduced with the dykes;
- 4. probably related to carbonatization of the gabbro;
- 5. locally a product of mobilization and concentration in response to late faulting;
- 6. associated with a pyritic, sericitic and carbonatized feldspar porphyry dyke in the Main Zone;
- 7. not associated with early fault structures;
- 8. not directly associated with major (regional) faults;
- 9. commonly present in quartz vein leakage haloes.

REFERENCES

Balles, A.H.
1971: Preliminary compilation of the geology of the Snow Lake-Flin Flon-Sherridon area; Manitoba Mines Branch, Geological Paper 1/71, 27 p.

Balles, A.H. and Syme, E.C.
1987: Geology of the Flin Flon-White Lake area; Manitoba Energy and Mines, Geological Map GR87-1-1, Scale 1:20 000.

Bateman, J.D.
1945: Gold deposits east of Flin Flon, Manitoba; Geological Survey of Canada, Paper 45-12, p. 3-5.

Bateman, J.D. and Harrison, J.M.
1945: Mikanagan Lake, Manitoba; Geological Survey of Canada, Map 632A, Scale 1:63 360.

Bruce, E.L.
1918: Amisk-Athapapuskow Lake district; Geological Survey of Canada, Memoir 105.

Carmichael, I.S.E., Turner, J.F., and Verhoogen, J.
1974: Igneous Petrology; McGraw Hill, 739 p.

Gilbert, H.P.
1986: Geological investigations in the Tartan Lake-Lac Almée area; in Manitoba Energy and Mines, Report of Field Activities 1986, p. 43-48.

Josse, G.R.
1974: Rubidium-strontium age determinations from the Flle-Morton-Woosey lakes area of the Flin Flon volcanic belt, west central Manitoba; University of Manitoba, M.Sc. thesis, unpublished.

Mineral Inventory Card 63K/13 Au2;
Manitoba Energy and Mines, Minerals Division.

Mukherjee, A.C., Stauffer, M.R. and Baadsgaard, H.
1971: The Hudsonian Orogeny near Flin Flon, Manitoba: a tentative interpretation of Rb/Sr and K-Ar ages; Canadian Journal of Earth Sciences, v. 8, p. 939-946.

Peloquin, S. and Gale, G.H.
1985: Geological setting of the Tartan Lake gold deposit; in Manitoba Energy and Mines, Report of Field Activities 1985, p. 71-73.

Peloquin, S. Tannahill, B. and Gale, G.H.
1986: Geology of the Tartan Lake gold deposit; in Manitoba Energy and Mines, Report of Field Activities 1985, p. 56-64.

Shanks, R.J. and Balles, A.H.
1977: "Missi Group" Rocks, Wekusko Lake Area; in Manitoba Mineral Resources Division, Report of Field Activities 1977, p. 83-87.

Stauffer, M.S., Mukherjee, A.C. and Koo, J.
1975: The Amisk Group: an Aphebian(?) island arc deposit; Canadian Journal of Earth Sciences, v. 12, p. 2021-2035.

Tanton, T.L.
1941: Flin Flon, Saskatchewan and Manitoba; Geological Survey of Canada, Map 613A, Scale 1:63 360.

APPENDIX I: TARTAN LAKE - MAJOR ELEMENT ANALYSES.

Sample Number	SiO_2 (%)	Al_2O_3 (%)	FeO(T) (%)	CaO (%)	MgO (%)	Na_2O (%)	K_2O (%)	TiO_2 (%)	P_2O_5 (%)	MnO (%)	LOI (%)	TOTAL (%)	CO_2 (%)
TL-23-G-1	49.4	19.4	9.80	12.80	3.20	0.70	0.30	0.6	0.35	0.14	2.9	99.59	-
TL-23-G-2	48.7	20.5	6.80	13.20	6.10	2.30	0.10	0.3	0.04	0.11	2.4	100.55	-
TL-25-G-1	46.6	13.4	18.00	8.30	5.90	3.30	0.10	1.7	0.05	0.18	2.8	100.33	-
TL-27-G-5	51.4	13.2	12.00	8.80	7.80	1.80	1.40	0.2	0.11	0.19	2.0	98.90	-
TL-31-G-1	47.9	17.0	8.40	13.50	8.40	1.60	0.10	0.4	0.03	0.15	2.4	99.88	-
TL-52.3	65.7	12.5	6.33	6.69	2.95	3.51	1.54	0.3	0.09	0.10	3.4	103.11	0.94
TL-87-14	78.8	9.3	0.94	1.35	0.17	3.56	1.46	0.2	0.09	0.03	1.4	97.32	-
TL-162A	48.3	14.4	14.00	10.00	7.70	1.80	0.20	0.5	0.05	0.22	2.2	99.37	-
TL-162C	46.4	15.3	12.10	9.70	7.40	3.00	0.30	0.5	0.05	0.18	5.0	99.93	-
TL-553.1	48.2	12.1	5.88	8.39	10.51	1.31	0.81	0.2	0.03	0.13	11.5	99.06	4.50
TL-563.1	39.1	12.6	4.96	11.10	7.62	0.57	3.31	0.2	0.03	0.13	19.0	98.62	14.74
TL-570.3	48.0	18.0	8.81	7.65	4.35	5.03	0.43	0.8	0.35	0.17	5.7	99.29	2.58
TL-573.1	60.4	17.0	5.36	4.40	2.47	5.83	1.86	0.6	0.24	0.07	1.8	100.03	0.93
TL-573.2	47.8	10.8	6.78	14.91	14.78	0.47	0.16	0.3	0.02	0.15	2.4	98.57	0.64
TL-574.1	44.7	19.1	10.25	11.28	5.02	2.59	1.38	1.0	0.49	0.21	2.5	98.52	0.07
TL-574.2	49.1	13.9	6.24	13.56	11.49	1.22	1.05	0.3	0.02	0.16	1.9	98.94	0.34
TL-586.1	37.2	15.5	13.51	10.86	7.64	0.85	0.53	1.6	1.10	0.15	7.3	96.24	3.04
TL-606.1	52.8	15.6	8.64	10.54	5.79	2.09	0.86	0.4	0.13	0.14	2.3	99.29	0.62
TL-662.1	61.8	16.4	4.48	4.69	2.57	5.37	2.06	0.5	0.19	0.07	1.3	99.44	-
TL-667.1	65.6	13.5	8.21	3.55	1.77	2.40	2.68	0.5	0.25	0.17	1.0	99.63	0.12
TL-669.1a	62.5	16.4	3.33	3.67	1.42	4.25	2.93	0.4	0.15	0.05	3.9	99.00	1.39
TL-669.1b	62.3	15.8	3.39	7.47	1.70	2.38	4.14	0.4	0.15	0.05	4.9	102.68	1.87
TL-672.1	56.3	12.9	16.88	2.22	2.91	0.56	2.73	0.4	0.22	0.09	2.6	97.82	-
TL-674.1	62.0	16.0	3.58	4.33	2.67	6.48	0.49	0.5	0.13	0.05	3.3	99.53	1.25
TL-676.1	55.3	16.4	6.11	4.48	2.20	5.17	2.34	0.5	0.26	0.08	5.7	98.58	-
TL-678.1	57.6	16.7	5.76	5.09	2.26	4.46	2.99	0.6	0.25	0.11	3.0	98.78	-
TL-682.1	62.0	16.4	4.39	4.86	2.47	5.20	1.91	0.5	0.19	0.06	0.9	98.90	-
TL-687.1	60.0	17.1	5.30	5.08	2.06	5.90	0.59	0.5	0.25	0.09	2.4	99.30	-
TL-689.3	49.6	12.1	15.25	6.04	6.82	2.78	1.04	2.3	0.16	0.27	2.3	98.66	0.15
TL-689.4	46.5	12.9	8.11	14.58	9.14	1.29	0.79	0.6	0.07	0.17	3.9	98.05	1.52
TL-690.1	48.5	13.6	5.85	12.72	9.33	1.65	1.14	0.3	0.06	0.13	5.4	98.68	2.82
TL-691.1	45.6	15.2	12.60	11.07	7.43	1.56	0.18	0.8	0.07	0.20	3.4	98.11	0.84
TL-696.1	63.8	12.6	8.82	3.43	2.10	2.73	1.17	0.4	0.28	0.17	2.8	98.29	-
TL-697.1	56.4	13.4	4.63	13.32	6.41	0.54	0.33	0.2	0.05	0.10	3.3	98.68	1.37
TL-699.1	64.4	13.4	9.67	0.85	2.56	2.07	2.11	0.3	0.10	0.18	3.2	98.85	-
TL-712.1	52.9	18.6	7.55	7.71	3.39	3.27	2.89	0.8	0.35	0.18	1.5	99.14	0.14
TL-720.1	51.8	17.0	7.50	5.53	3.05	3.73	2.94	0.9	0.38	0.14	6.3	99.27	2.92
TL-727.1	67.3	13.7	5.65	3.55	1.25	3.60	2.38	0.4	0.28	0.13	1.1	99.33	-
TL-728.1	63.7	12.8	9.13	3.64	1.98	2.58	2.12	0.4	0.25	0.19	2.7	99.44	-
TL-729.2	62.1	13.2	9.28	4.70	2.03	2.63	1.69	0.4	0.34	0.26	2.6	99.24	-
TL-730.1	63.7	13.5	8.18	4.46	1.72	3.10	1.28	0.3	0.24	0.24	2.3	99.10	-
TL-731.1	54.3	11.4	9.28	7.84	9.97	3.12	0.72	0.3	0.11	0.16	1.7	98.90	0.12
RL-586	58.5	17.1	5.84	6.08	2.18	4.88	0.89	0.5	0.30	0.06	1.9	98.27	-
RL-591A	57.7	15.8	4.41	6.27	2.33	2.21	3.84	0.5	0.21	0.12	5.7	99.07	-
RL-615	63.0	16.0	3.60	4.72	1.66	6.41	0.42	0.4	0.16	0.03	3.0	99.40	-
RL-617A	59.6	16.1	5.13	3.96	2.26	4.77	2.14	0.5	0.23	0.05	4.8	99.58	-
RL-617B	52.4	13.1	9.99	5.34	5.56	1.80	0.97	0.9	0.12	0.18	7.6	97.98	-
RL-622	55.3	16.5	8.29	4.35	2.59	5.47	2.44	0.7	0.31	0.16	2.7	98.82	-
RL-623	62.2	15.2	7.27	4.89	2.16	1.46	3.65	0.7	0.22	0.14	1.3	99.18	-
RL-627	55.1	17.7	4.57	5.58	3.06	5.61	1.56	0.8	0.39	0.08	4.6	99.03	-
RL-629	66.0	16.2	2.88	2.04	1.11	5.37	2.50	0.3	0.13	0.02	2.6	99.15	-
RL-638	53.8	16.5	9.85	5.89	3.12	4.55	2.34	0.8	0.44	0.16	1.4	98.85	-

APPENDIX II: ICP ANALYSES FOR ROCKS FROM THE TARTAN LAKE AREA.

Sample Number	Mo (ppm)	Cu (ppm)	Pb (ppm)	Zn (ppm)	Ag (ppm)	Ni (ppm)	Mn (ppm)	Fe (%)	As (ppm)	U (ppm)	Th (ppm)	Sr (ppm)	Cd (ppm)	Sb (ppm)
RL-501	1	18	2	79	0.1	32	705	4.28	2	5	1	13	1	2
RL-502	1	1	2	44	0.1	5	368	2.99	2	5	6	98	1	2
RL-504	1	163	2	22	0.2	12	208	1.04	35	5	1	32	1	2
RL-506	1	200	17	44	0.4	22	389	3.04	5	5	3	45	1	2
RL-515	1	4	6	64	0.2	8	503	2.13	2	5	9	162	1	2
RL-516	1	480	3	49	0.1	5	423	2.80	2	5	1	43	1	2
RL-519	1	81	4	31	0.1	7	274	2.79	30	5	6	80	1	2
RL-523	1	129	4	74	0.1	29	630	4.51	2	5	1	23	1	2
RL-533	1	205	3	21	0.1	21	226	1.93	8	5	1	35	1	2
RL-548	1	1	2	57	0.2	7	611	3.04	7	5	5	102	1	2
RL-551	1	411	7	43	0.2	31	950	3.56	6	5	1	125	1	2
RL-569	1	25	2	24	0.2	17	375	1.99	33	5	1	44	1	3
RL-573	1	5	2	64	0.1	50	1011	5.42	35	5	1	86	1	164
RL-576	1	8	4	77	0.1	36	930	6.12	40	5	1	39	1	2
RL-579A	1	12	3	50	0.1	10	481	3.04	2	5	4	62	1	2
RL-586	1	32	2	36	0.1	4	329	3.24	10	5	7	56	1	4
RL-591A	1	14	8	84	0.2	6	725	1.99	3	5	5	105	1	2
RL-597	1	3	2	15	0.1	32	331	1.24	12	5	1	61	1	2
RL-615	1	12	2	18	0.1	6	227	2.00	2	5	3	46	1	2
RL-616	1	128	3	50	0.1	22	561	4.42	37	5	1	35	1	2
RL-617A	1	3	6	50	0.2	4	351	3.15	2	5	7	96	1	2
RL-617B	1	89	3	76	0.1	29	1068	6.64	5	5	1	132	1	2
RL-622	1	144	6	96	0.1	7	1057	5.68	9	5	2	62	1	2
RL-623	1	96	2	117	0.1	5	787	4.46	5	5	2	28	1	2
RL-627	1	34	2	36	0.1	8	526	3.02	4	5	7	51	1	2
RL-629	1	7	3	17	0.1	1	127	1.56	3	5	8	40	1	2
RL-638	1	235	5	67	0.2	4	789	5.47	8	5	3	44	1	2
TL-513A	2	9	7	68	0.1	7	700	5.60	4	5	2	65	1	2
TL-513C	1	75	3	60	0.1	22	502	4.21	7	5	1	101	1	2
TL-528.2	1	22	2	31	0.1	129	807	3.89	7	5	2	88	1	2
TL-553.1	2	5	5	47	0.2	112	815	3.56	5	5	3	109	1	2
TL-563.1	1	5	4	25	0.1	74	857	3.10	3	6	2	153	1	2
TL-570.2	1	69	2	73	0.1	7	544	5.68	2	5	2	21	1	4
TL-573.1	1	20	48	253	0.2	4	371	3.21	3	5	5	77	1	2
TL-577.1	1	12	6	34	0.1	3	223	2.15	3	5	6	84	1	2
TL-586.1	1	215	2	80	0.2	8	833	8.15	21	5	3	103	1	2
TL-588.4	1	709	2	19	0.2	34	908	1.77	2	10	3	292	1	2
TL-589.1	1	267	5	94	0.1	7	741	8.54	8	5	2	91	1	2
TL-592.1	1	18	2	73	0.1	4	578	3.05	4	5	5	74	1	2
TL-656.1	2	108	2	222	0.1	1	1191	5.23	34	5	2	25	1	2
TL-660.1	1	90	8	108	0.1	3	974	5.94	2	5	2	32	1	2
TL-662.1	1	1	4	40	0.3	24	363	2.36	2	5	4	90	1	2
TL-667.1	2	79	4	79	0.1	1	755	5.78	4	5	1	16	1	2
TL-672.1	1	436	9	177	0.1	5	553	12.64	26	5	2	13	1	2
TL-678.1	1	16	3	60	0.1	4	717	3.77	7	5	6	64	1	2
TL-682.1	1	2	4	36	0.1	21	288	2.18	2	5	4	97	1	2
TL-687.1	3	135	2	71	0.2	8	541	3.29	17	5	4	60	1	2
TL-689.3	1	52	6	89	0.1	13	845	6.33	4	5	1	9	1	2
TL-689.4	1	28	3	31	0.1	53	423	2.01	16	5	2	55	1	2
TL-696.1	1	159	9	249	0.1	4	1252	6.55	6	5	2	29	1	2
TL-699.1	1	4	3	199	0.1	1	1249	7.04	3	5	2	22	1	2
TL-720.2	1	2	2	90	0.1	7	619	6.18	6	5	5	113	1	2

Sample Number	Mo (ppm)	Cu (ppm)	Pb (ppm)	Zn (ppm)	Ag (ppm)	Ni (ppm)	Mn (ppm)	Fe (%)	As (ppm)	U (ppm)	Th (ppm)	Sr (ppm)	Cd (ppm)	Sb (ppm)
TL-727.1	1	125	2	83	0.2	1	742	3.41	2	5	2	34	1	2
TL-728.1	1	74	2	143	0.1	1	1297	6.64	6	5	2	26	1	2
TL-729.2	1	173	6	180	0.2	1	1756	6.51	2	5	2	64	1	2
TL-730.1	1	68	6	263	0.1	2	1541	5.60	2	5	2	48	1	2
TL-731.1	1	10	3	30	0.3	21	350	2.78	2	5	1	12	1	2

Sample Number	Bi (ppm)	Ca (%)	P (%)	La (ppm)	Cr (ppm)	Mg (%)	Ba (ppm)	Ti (%)	B (ppm)	Al (%)	Na (%)	K (%)	Au (ppb)
RL-501	2	0.38	0.044	2	123	3.81	149	0.11	2	2.94	0.08	0.52	1
RL-502	2	1.57	0.092	25	2	1.13	281	0.12	4	1.88	0.13	0.64	1
RL-504	2	0.66	0.035	2	10	0.52	44	0.10	4	0.81	0.13	0.18	1
RL-506	2	0.89	0.100	12	35	1.58	49	0.15	2	1.57	0.13	0.09	1
RL-515	2	1.64	0.087	32	6	1.11	127	0.13	3	1.53	0.15	0.26	1
RL-516	2	2.27	0.022	2	5	1.29	139	0.14	3	1.80	0.13	1.14	1
RL-519	2	1.59	0.092	24	5	1.11	126	0.04	4	1.62	0.14	0.28	94
RL-523	2	4.09	0.055	2	59	3.59	56	0.11	2	3.02	0.13	0.30	1
RL-533	2	0.79	0.032	2	82	0.78	48	0.07	6	0.81	0.12	0.13	1
RL-548	2	3.14	0.094	23	11	1.27	120	0.09	5	1.85	0.12	0.23	1
RL-551	2	12.14	0.018	2	98	2.18	68	0.04	2	2.15	0.15	0.30	2
RL-569	2	1.84	0.043	2	38	0.93	165	0.08	3	1.27	0.10	0.57	4
RL-573	2	10.02	0.038	6	309	3.24	5	0.03	2	3.18	0.13	0.03	2
RL-576	2	2.03	0.046	2	89	3.74	22	0.08	2	3.63	0.10	0.07	6
RL-579A	2	1.16	0.089	18	8	1.57	108	0.16	3	1.99	0.16	0.53	3
RL-586	2	1.13	0.113	28	3	1.18	78	0.14	3	1.49	0.15	0.19	2
RL-591A	2	4.85	0.074	16	5	1.01	132	0.09	8	1.46	0.11	0.57	1
RL-597	2	8.16	0.026	5	123	0.94	28	0.09	3	1.27	0.11	0.14	1
RL-615	2	2.58	0.059	13	10	0.81	44	0.10	10	1.12	0.18	0.11	1
RL-616	2	0.77	0.018	2	2	1.70	266	0.43	5	2.00	0.10	0.74	2
RL-617A	2	3.46	0.088	30	8	1.21	166	0.04	3	1.76	0.15	0.29	1
RL-617B	2	4.85	0.041	6	43	3.38	46	0.05	2	3.44	0.12	0.06	3
RL-622	2	1.66	0.111	5	18	1.52	440	0.28	2	2.60	0.15	1.57	2
RL-623	3	0.50	0.076	5	4	1.15	310	0.25	3	2.39	0.08	1.79	6
RL-627	2	3.63	0.148	32	10	1.86	103	0.15	2	2.04	0.16	0.51	45
RL-629	2	1.08	0.047	28	3	0.47	186	0.02	6	0.78	0.12	0.27	3
RL-638	2	0.99	0.156	9	1	1.40	617	0.28	2	2.39	0.14	1.62	2
TL-513A	2	1.95	0.188	5	3	2.12	126	0.16	2	2.68	0.14	0.30	1
TL-513C	2	1.67	0.047	2	22	2.46	85	0.25	2	2.63	0.13	0.30	7
TL-528.2	3	8.16	0.004	2	419	6.69	5	0.01	2	2.26	0.14	0.01	1
TL-553.1	3	6.63	0.007	2	346	5.59	9	0.01	2	3.61	0.12	0.02	3
TL-563.1	3	8.88	0.009	2	41	4.31	25	0.01	2	1.06	0.14	0.15	1
TL-570.2	2	3.92	0.118	6	3	3.85	50	0.03	2	2.83	0.13	0.09	10
TL-573.1	2	1.28	0.092	18	1	1.36	358	0.17	2	1.77	0.17	0.73	1
TL-577.1	2	0.91	0.094	22	3	0.84	294	0.22	5	1.29	0.17	0.55	9
TL-586.1	2	4.80	0.526	6	1	4.57	15	0.13	2	4.26	0.12	0.04	1
TL-588.4	3	13.75	0.023	3	92	1.24	26	0.01	2	1.14	0.17	0.06	24
TL-589.1	2	3.67	0.194	3	1	4.31	48	0.04	2	4.56	0.11	0.15	9
TL-592.1	2	0.83	0.094	21	4	1.42	90	0.18	2	1.81	0.16	0.23	1
TL-656.1	2	0.89	0.028	9	2	1.21	97	0.14	2	2.39	0.10	0.96	1
TL-660.1	2	1.46	0.072	8	1	1.75	63	0.08	2	2.70	0.10	0.46	1
TL-662.1	2	0.99	0.068	13	12	1.37	390	0.19	2	1.81	0.18	1.07	1
TL-667.1	2	0.44	0.089	3	3	0.93	581	0.20	2	2.58	0.11	1.67	1
TL-672.1	2	0.26	0.070	3	1	1.76	391	0.21	7	4.35	0.07	1.65	36
TL-678.1	2	2.25	0.091	22	4	1.30	534	0.23	4	2.18	0.16	1.44	1

Sample Number	Bi (ppm)	Ca (%)	P (%)	La (ppm)	Cr (ppm)	Mg (%)	Ba (ppm)	Ti (%)	B (ppm)	Al (%)	Na (%)	K (%)	Au (ppb)
TL-682.1	2	0.78	0.070	13	13	1.10	405	0.19	3	1.58	0.18	0.83	1
TL-687.1	2	1.65	0.089	14	8	1.26	68	0.17	2	1.75	0.15	0.18	3
TL-689.3	2	0.97	0.053	2	1	2.01	271	0.64	2	2.43	0.16	0.62	1
TL-689.4	3	3.26	0.023	2	202	1.58	84	0.15	3	1.61	0.10	0.31	4
TL-696.1	2	1.31	0.097	3	2	1.27	105	0.13	2	2.65	0.11	0.50	2
TL-699.1	2	0.45	0.034	9	1	1.52	76	0.07	2	2.88	0.08	0.43	3
TL-720.2	2	2.39	0.181	23	3	2.66	85	0.04	32	3.33	0.09	0.37	1
TL-727.1	3	0.67	0.097	5	1	0.68	349	0.18	2	1.64	0.12	1.14	4
TL-728.1	2	1.44	0.084	3	1	1.12	349	0.19	2	2.75	0.12	1.25	1
TL-729.2	2	1.52	0.121	4	1	1.20	433	0.20	2	2.75	0.11	1.09	2
TL-730.1	2	1.21	0.079	4	3	0.93	188	0.16	2	2.34	0.12	0.74	1
TL-731.1	2	0.56	0.036	2	144	1.94	176	0.09	2	1.56	0.12	0.42	1

APPENDIX III: GOLD AND SILVER ANALYSES FOR GRAB SAMPLES FROM THE TARTAN LAKE AREA.

Sample Number	Au (ppb)	Ag (ppm)	Sample Location	Field	Description
TL-1.2	< 12	< 1	26 + 00N/ 19 + 00W	RLE	Quartz from small shear
TL-4.4	45	< 1	17 + 80S/ 20 + 50W	RLE	Quartz-tourmaline vein
TL-4.5A	< 12	< 1	17 + 80S/ 20 + 50W	RLE	Quartz-tourmaline vein, from shear
TL-4.5B	< 12	< 1	17 + 80S/ 20 + 50W	RLE	Quartz-tourmaline vein, not from shear
TL-5.1	17	< 1	14 + 70S/ 22 + 30W	RLE	Quartz vein
TL-5.5	< 12	< 1	14 + 70S/ 22 + 30W	RLE	Quartz vein
TL-13.1	45	< 1	14 + 50S/ 21 + 25W	RLE	Quartz vein, from shear
TL-13.2	< 12	< 1	14 + 50S/ 21 + 25W	RLE	Shear
TL-17.2	< 12	< 1	9 + 50S/ 17 + 30W	RLE	Feldspar porphyry
TL-18.1	< 12	< 1	16 + 20S/ 15 + 30W	RLE	Massive basalt flow
TL-18.X	< 12	< 1	16 + 20S/ 15 + 30W	RLE	Feldspar porphyry or crystal tuff
TL-22.2	< 12	< 1	21 + 00N/ 18 + 30W	RLE	Quartz vein
TL-23-G-2	< 12	< 1	20 + 70N/ 24 + 00W	RLE	Gabbro
TL-23-G-1	< 12	3	20 + 70N/ 24 + 00W	RLE	Intermediate dyke
TL-25-G-1	< 12	< 1	16 + 00N/ 26 + 80W	RLE	Gabbro
TL-26-A-G.1	< 12	< 1	12 + 50N/ 26 + 30W	RLE	Layered volcaniclastic rocks
TL-26-A-G-1	< 12	< 1	12 + 50N/ 26 + 30W	RLE	Layered volcaniclastic rocks
TL-27-C-G-1	< 12	< 1	10 + 00N/ 27 + 20W	RLE	Felsic tuff
TL-27-G-2	< 12	< 1	10 + 00N/ 27 + 20W	RLE	Quartz and gossan
TL-27-G-3	< 12	< 1	10 + 00N/ 27 + 20W	RLE	Volcaniclastic rock
TL-27-G-5	< 12	< 1	10 + 00N/ 27 + 20W	RLE	Pyroxene-phyric breccia
TL-31-G-1	< 12	< 1	23 + 70N/ 25 + 80W	RLE	Gabbro
TL-49.1	< 12	< 1	14 + 80S/ 6 + 70W	RLE	Quartz vein
TL-59.1	< 12	< 1	11 + 80S/ 28 + 30W	RLE	Quartz vein, from shear
TL-71.1A	< 12	< 1	30 + 00S/ 19 + 00E	TL	Feldspar porphyry
TL-72.2	< 12	< 1	29 + 50S/ 24 + 30E	TL	Feldspar porphyry
TL-74-A-1	< 12	< 1	22 + 00S/ 22 + 50E	TL	Quartz
TL-74-A-A	< 12	< 1	22 + 00S/ 22 + 50E	TL	Gabbro
TL-74-B-3	< 12	< 1	21 + 20S/ 21 + 30E	TL	Aphanitic intermediate dyke, gossan
TL-141-A-1	< 12	< 1	23 + 70N/ 0 + 20E	TL	Quartz vein
TL-145.1	< 12	< 1	14 + 00N/ 0 + 00E		Pyroxene-phyric andesite
TL-153.2	< 12	< 1	32 + 00N/ 34 + 20E	TL	Quartz vein
TL-156.6	< 12	< 1	24 + 00N/ 31 + 50E	TL	Quartz
TL-157-A-1	< 12	< 1	26 + 00N/ 29 + 00E		Feldspar porphyry
TL-157-A-3	< 12	< 1	26 + 00N/ 29 + 00E		Fine grained intermediate dyke, gossan
TL-157-A-4	< 12	< 1			Shear zone
TL-159.1	< 12	< 1	30 + 50N/ 27 + 50E	TL	Quartz from pit
TL-159.2	< 12	< 1	30 + 50N/ 27 + 50N	TL	Gossan from pit
TL-161.2	17	< 1	35 + 00N/ 34 + 00E	TL	Gossaned zone from trench
TL-161.3	< 12	< 1	35 + 00N/ 34 + 00E	TL	Quartz from trench
TL-162	101	< 1	36 + 50N/ 31 + 00E	TL	Gabbro
TL-162A	< 12	< 1	36 + 50N/ 31 + 00E	TL	Gabbro
TL-162B	< 12	6	36 + 50N/ 31 + 00E	TL	Rusty weathering schist from shear zone
TL-162C	< 12	3	36 + 50N/ 31 + 00E	TL	Knotted gabbro
TL-162.2	69	1	36 + 20N/ 31 + 00E	TL	Clinker or cinder graphite
TL-162.3	< 12	< 1	36 + 20N/ 31 + 00E	TL	Gossan zone
TL-162.4	17	< 1	36 + 20N/ 31 + 00E	TL	Graphite (clinker) with talc?
TL-162.5	< 12	< 1	36 + 20N/ 31 + 00E	TL	Quartz-rich zone from trench
TL-162.7	< 12	< 1	36 + 20N/ 31 + 00E	TL	Quartz, talc and gossan, from trench
TL-162.8	17	< 1	36 + 20N/ 31 + 00E	TL	Quartz in gossan, from trench

Sample Number	Au (ppb)	Ag (ppm)	Sample Location	Field	Description
TL-162.9	< 12	< 1	36 + 20N/31 + 00E	TL	Quartz in gossan, from trench
TL-162.1	< 12	< 1	36 + 20N/31 + 00E	TL	Grey schist
TL-176.2	< 12	< 1	15 + 60N/16 + 50E		Quartz vein
TL-193.1	< 12	< 1	6 + 55N/ 2 + 00E		Quartz from main zone
TL-378.1	< 12	< 1	25 + 00S/33 + 25E	TL	Quartz
TL-385-A	29	< 1	33 + 30N/33 + 80N	TL	Pyrite zone
TL-385-B	75	2	33 + 30N/33 + 80N	TL	Graphite zone
TL-385-C	57	3	33 + 30N/33 + 80N	TL	Graphite zone
TL-RLG-414	< 12	< 1	4 + 00S/15 + 40W	RL	Quartz vein
TL-415	< 12	< 1	4 + 75S/15 + 00E	RL	Chlorite schist from shear zone
TL-420	< 12	< 1	3 + 00N/ 5 + 00W	RL	Quartz from trench
TL-421	17	< 1	3 + 00N/ 5 + 00W	RL	Feldspar porphyry from trench
TL-422	162	< 1	3 + 00N/ 5 + 00W	RL	Quartz from trench
TL-423	< 12	< 1	3 + 00N/ 5 + 00W	RL	Volcanic rock
TL-424	508	< 1	3 + 00N/ 8 + 00W	RL	Quartz from trench
TL-425	< 12	< 1	3 + 00N/ 8 + 00W	RL	Feldspar porphyry from trench
TL-446	214	< 1	17 + 00S/20 + 00E	TL	Quartz from shear
TL-526.0	< 12		3 + 35N/ 9 + 15E	TL	Quartz
TL-528.3	55		3 + 75N/ 4 + 90E	TL	Intermediate dyke
TL-529.2	46		3 + 40N/ 4 + 20E	TL	Schist
TL-528.4	63		3 + 75N/ 4 + 90E	TL	Schist
TL-530.2	< 12		2 + 35N/ 4 + 35E	TL	Schist
TL-531.1	51		1 + 20N/ 3 + 20E	TL	Schist
TL-533.1	17		1 + 40S/ 3 + 90E	TL	Quartz
TL-551.1	8500		0 + 30N/ 8 + 00E	TL	Quartz
TL-551.2	< 12		0 + 30N/ 8 + 00E	TL	Schist
TL-556.2	< 12		0 + 25S/ 8 + 15E	TL	Diorite, altered
TL-566.1	< 12		5 + 00N/ 7 + 00E	TL	Diorite, altered
TL-566.2	< 12		5 + 00N/ 7 + 00E	TL	Chlorite-carbonate schist
TL-566.3	38		5 + 00N/ 7 + 00E	TL	Intermediate rock, fine grained, non-poorly schistose
TL-570.1	< 12		3 + 80N/ 6 + 00E	TL	Shear (schist)
TL-570.2	< 12		3 + 80N/ 6 + 00E	TL	Diorite, altered, fine grained
TL-575.1	< 12		0 + 55S/ 0 + 20E	TL	Intermediate dyke, fine grained
TL-576.1	< 12		0 + 60S/ 1 + 10E	TL	Feldspar quartz porphyry dyke
TL-579.1	< 12		0 + 20S/ 0 + 30E	TL	Feldspar quartz porphyry dyke
TL-581.2	17		1 + 25N/ 5 + 30E	TL	Schist and quartz
TL-585.1	20000		0 + 20S/ 9 + 50E	TL	Feldspar quartz porphyry dyke
TL-589.1	405		4 + 70N/10 + 75E	TL	Chlorite schist
TL-591.1	< 12		7 + 30N/13 + 00E	TL	Schist and quartz
TL-663.1	< 12		12 + 35N/10 + 95E	TL	Chlorite schist and quartz
TL-669.4	1079		14 + 20N/17 + 40E	TL	Quartz and schist
TL-674.2	1020		6 + 75N/ 1 + 15E	TL	Chlorite schist and quartz
TL-676.1	40		5 + 95N/ 0 + 50E	TL	Feldspar-quartz porphyry, from trench
TL-676.3	6000		5 + 95N/ 0 + 50E	TL	Quartz rubble
TL-685.1	13		8 + 45N/ 3 + 40E	TL	Chlorite schist
TL-720.2	< 12		19 + 30N/ 4 + 20E	TL	Chlorite schist
TL-721.1	< 12		17 + 55N/ 5 + 60E	TL	Quartz-chlorite schist

APPENDIX IV: SAMPLE LOCATIONS.

Figure A: Sample locations for the Mine Peninsula area.

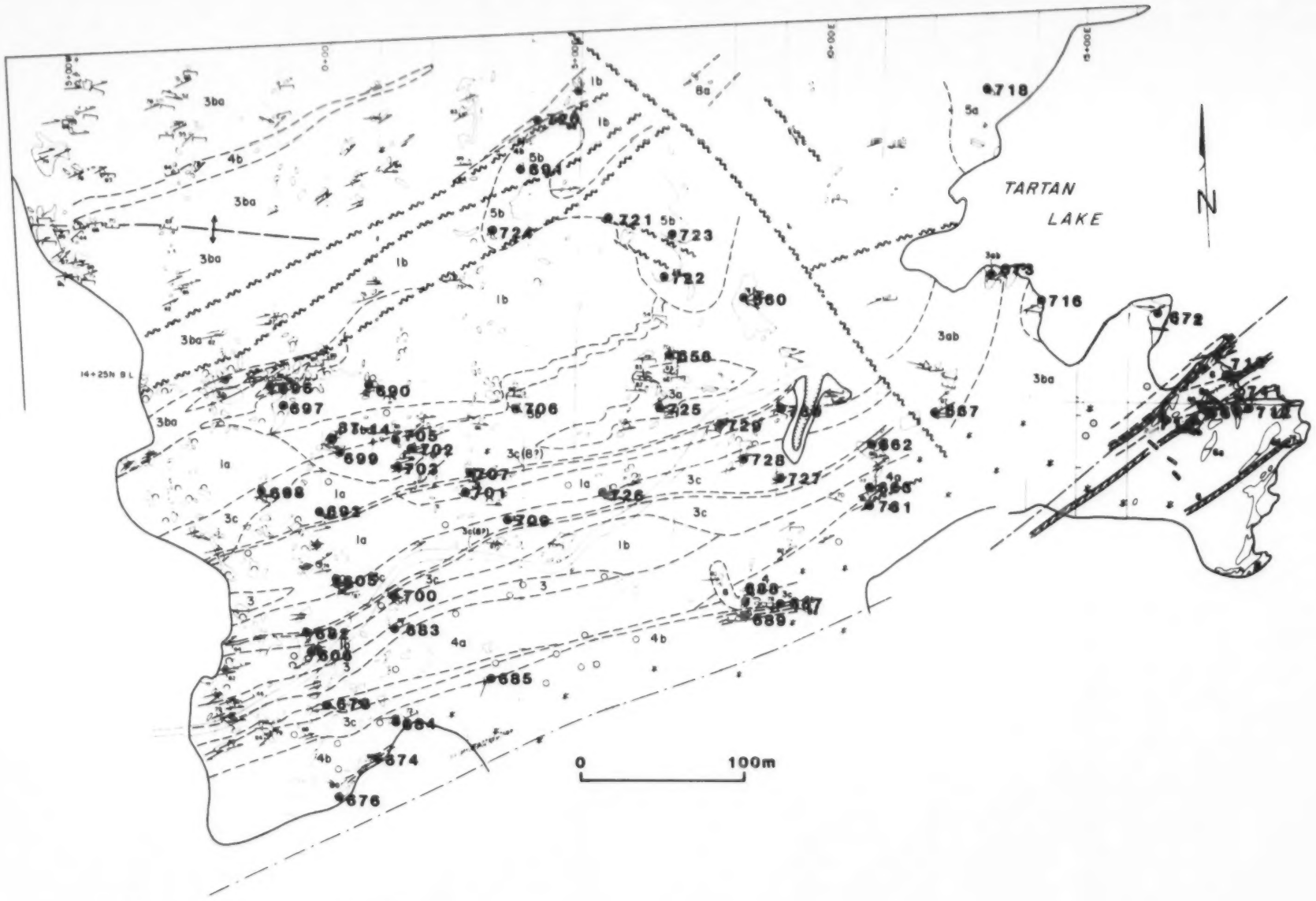

Figure B: Sample locations for the South Block.

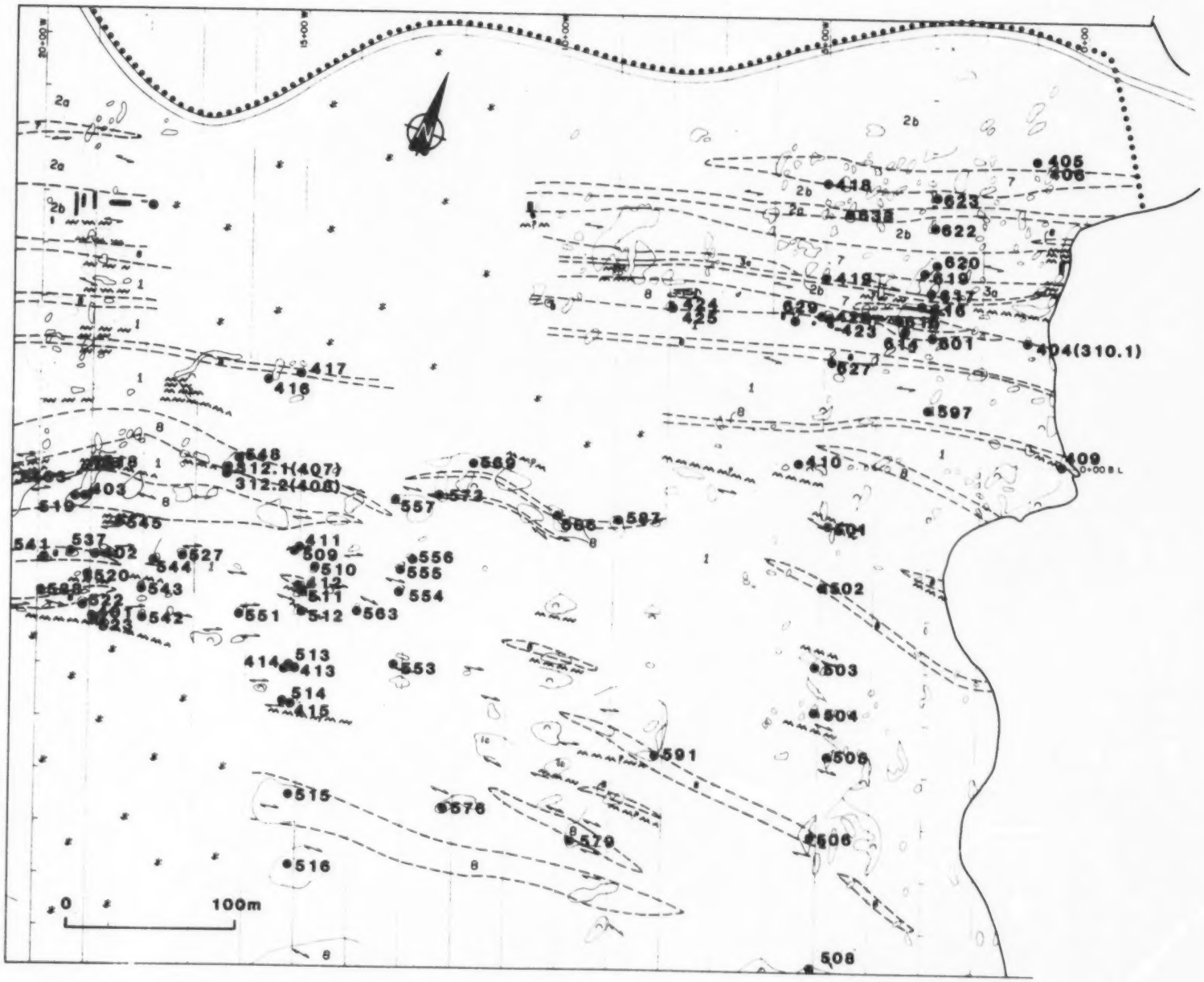

Figure C: Sample locations for the Ruby Lake grid.

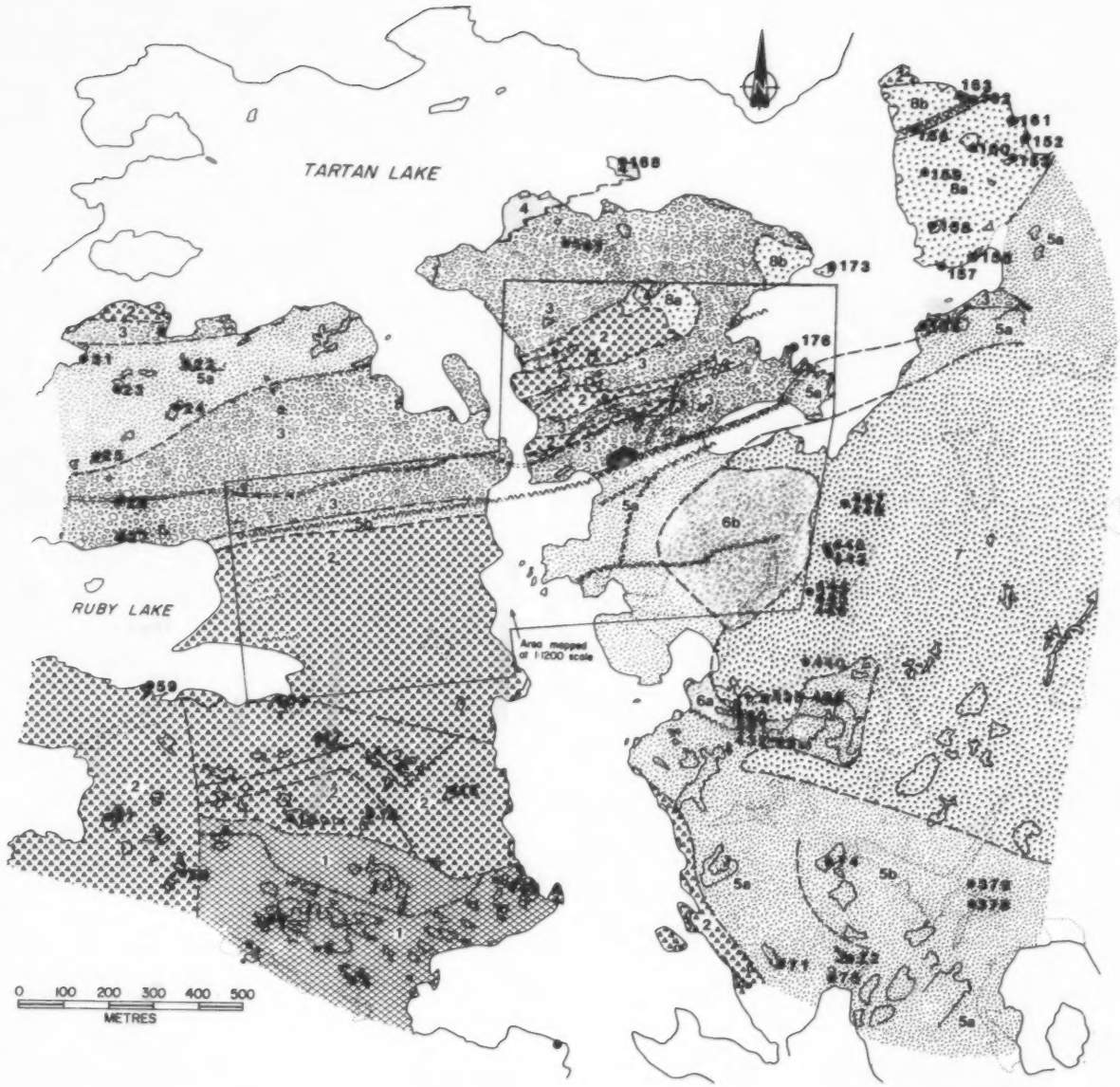

Figure D: Sample locations for the Tartan Lake (1:5000) grid.

APPENDIX V: SELECTED PETROGRAPHIC DESCRIPTIONS.

Due to the large number of petrographic descriptions and their repetitiveness, only two or three representative descriptions for each rock type are presented here.

42-86-RL-506
FIELD NAME: Feldspar porphyry
4 + 80W/7 + 10S

Sample RL-506 contains 10%, subhedral to euhedral plagioclase phenocrysts that are up to 3 mm, moderately epidotized, irregularly distributed and randomly oriented. They can be polycrystalline, and are commonly broken *in situ*. The phenocrysts are variable in size, the smaller crystals appearing subhedral and broken more commonly. Fine grained epidote, up to 20%, occurs interstitially and as crosscutting veinlets. 2% chlorite and 1% biotite occur as tabular intergrowths commonly associated with epidote. 2 - 3%, subhedral hornblende, up to 1.5 mm, is associated with epidote and can be hematized along cleavage planes. 2%, irregularly shaped opaque minerals are associated with epidote and have traces of hematization. The remainder of the sample consists of very fine grained ($\leq$ 0.05 mm), anhedral quartz, plagioclase and interstitial muscovite and chlorite. Although the groundmass does not have a layered or sheared appearance, epidote veinlets can have a vague foliation.

42-86-RL-515
FIELD NAME: Feldspar-quartz porphyry
15 + 15W/7 + 80S

Sample RL-515 contains 15%, subhedral, moderately saussuritized plagioclase phenocrysts up to 8 mm, which occur as single crystals and polycrystalline aggregates. The larger phenocrysts are commonly broken *in situ*, and the resulting microfracture infilled with a quartz $\pm$ carbonate $\pm$ muscovite $\pm$ epidote mosaic. 5%, anhedral quartz phenocrysts, average 1.0 - 1.5 mm, are commonly polycrystalline and crosscut by a quartz $\pm$ carbonate mosaic. Carbonate is commonly associated with quartz at the edges of the phenocryst. 10 - 15% carbonate occurs as fine grained anhedral crystals, mosaics, and as fine grained lenticular areas up to 1.5 x 8 mm. These lenticular areas are affected by two directions of deformation: an earlier event imposed an alignment of lenses and foliation of crystals, and a later event imposed a crenulation nearly perpendicular to the earlier foliation. 5%, fine grained muscovite intergrowths occur as irregular patches. 15%, fine grained epidote aggregates and subhedral crystals are associated with 7 - 10% anhedral chlorite and 2 - 37% tabular biotite. 1%, subhedral opaque minerals up to 1 mm have epidote inclusions and are hematized along the crystal edges in places. Quartz and plagioclase, $\leq$ 0.05 mm, comprise the remainder of the groundmass. Mafic minerals have a poor foliation. Near the carbonate lenses the replacement micas in plagioclase phenocrysts are roughly aligned.

42-86-TL-573.1
FIELD NAME: Feldspar porphyry
0 + 30E/0 + 40N

Sample TL-573.1 contains 50%, randomly oriented, subhedral to euhedral plagioclase phenocrysts, up to 2 mm, average 1.2 mm. While these crystals may be incidentally touching in places, they are not polycrystalline aggregates; some crystals are broken *in situ*. The plagioclase phenocrysts are moderately to heavily saussuritized, and many cores are epidotized as in sample TL-579.1. The sample also contains 5%, irregular to euhedral pyrite crystals, 10% epidote, 1% hornblende, 5% biotite, and 5% chlorite. The remainder of the sample consists of very fine grained ($\leq$ 0.02 mm) quartz, plagioclase, and biotite.

42-86-TL-715.1
FIELD NAME: Feldspar porphyry
16 + 65E/14 + 10N
FIELD COMMENTS: Dyke

Sample TL-715.1 is similar to TL-687.1. 1% quartz and 15% plagioclase phenocrysts occur, broken *in situ* in places. Plagioclase crystals are moderately saussuritized. Some plagioclase crystals have grown around pre-existing plagioclase crystals, indicating that at least some of the feldspars are partly porphyroblastic. The nucleating plagioclase crystal in these porphyroblasts is significantly larger than individual crystals in the groundmass. Many plagioclase phenocrysts/porphyroblasts are rimmed by epidote and/or very fine grained opaque minerals. Areas up to 3 mm demarcated by the growth of very fine grained epidote bear 0.5 - 1 mm plagioclase $\pm$ quartz crystals with finer grained quartz, plagioclase, carbonate, muscovite, and biotite. A very fine grained groundmass of quartz, feldspar, biotite, and carbonate appears to flow around phenocrysts/porphyroblasts. The grain size and carbonate content increase slightly in the pressure shadows of these crystals.

RL-617A
FIELD NAME: Felsic tuff
3 + 30N/3 + 00W

Sample RL-617A contains 20%, randomly oriented, broken crystals up to 4 mm with highly variable grain size. Most of the crystals are lightly epidotized plagioclase with less than 1% quartz.

The matrix, average grain size less than 0.05 mm, consists of plagioclase (+ quartz?), 20% biotite and

epidote, 10% carbonate, and 2% opaque oxide minerals. Sericite, 5%, occurs in the matrix and along some crystal boundaries.

Lithic clasts are virtually absent. Traces of euhedral pyrite overgrow pre-existing mineralogy.

RL-617B
FIELD NAME: Felsic tuff
3 + 30N/3 + 00W

Sample RL-617B is thinly laminated with layers distinguishable by variations in grain size and composition. The rock is very fine grained with an apparently bimodal grain size distribution, 0.1 mm and 0.05 mm.

Subhedral plagioclase, 50%, some broken, is randomly oriented with layers. Biotite, 35%, forms subparallel mafic-rich layers and is interstitial to plagioclase in felsic layers. Subhedral carbonate, 15%, average 0.15 mm, forms crystal aggregates which overprint the existing mineralogy. Anhedral opaque oxide minerals, 1%, less than 0.05 mm, form disseminations and elongate smears parallel to foliation. Anhedral to subhedral sulphide minerals, 1%, are concentrated in carbonate-rich areas and overgrow pre-existing mineralogy, including carbonate.

42-86-TL-696.1
PETROGRAPHIC NAME: Intermediate tuff
FIELD NAME: Intermediate feldspar crystal tuff
1 + 05W/14 + 10N
FIELD COMMENTS: Prominent layering in hand sample

Sample 696.1 is characterized by felsic, 85%, and mafic, 15%, layering. The felsic layers consist of 0.05 mm plagioclase and quartz crystals with about 15% biotite and lesser amounts of carbonate, epidote, and opaque minerals. Mafic layers are variable from 0.3 to 13 mm thick, may bend slightly, and are discontinuous. They consist of subparallel, 0.1 mm biotite with 20-30% plagioclase, quartz, epidote, carbonate, chlorite, and opaque minerals.

1 - 3%, subhedral plagioclase crystals are up to 0.4 mm. The coarser grained plagioclase crystals exhibit irregularities along their boundaries. Possible inclusion trails were identified within some plagioclase crystals. One carbonate lens up to 2 mm wide consists of a mosaic of 0.5 mm carbonate crystals with minor quartz, feldspar, epidote, biotite, and opaque minerals. Minor blebs of very fine grained carbonate occur throughout the sample.

42-86-TL-703.1
PETROGRAPHIC NAME: Intermediate tuff
FIELD NAME: Feldspar crystal tuff
1+ 60E/12 + 55N
FIELD COMMENTS: "Epidote pod"

Sample TL-703.1 is compositionally layered, with mafic layers, 15% alternating with felsic layers, and an average grain size of 0.05 mm. Individual layers average about 0.3 - 0.5 mm thick. There are 1 - 3%, 0.1 - 0.15 mm plagioclase crystals which are anhedral to subhedral and broken in places. The felsic layers consist of: anhedral, irregularly shaped grains of undulatory quartz and plagioclase; 10 - 25%, subparallel biotite; and 5%, subparallel, but more irregularly shaped, chlorite. The mafic layers consist of: subparallel biotite with 10%, irregular to subparallel chlorite; 15%, irregular, granular quartz and plagioclase; and 1%, irregular, opaque oxide minerals which are concentrated in mafic and epidotized areas.

Carbonate occurs in irregular patches throughout the section. Epidote occurs in irregular patches, particularly concentrated in mafic layers where it constitutes 5 - 20% of the mafic area, and as the major constituent of an epidote pod 1 cm across.

The pod is crisscrossed by multidirectional fractures that are infilled by patches of polycrystalline quartz accompanied by irregular chlorite, 1% sulphide minerals, and trace amounts of biotite. Minor single euhedral crystals of quartz are also scattered throughout the pod; the overall quartz content of the pod is about 15%. The layering bends around the margins of the pod, and some layers are apparently truncated by the pod. A layer of very fine grained granular quartz, epidote, and plagioclase surrounds the epidote pod.

Notes: Despite the presence of small feldspar crystals there is an insufficient amount of crystals present to properly name this rock a crystal tuff. More properly it might be named simply, intermediate tuff. Evidence of reworking in a sedimentary environment is not conclusive. The extremely fine grain size makes the examination of grain shapes difficult: rounding and sorting are not evident but are not precluded.

42-86-TL-660.1
PETROGRAPHIC NAME: Intermediate lapilli-tuff
FIELD NAME: Intermediate tuff
8 + 30E/16 + 05N

Sample TL-660.1 consists of 50%, 2-8 mm, rounded to flattened aggregates (lapilli) of very fine grained (0.05 mm) quartz, plagioclase, biotite, carbonate, and chlorite. 10 - 15%, plagioclase crystals, 0.05 - 2.5 mm, average 1 - 1.5 mm, some of which are broken, occur in a matrix composed of subparallel biotite with lesser chlorite, epidote, carbonate, and opaque minerals, and with an average grain size of 0.05 mm. Some feldspar crystals

exhibit minor chlorite alteration. Some biotite is partially bent around feldspar crystals. In the 'lapilli' the biotite is randomly oriented.

42-86-TL-728.1
PETROGRAPHIC NAME: Intermediate volcaniclastic rock
FIELD NAME: "Gritty" tuff
8 + 30E/12 + 95N

Sample TL-728.1 is prominently layered with laminae 0.5 - 1 cm thick. The grains, 0.03-0.05 mm, are angular. The majority of the rock consists of quartz and plagioclase with 30% mafic minerals. Biotite with very fine grained epidote (± chlorite) occurs in layers up to 0.8 mm wide and within felsic layers. Within mafic layers, the biotite is aligned parallel to layering; biotite is interstitial within felsic layers. 1 - 3% carbonate, 0.35 mm, occurs in aggregates up to 1 cm long parallel to layering. 1%, anhedral tourmaline (var. schorl) and trace amounts of fine grained muscovite are present.

42-86-TL-727.1
PETROGRAPHIC NAME: Intermediate volcaniclastic tuff
FIELD NAME: "Gritty" tuff
9 + 95E/12 + 55N

Sample TL-727.1 consists of angular grains with mostly uniform grain sizes, average 0.025 mm. Anhedral plagioclase and undulatory quartz are dominant, accompanied by about 30% interstitial epidote and biotite that partially overgrow the edges of plagioclase and quartz. Fine laminations are defined by a subparallel alignment of biotite. 1%, anhedral sulphide minerals, average 0.2 mm, are associated with epidote pods and are hematized in places at crystal edges. Lenses and aggregates of epidote and/or quartz ± carbonate ± opaque minerals occur. They are 0.1 - 10 mm and may be elongate parallel to the alignment of biotite.

42-86-TL-528.1
FIELD NAME: Gabbro
4 + 90E/3 + 75N
FIELD COMMENTS: Medium grained

Sample TL-528.1 consists of: 65% tremolite-actinolite, avg. 0.7 - 1.3 mm, subhedral to anhedral polycrystalline aggregates and fibrous aggregates; 25% epidote, 0.1 mm, forming pseudomorphs after plagioclase and fine grained aggregates interstitial to tremolite-actinolite; 5 - 10%, intergranular plagioclase mostly pseudomorphed by epidote; 3% sericite in irregularly shaped areas and overgrowing amphibole in places; 1%, 0.1 mm anhedral tourmaline overgrowing tremolite-actinolite; and 1%, 0.1 mm, secondary anhedral sulphide minerals, irregularly distributed. The thin section is non-foliated.

42-86-TL-573.2
FIELD NAME: Gabbro
0 + 30E/0 + 40N

Sample TL-573.2 consists of: 50% uralite pseudomorphs, up to 3 mm, after interconnected polycrystalline pyroxene aggregates; 25%, irregularly shaped, interstitial, fine grained, anhedral crystal aggregates of epidote; 15%, relict plagioclase crystals, up to 1.4 mm in optical continuity, that are heavily saussuritized and overgrown by minute amphibole overgrowths; 1%, secondary carbonate crystals, up to 1 mm; 1%, anhedral sulphide minerals, up to 0.7 mm; and 1%, secondary chlorite intergrown with and associated with sulphide minerals.

42-86-TL-575.3
FIELD NAME: Gabbro
0 + 20E/0 + 65S

Sample TL-575.3 contains 44%, 1.4 mm, ragged, subhedral to anhedral, prismatic crystals and fibrous aggregates of tremolite-actinolite. The larger crystals of tremolite-actinolite bear smaller (about 0.1 mm), randomly oriented tremolite-actinolite prisms within the crystals. 0.05 mm, randomly oriented epidote crystals, 40%, occur in interstitial aggregates. Very fine grained plagioclase, 15%, is interstitial to epidote. The sample also includes 0.35 mm, anhedral carbonate and < 1%, anhedral, opaque sulphide minerals, average 0.02 mm. The thin section is crosscut by a 0.5 mm wide veinlet consisting of very fine grained epidote and plagioclase that brecciates the gabbro.

42-86-TL-570.3
PETROGRAPHIC NAME: Gabbro
6 + 00E/3 + 80N
FIELD COMMENTS: Diorite, fine grained

Sample TL-570.3 consists of: 40%, subhedral, moderately to heavily saussuritized plagioclase; 20% epidote replacing plagioclase and forming fine grained networks around plagioclase crystals and aggregates; 15% chlorite; 15% anhedral carbonate; 5% muscovite/sericite in anhedral crystals and altered feldspar; 3% subhedral tourmaline; and 2%, anhedral to euhedral, sulphide minerals associated with carbonate and/or chlorite. The grain size averages 0.25 mm and is up to 2 mm.

42-86-TL-722.1
FIELD NAME: Gabbro
6 + 70E/16 + 40N
FIELD COMMENTS: Fine grained

Sample TL-722.1 has an average grain size of 0.7

mm. It contains 5% hornblende in optically continuous areas up to 3 mm that are highly disrupted internally and at crystal boundaries by the growth of chlorite ± quartz ± biotite. In addition to these areas, an additional 35% hornblende occurs in anhedral to subhedral crystals. This sample also contains: 25%, 0.35 mm, anhedral tabular intergrowths of chlorite; 15% epidote, very fine grained aggregates and irregularly distributed, anhedral to subhedral pseudomorphs after plagioclase; 17%, very fine grained, interstitial plagioclase; 2%, 0.1 mm, subhedral pyroxene associated with hornblende and chlorite; 1% anhedral carbonate; and 1%, very fine grained biotite associated with chlorite.

42-86-TL-574.4
FIELD NAME: Diorite
3 + 30E/2 + 00S
FIELD COMMENTS: Dyke, aphanitic

Sample TL-574.4 has been variably altered by epidote and chlorite in veinlets and irregular shapes. The least altered material consists of: 65%, euhedral to subhedral plagioclase; 20% epidote; and 15% chlorite. Less than 1%, euhedral cubic to anhedral pyrite averages 0.07 mm. The most altered material consists of epidote and chlorite patches that have destroyed original textures and mineralogy.

42-86-TL-575.2
FIELD NAME: Diorite
0 + 20E/0 + 65S
FIELD COMMENTS: Dyke, aphanitic

Sample TL-575.2 contains: 35%, fine grained, disseminated epidote; 57% plagioclase whose shapes are obscured to completely pseudomorphed by epidote; 7%, anhedral to euhedral, disseminated sulphide minerals, average 0.1 mm, up to 1.4 mm; 1% anhedral carbonate; and 1% anhedral undulatory quartz associated with epidote. The average grain size in this sample is < 0.1 mm, but individual epidote grains are much smaller (≤ 0.05 mm).

42-86-TL-718.1
FIELD NAME: Knotted Gabbro
13 + 10E/20 + 25N

Sample TL-718.1 contains 15% hornblende poikiloblasts up to 4 mm consisting of optically continuous hornblende disrupted by fine grained epidote, biotite, plagioclase, and finer grained hornblende. The groundmass consists of: 35%, very fine grained epidote in anhedral patches; 10% epidote pseudomorphous after plagioclase; 15% hornblende with variable grain size but finer grained than the poikiloblasts; 8%, very fine grained, anhedral plagioclase; 7%, very fine grained, subhedral, tabular biotite; 5%, anhedral carbonate; and 5%, opaque oxide minerals in elongate streaks up to 0.05 x 0.75 mm.

42-86-TL-691.1
FIELD NAME: Gabbro
3 + 80E/18 + 55N
FIELD COMMENTS: Fine grained

Sample TL-691.1 has a subophitic texture and an average grain size of 0.75 mm. The sample consists of: 35% epidote, primarily as pseudomorphs after plagioclase and also as 0.05 mm, subhedral crystals; 40%, anhedral, polycrystalline clinopyroxene, up to 4 mm across, altered by epidote and biotite; 15% chlorite; 5%, fibrous actinolite; 3%, anhedral, opaque sulphide minerals, average 0.1 mm; 1%, anhedral carbonate crystals, and 1% quartz associated with chlorite and interstitial crystalline aggregates. Rare microfractures yield very minor offsets in crystals.

42-86-TL-731.1
FIELD NAME: Mafic schist
10 + 90E/12 + 05N

Sample TL-731.1 consists of: tremolite-actinolite, 45%, 0.45 mm, equant, mono- and polycrystalline, and as aggregates of prismatic subhedral crystals, 0.06 mm; plagioclase, 20%; epidote, 30%, in very fine grained aggregates; quartz (+ plagioclase), 5%, 0.05 - 3 mm in 1 - 1.5 mm mosaics, irregularly distributed, epidotized and sericitized; and < 1%, 0.45 mm, anhedral sulphide minerals.

The sample has well developed foliation defined by the elongation of quartz mosaics and streaks of amphibole-rich areas, and by the subparallel alignment of some amphibole and plagioclase crystals.

42-86-TL-674.4
FIELD NAME: Chlorite schist
1 + 30E/6 + 70N

Sample TL-674.4 consists of: plagioclase + quartz, 40%, lightly to moderately saussuritized, with an apparent bimodal distribution of grain sizes, average 0.7 mm and 0.05 mm; chlorite, 35%, forming fibrous aggregates interstitial to plagioclase; carbonate, 9%, forming patches of anhedral crystals, average 0.7 mm, associated with plagioclase and quartz; epidote, 7%, in fine grained granular aggregates; biotite, 2%, in tabular aggregates; pyrite, 1%, anhedral to euhedral cubic, up to 0.35 mm, avg. 0.05 mm, associated with chlorite and rimmed in places by opaque oxide minerals; opaque oxide minerals, 6%, similar to the occurrence of sulphide minerals. A rough compositional "layering" on a 1 cm scale may be present; the amount of chlorite and opaque minerals is variable between the layers.

Note: This rock appears to a chlorite-rich chemical sediment mixed with reworked volcaniclastic material.

42-86-TL-563.1
FIELD NAME: Schist
10 + 50E/0 + 45S

Sample TL-563.1 contains bands of crenulated micas separated by non-crenulated bands of carbonate and plagioclase. The crenulated streaks comprise fibrous aggregates of muscovite, 15%, intergrown with chlorite, 5%. Carbonate, 60%, is anhedral and averages 0.12 mm. Lightly saussuritized plagioclase, 15%, forms anhedral, 0.2 - 0.35 mm crystals associated with carbonate and brecciated crystals up to 1.5 mm with finer grained plagioclase (+ muscovite + carbonate + tourmaline) infilling fractures. Euhedral tourmaline, 3%, avg. 0.05 mm, is irregularly distributed; 2% quartz, 0.25 mm, forms polycrystalline streaks. Less than 1%, 0.07 mm, subhedral to euhedral pyrite is also present. In places carbonate and tourmaline appear to overgrow the micaceous bands, but generally there is a demarcation of carbonate - mica boundaries.

42-86-TL-669.3
FIELD NAME: Chlorite-calcite-quartz schist
17 = 40/14 + 20N

Sample TL-699.3 contains: carbonate, 30%, avg. 0.1 mm; sericite, 30%, and chlorite, avg. $\leq$ 0.2 mm; plagioclase and quartz, 15%, 0.05 mm; and 1%, anhedral opaque sulphide (?) and oxide minerals up to 0.55 mm, appearing in places as dusty streaks parallel to foliation. Micas are well foliated. A second deformational event has imposed crenulations oblique to foliation. Microfractures along some of the intersections of these two directions of foliation cause minor displacement of layers.

MAPS
NOT
FILMED

CARTES
OMISES